

**Generation of novel intracellular binding reagents  
based on the human  $\gamma$ B-crystallin scaffold**

**Dissertation**

zur Erlangung des akademischen Grades

*doctor rerum naturalium*

(Dr. rer. nat.)

vorgelegt der

Naturwissenschaftlichen Fakultät I-Biowissenschaften

der Martin-Luther-Universität Halle-Wittenberg

Institut für Biochemie und Biotechnologie

von Ewa Mirecka

geboren am 17. Dezember 1976 in Gdynia, Polen

## Table of contents

<b>1. INTRODUCTION</b>	1
<b>1.1 Monoclonal antibodies as a biomolecular scaffold</b>	1
<b>1.2 Binding molecules derived from non-immunoglobulin scaffolds</b>	3
1.2.1 Alternative protein scaffolds – general considerations	3
1.2.2 Application of alternative binding molecules	6
<b>1.3 Affilin – novel binding molecules based on the human <math>\gamma</math>B-crystallin scaffold</b>	6
1.3.1 Human $\gamma$ B-crystallin as a molecular scaffold	6
1.3.2 Generation of a human $\gamma$ B-crystallin library and selection of first-generation Affilin molecules	8
<b>1.4 Selection of binding proteins by phage display</b>	9
<b>1.5 Human papillomavirus E7 protein as a model target for the generation of intracellular Affilin molecules</b>	11
1.5.1 Human papillomaviruses and associated diseases	12
1.5.2 Genomic organization of human papillomaviruses	12
1.5.3 Viral life cycle	13
1.5.4 Human papillomavirus E7 protein	14
1.5.4.1 Biological activities and cellular targets of the E7 protein	14
1.5.4.2 Biochemical characterization of the E7 protein	16
<b>1.6 Options for delivery of therapeutic proteins into mammalian cells</b>	18
<b>1.7 Aim of the study</b>	20
<b>2. MATERIALS AND METHODS</b>	21
<b>2.1 Materials</b>	21
2.1.1 Bacterial strains	21
2.1.2 Eukaryotic cells	21
2.1.3 Phage	21
2.1.4 Vectors	22
2.1.5 Oligonucleotides	23
2.1.6 Chemicals	23
2.1.7 Enzymes	24
2.1.8 Proteins	24
2.1.9 Antibodies	24
2.1.10 Kits and standards	25
2.1.11 Buffers and solutions	25
2.1.12 Media and antibiotics for cultivation of <i>E. coli</i>	26
2.1.13 Media for mammalian cell culture	27
2.1.14 Chromatography columns	27
2.1.15 Laboratory equipment	27
2.1.16 Miscellaneous	28
<b>2.2 Methods</b>	28
2.2.1 Molecular biology	28
2.2.1.1 Plasmid DNA preparation	28
2.2.1.2 Determination of DNA concentration	28
2.2.1.3 Polymerase chain reaction	28
2.2.1.4 DNA digestion	29
2.2.1.5 Generation of double-stranded oligonucleotides	29
2.2.1.6 Dephosphorylation of DNA	30
2.2.1.7 Agarose gel electrophoresis	30
2.2.1.8 DNA gel extraction	30
2.2.1.9 DNA ligation	30
2.2.1.10 Site-directed mutagenesis	30
2.2.1.11 DNA sequencing	31

## Table of contents

---

2.2.2	Transformation of <i>E. coli</i> cells	31
2.2.2.1	Chemically competent <i>E. coli</i> cells	31
2.2.2.2	Electrocompetent <i>E. coli</i> cells	31
2.2.3	Phage display selection of anti-E7 Affilin molecules	32
2.2.4	Protein expression using recombinant <i>E. coli</i>	35
2.2.5	Protein purification and chromatographic analysis	36
2.2.6	Protein characterization	37
2.2.6.1	Quantification of protein concentration	37
2.2.6.2	SDS-PAGE	38
2.2.6.3	Western blotting	38
2.2.6.4	ELISA	38
2.2.6.5	Surface plasmon resonance	39
2.2.7	Cell biology	40
2.2.7.1	Mammalian cell propagation	40
2.2.7.2	Tat-mediated internalization of Affilin molecules into mammalian cells	40
2.2.7.3	Transfection of mammalian cells	41
2.2.7.4	Immunofluorescence microscopy	41
2.2.7.5	Bromodeoxyuridine incorporation assay	42
2.2.7.6	Analysis of apoptosis	42
<b>3.</b>	<b>RESULTS</b>	<b>43</b>
<b>3.1</b>	<b>Recombinant production of the HPV-16 E7 protein</b>	<b>43</b>
3.1.1	Cloning, expression and purification of the HPV-16 E7 protein	43
3.1.2	Biophysical characterization of the HPV-16 E7 protein	47
3.1.2.1	Western blot analysis	47
3.1.2.2	Binding of the HPV-16 E7 protein to pRb	47
<b>3.2</b>	<b>Phage display selection of anti-E7 Affilin molecules from a <math>\gamma</math>B-crystallin library</b>	<b>50</b>
3.2.1	Conventional phage display selection of anti-E7 Affilin molecules	50
3.2.1.1	Affinity selection	50
3.2.1.2	Analysis of individual clones by ELISA	51
3.2.1.3	Sequence analysis of individual clones	52
3.2.1.4	Affinity determination	54
3.2.1.5	Effect of the Cys to Ser exchange on the affinity of Affilin D1	56
3.2.2	Selection of Affilin molecules against the HPV-16 E7 protein by phage display with proteolysis	57
3.2.2.1	Affinity selection	57
3.2.2.2	Analysis of individual clones by ELISA	58
3.2.2.3	Sequence analysis of individual clones	59
3.2.2.4	Affinity determination	60
<b>3.3</b>	<b>Investigation of the Tat-mediated delivery of Affilin molecules</b>	<b>61</b>
3.3.1	Generation of Affilin-Tat fusion proteins	62
3.3.2	Expression and purification of Affilin-Tat fusion proteins and $\gamma$ B-crystallin-Tat	62
3.3.2.1	Optimization of the bacterial expression of Affilin-Tat fusion proteins	63
3.3.2.2	Purification of Tat-fused Affilin variants and $\gamma$ B-crystallin-Tat	64
3.3.3	Characterization of Tat-fused Affilin variants and $\gamma$ B-crystallin-Tat	66
3.3.3.1	Western blot analysis	66
3.3.3.2	Effect of the Tat peptide on the affinity of Affilin variants	67
3.3.3.3	Binding characteristics of Affilin molecules investigated by surface plasmon resonance	68
3.3.3.4	Evaluation of the specificity of Affilin variants	69
3.3.4	Analysis of the cellular uptake of Affilin-Tat fusion proteins	70
3.3.4.1	Western blot analysis of the Tat-mediated uptake	70
3.3.4.2	Microscopic examination of the Tat-mediated internalization	72
<b>3.4</b>	<b>Intracellular activity of transiently expressed Affilin molecules</b>	<b>76</b>
3.4.1	Transient expression of Affilin molecules in mammalian cells	76
3.4.2	Evaluation of the intracellular activity of Affilin molecules	77
3.4.2.1	Antiproliferative effect of Affilin molecules	77
3.4.2.2	Influence of the Affilin expression on the apoptosis of E7-positive cells	81

<b>4.</b>	<b>DISCUSSION</b> .....	82
<b>4.1</b>	<b>Recombinant production of the E7 protein</b> .....	82
<b>4.2</b>	<b>Generation of intracellular Affilin molecules</b> .....	84
4.2.1	Phage display selection of Affilin molecules from a $\gamma$ B-crystallin library .....	84
4.2.2	Sequence analysis of selected Affilin variants .....	86
4.2.3	Comparison of binding affinities of Affilin molecules and other binding proteins .....	88
4.2.4	Specificity of Affilin molecules .....	90
4.2.5	Recombinant production of Affilin molecules .....	90
<b>4.3</b>	<b>Tat-mediated delivery of Affilin molecules into mammalian cells</b> .....	92
<b>4.4</b>	<b>Intracellular activity of Affilin molecules</b> .....	94
<b>5.</b>	<b>CONCLUSIONS</b> .....	97
<b>6.</b>	<b>SUMMARY</b> .....	98
<b>7.</b>	<b>ZUSAMMENFASSUNG</b> .....	100
<b>8.</b>	<b>REFERENCES</b> .....	102
<b>9.</b>	<b>PUBLICATIONS</b> .....	119
<b>10.</b>	<b>ABBREVIATIONS</b> .....	120
	<b>ERKLÄRUNG</b> .....	121
	<b>CURRICULUM VITAE</b> .....	122

# 1. Introduction

## 1.1 Monoclonal antibodies as a biomolecular scaffold

The antibody structure is the best-known example of a protein scaffold used naturally by the immune system to display well-defined binding motifs for molecular recognition (Janeway *et al.*, 2001). The binding site of the antibody corresponds to six loops, known as complementarity-determining regions (CDRs) or hypervariable regions, anchored and oriented by a conserved framework consisting of light-chain and heavy-chain variable domains (Fig. 1). The polypeptide segments comprising CDRs show hypervariability in length, sequence, conformation and relative disposition imparting the unique antigen specificity to each antibody molecule (Padlan, 1994).

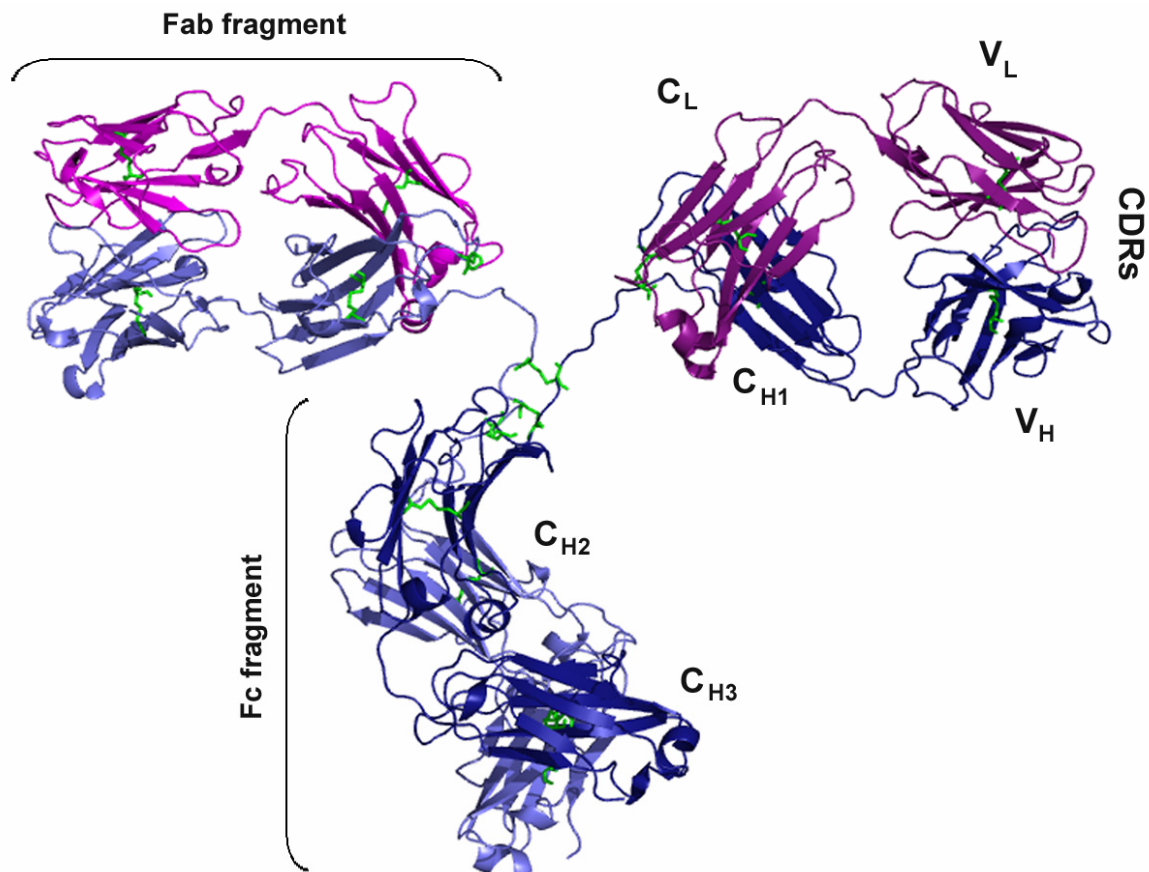


**Figure 1.** Structural model of the IgG molecule (PDB code 1IGT). The antibody is composed of two pairs of identical heavy (blue) and light (violet) chains linked by disulfide bonds (stick mode, green). Each light chain consists of one variable (V<sub>L</sub>) and one constant (C<sub>L</sub>) domain, whereas each heavy chain comprises one variable domain (V<sub>H</sub>) and three constant domains (C<sub>H1</sub>, C<sub>H2</sub>, and C<sub>H3</sub>). Functionally, antibody is divided into two antigen-binding fragments (Fabs) and a constant (Fc) region. The antigen-binding site comprises hypervariable regions of V<sub>H</sub> and V<sub>L</sub> chains (called complementarity-determining regions - CDRs). Each antibody domain has a typical immunoglobulin fold composed of two tightly packed antiparallel β-sheets. The figure was generated using PyMOL (<http://pymol.org>).

The ability of the immune system to produce antibodies specific to almost any target has led to the widespread use of antibodies in biomedical research and diagnostics. More recently, advances in recombinant technologies have extended the application of antibodies into human therapy (Lonberg, 2008). Consequently, monoclonal antibodies have become the most-rapidly growing sector of pharmaceutical biotechnology with over 20 antibody-based drugs already approved by the U.S. Food and Drug Administration and many other therapeutic antibodies being currently evaluated in preclinical and advanced clinical studies (reviewed in Reichert, 2008).

As binding molecules, monoclonal antibodies possess intrinsic strengths such as unlimited diversity as well as high specificity and affinity for pre-defined targets. With respect to the therapeutic applications, antibodies offer a wide variety of mechanisms of action such as target neutralization, ligand and/or receptor binding and antagonism, sensitization of cells to chemotherapy and induction of antibody-dependent cell-mediated or complement-dependent cytotoxicity (Carter, 2006). The low immunogenicity of antibody-based drugs has been achieved primarily by chimerization or humanization and most recently by the use of fully human monoclonal antibodies (Presta, 2006).

Despite of these attributes, certain limitations of antibodies associated with their large size and complex structure exist. They include demanding and expensive manufacturing in mammalian cell culture systems as well as complicated patent situation, which makes the commercial exploitation of antibody technologies difficult. Furthermore, due to the dependence of antibody structure on disulfide bonds, the use of therapeutic antibodies is restricted to extracellular or cell-surface antigens (Carter, 2006). Poor tissue penetration is another significant obstacle to the development of successful antibody drugs for immunotherapy of solid tumors (Thurber *et al.*, 2008).

To circumvent problems associated with the large size of immunoglobulins, smaller antibody formats, such as single-chain variable antibody fragments (scFvs) or domain antibodies, have been generated (Kipriyanov & Le Gall, 2004; Holliger & Hudson, 2005; Fig. 2). These antibody fragments can be produced in the periplasm of *E. coli*, however, many of them are expressed at low yields, have poor thermodynamic stability and increased aggregation behavior (Demarest & Glaser, 2008). To improve folding properties and production yields of recombinant antibody fragments, several engineering approaches in combination with innovative maturation methods can be employed (Worn & Pluckthun, 2001; Ewert *et al.*, 2003; Honegger, 2008). As an alternative, the favorable features of antibodies, *i.e.* tight and specific binding can be transferred to the alternative protein frameworks with high thermodynamic stability and efficient folding properties (Skerra, 2000; Binz *et al.*, 2005).

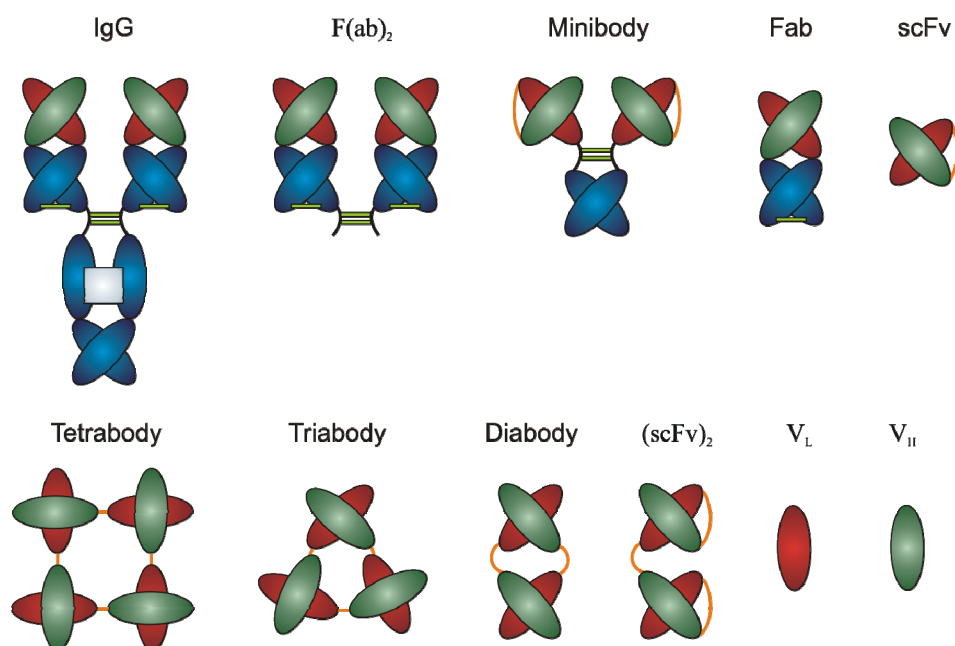


**Figure 2.** Representative antibody formats. For simplicity, all antibody formats are depicted as being monospecific. The variable domains of heavy ( $V_H$ ) and light ( $V_L$ ) chains are depicted in green and red, respectively. Constant domains of heavy and light chains are shown in blue. Glycosylation is shown as a light blue box. Inter-chain disulfide bonds are depicted as green bars, whereas peptide and chemical linkers are shown as orange lines. Modified from Carter, 2006.

## 1.2 Binding molecules derived from non-immunoglobulin scaffolds

### 1.2.1 Alternative protein scaffolds – general considerations

The novel binding proteins based on alternative scaffolds can be generated using rational or combinatorial protein engineering methods initially developed for recombinant antibodies (reviewed in Lutz & Bornscheuer, 2009). In combinatorial engineering approaches, certain surface-exposed amino acid residues within the underlying scaffold are randomly mutated to produce a protein library, which can then be used for *in vitro* selection of variants against pre-defined targets using well established display techniques such as phage display, ribosome display, mRNA display or cell surface display (reviewed in Wittrup, 2001; Lipovsek & Pluckthun, 2004, Paschke, 2006; for detailed description of the phage display technology see section 1.4).

In general, the concept of an alternative binding protein requires protein architectures that tolerate a number of amino acid exchanges such as multiple insertions, deletions and substitutions. The protein scaffold should preferably be of small size and constitute a single polypeptide chain to facilitate the library construction and cost-effective production using bacterial or yeast expression systems (Binz *et al.*, 2005). For therapeutic applications, it is intended to use protein scaffolds that are of human origin in order to reduce

the probability of immune response (Hey *et al.*, 2005; Skerra, 2007). Alternative scaffolds that lack disulfide bonds have a potential to be used in intracellular applications providing a clear advantage over antibody fragments, which typically rely on intra-chain disulfide bonds for their stability (Cattaneo & Biocca, 1999; Worn *et al.*, 2000).

Throughout the past decade, several classes of proteins have been evaluated as scaffolds for the generation of alternative binding reagents (summarized in Tab. 1; reviewed in Binz & Pluckthun, 2005; Hey *et al.*, 2005; Hosse *et al.*, 2006).

**Table 1.** Examples of validated protein scaffolds of non-immunoglobulin origin used for development of novel affinity proteins.

Name	Protein scaffold	Origin	No. of residues	Binding motif	Application	Selected references
Affibody	Z-domain of Staphylococcal protein A	bacterial	58	13 residues in 2 $\alpha$ -helices	Therapy (cancer, Alzheimer's disease) Chromatography Molecular imaging	(Nord <i>et al.</i> , 1997; Wikman <i>et al.</i> , 2004)
AdNectin	Tenth fibronectin type III domain	human	94	2 to 3 loops	Therapy (ophthalmology, cancer)	(Xu <i>et al.</i> , 2002; Getmanova <i>et al.</i> , 2006)
Affilin	$\gamma$ B-crystallin, ubiquitin	human	174 76	8 residues in $\beta$ -sheets	Therapy (cancer, ophthalmology, inflammation) Chromatography	(Fiedler <i>et al.</i> , 2006; Ebersbach <i>et al.</i> , 2007)
Anticalin	Lipocalins	human insect	160 - 180	Up to 24 residues in 4 loops	Therapy (cancer, cardiovascular diseases)	(Skerra, 2000; Schlehuber & Skerra, 2005)
Avimer	A-domains	human	43	Mainly $\beta$ -turns	Therapy (autoimmunity, inflammation, cancer)	(Silverman <i>et al.</i> , 2005)
DARPin	Ankyrin repeat protein	human	33	$\beta$ -turn, 1 $\alpha$ -helix, 1 loop	Therapy (antiviral, cancer, intracellular) Diagnostics Biotechnology	(Stumpp & Amstutz, 2007; Stumpp <i>et al.</i> , 2008)
Evibody	cytotoxic T lymphocyte-associated antigen 4 (CTLA-4)	human	136	loops	Therapy (cancer)	(Hufton <i>et al.</i> , 2000)
Kunitz domain	Kunitz-type domain of trypsin inhibitor	human	58	1 or 2 inserted loops	Therapy (hereditary angioedema, cystic fibrosis, cancer)	(Williams & Baird, 2003; Attucci <i>et al.</i> , 2006)
Microbody	Proteins from the 'knottin' family	variety of species	23 - 113	$\beta$ -turn, $\beta$ -sheet and/or loop	Therapy (pain treatment, antiviral and antibacterial applications)	(Craig <i>et al.</i> , 2001)
PDZ domain	Class I PDZ domain	mouse	90	15 residues in $\alpha$ -helix	Western blotting Pull-down Chromatography	(Reina <i>et al.</i> , 2002)
Peptide aptamers	Thioredoxin-A and other scaffolds	bacterial or other	108 -	loop insertions or C-terminal fusions	Intracellular applications	(Borghouts <i>et al.</i> , 2005)

Depending on the engineering strategy, binding proteins based on alternative scaffolds recognize their pre-defined targets via amino acid residues located within single or multiple loops. Examples in this respect are engineered Kunitz-type protease inhibitors, binders based on the tenth fibronectin type III domain or lipocalins (Fig. 3A, B and C). Other protein scaffolds recruit surface-exposed side chains of secondary structure elements for binding, e.g. Z-domain of Protein A from *Staphylococcus aureus* or ankyrin repeat proteins (Fig. 3D and E).

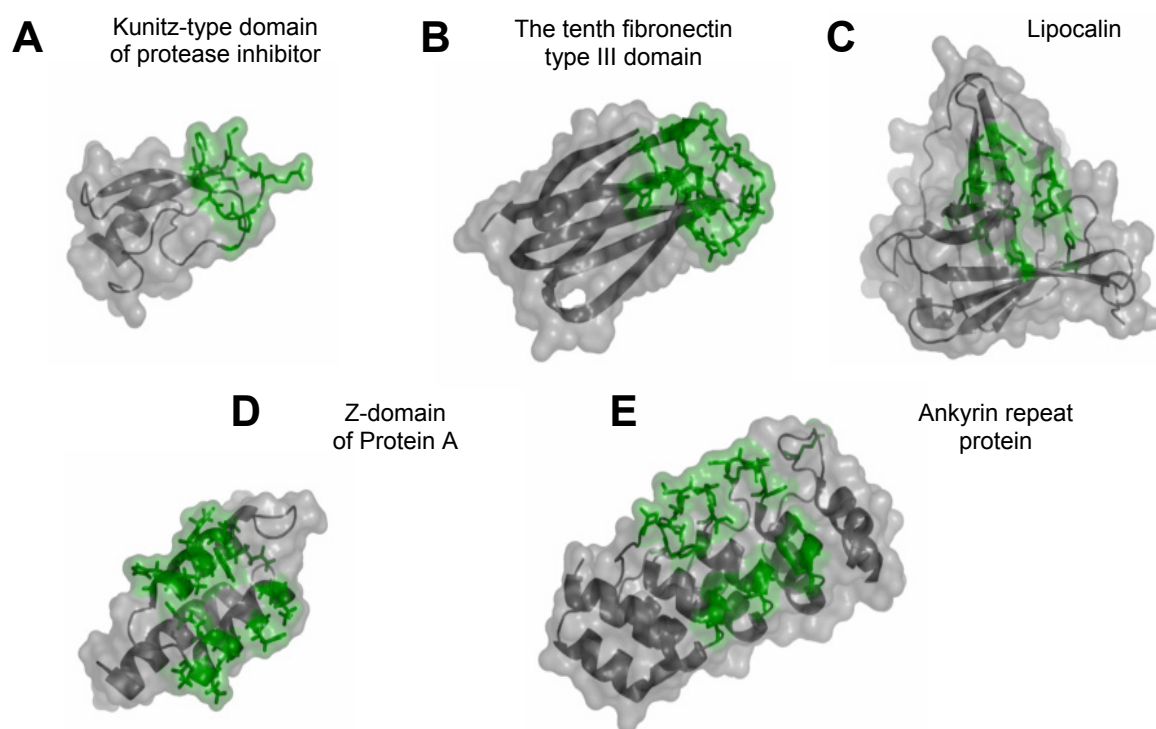


**Figure 3.** Graphical representations of different binding motifs on alternative protein scaffolds. (A), Kunitz-type domain of protease inhibitor (PDB code 1AAP); (B), the tenth fibronectin type III domain (PDB code 1FNA); (C), lipocalin (PDB code 1BBP); (D), Z-domain of Protein A (PDB code 2SPZ); (E), ankyrin repeat protein (PDB code 1MJ0). Depending on the scaffold architecture, target interaction is mediated by the surface-exposed amino acid residues located within single loop (A), multiple loops (B and C) or secondary structure elements (D and E). The secondary structure of conserved frameworks is depicted in grey, whereas randomized amino acid residues are highlighted in green. Modified from Hey *et al.*, 2005.

The alternative scaffolds have already proved to yield functional binders against different target molecules such as low-molecular-weight compounds, peptides and proteins. It is noteworthy that these molecules have achieved specificities and affinities comparable to those of conventional antibodies (Binz *et al.*, 2005; Skerra, 2007). As such, alternative binding proteins may become invaluable tools to be used in a wide range of biotechnological and biomedical application areas previously exclusively attributed to antibodies.

### 1.2.2 Application of alternative binding molecules

Binding proteins based on alternative scaffolds are currently being evaluated for various biotechnological applications such as affinity chromatography (Nord *et al.*, 2000; Reina *et al.*, 2002; Lamla & Erdmann, 2003), protein capture microarrays (Renberg *et al.*, 2005), molecular imaging (Orlova *et al.*, 2006), co-crystallization (Milovnik *et al.*, 2009) or targeted drug discovery (reviewed in Binz *et al.*, 2005; Gill & Damle, 2006; for more examples see Tab. 1). With regard to the human therapy, the development of alternative binding proteins as potential biopharmaceuticals resulted in some drug candidates (*i.e.* Kunitz derivatives, Avimer and AdNectin variants) currently undergoing clinical trials with some more subjected to preclinical studies (reviewed in Skerra, 2007; Gebauer & Skerra, 2009).

As several alternative scaffolds are devoid of disulfide bonds, they represent a rich source of affinity reagents suitable for intracellular applications, among which are intracellular target validation, study of protein function in cells as well as potentially intracellular therapy. Successful initial examples of alternative binding proteins used intracellularly include variants based on the fibronectin type III domain shown to discriminate between the agonist- and antagonist-bound form of the estrogen receptor  $\alpha$  in the yeast two-hybrid system (Koide *et al.*, 2002). Next, Junqueira and co-workers reported mutants of the PDZ domain derived from the serine protease Omi that recognize the C-terminus of the human c-Myc oncoprotein and induce the cell death in target-positive mammalian cells (Junqueira *et al.*, 2003). In another approach, variable peptide sequences termed peptide aptamers displayed on the *E. coli* thioredoxin A or other scaffold proteins have been shown to inhibit the activity of several intracellular targets essential in cancer development and progression (Borghouts *et al.*, 2005). More recent examples of alternative binding proteins generated to bind intracellular targets include DARPins derived from design ankyrin repeat proteins. High-affinity binding molecules selected from corresponding DARPIn libraries have been shown to inhibit intracellular kinase and proteinase in bacteria leading to a phenotype comparable to the genetic knockout (Amstutz *et al.*, 2005; Kawe *et al.*, 2006).

These results, indicating that binding molecules based on alternative scaffolds retain their functionality in the intracellular environment, are promising and encourage research and further development of this approach.

## 1.3 Affilin – novel binding molecules based on the human $\gamma$ B-crystallin scaffold

### 1.3.1 Human $\gamma$ B-crystallin as a molecular scaffold

The human  $\gamma$ B-crystallin is a member of a highly homologous family of vertebrate lens proteins called  $\gamma$ -crystallins (Jaenicke & Slingsby, 2001). Together with  $\beta$ -crystallins,

these proteins contribute to the refractive index and transparency of the lens structure (Bloemendal *et al.*, 2004). They are produced at very high concentrations by fiber cells during lens development, retaining their biological function in the absence of protein turnover for the lifetime of the organism (Wistow & Piatigorsky, 1988). To fulfill the requirement of longevity, crystallins must exhibit extraordinary stability and solubility. As an example of that, the bovine  $\gamma$ B-crystallin protein has been shown to preserve its native structure at pH 1 - 10 and to a temperature of 75°C being also resistant to denaturing agents such as 7 M urea (Rudolph *et al.*, 1990). The recombinant human  $\gamma$ B-crystallin shows a high degree of thermodynamic stability equivalent to that of bovine protein (Ebersbach *et al.*, 2007). It is noteworthy that the intrinsic stability of the  $\gamma$ B-crystallin does not depend on intramolecular disulfide bonds (Jaenicke, 1994).

Structurally, the human  $\gamma$ B-crystallin protein is a monomer composed of 174 amino acids with the molecular weight of approximately 21 kDa (Rudolph *et al.*, 1990). The molecule is composed of two highly symmetrical, independent domains with double Greek key fold, each consisting of about 40 amino acid residues arranged in four antiparallel  $\beta$ -strands (Fig. 4). The two domains are connected by a short linker and interact through a hydrophobic interface comprising amino acids Met43, Phe56, Ile81, Ile132, Leu145 and Val170 (Bloemendal *et al.*, 2004; Fig. 4). The intramolecular interactions between domains as well as the all- $\beta$  secondary structure of the Greek key motif have been shown to determine the overall stability of the protein (Jaenicke & Slingsby, 2001).

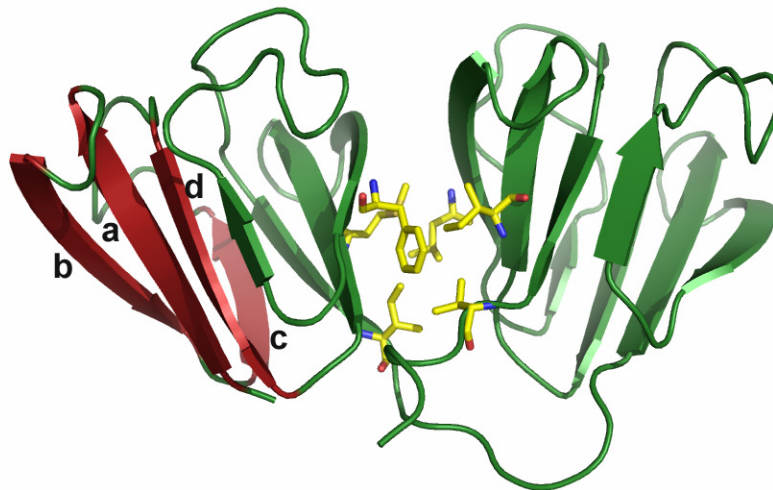


**Figure 4.** Overall structure model of the human  $\gamma$ B-crystallin protein (PDB code 2JDF). The molecule consists of two independent domains with double Greek key fold (the first N-terminal Greek key motif composed of  $\beta$ -strands a, b, c and d is shown in red). Both domains interact through a hydrophobic interface (amino acids Met43, Phe56, Ile81, Ile132, Leu145 and Val170; stick mode) and are connected via a short linker peptide. The figure was generated using PyMOL (<http://pymol.org>).

Owing to its favorable biophysical properties, the  $\gamma$ B-crystallin protein has been proposed as a scaffold candidate for the generation of novel affinity reagents named Affilin molecules (Fiedler & Rudolph, 2001; Ebersbach *et al.*, 2007).

### 1.3.2 Generation of a human $\gamma$ B-crystallin library and selection of first-generation Affilin molecules

The technology to use the human  $\gamma$ B-crystallin protein as a scaffold for the generation of alternative binding reagents has been established by Fiedler & Rudolph, 2001. Based on the structural considerations with respect to the tolerance of amino acid positions to diverse substitutions as well as their surface accessibility, eight amino acid residues located within the first, second and fourth  $\beta$ -strand of the N-terminal domain of  $\gamma$ B-crystallin, have been selected for the generation of a universal binding site (Fiedler & Rudolph, 2001). Their location in the three-dimensional structure model of the human  $\gamma$ B-crystallin as well as the accessible surface area of the binding site are illustrated in Fig. 5. The selected amino acid codons have been randomized using the *de novo* gene synthesis with NNK randomization (N: A, T, G and C; K: T or G nucleotides) which represents 32 codons and encodes all 20 amino acids and one amber stop codon. The resulting pool of DNA molecules has been inserted into an appropriate phagemid vector yielding a library of  $4.5 \times 10^8$  independent  $\gamma$ B-crystallin variants (Fiedler & Rudolph, 2001; Ebersbach *et al.*, 2007).

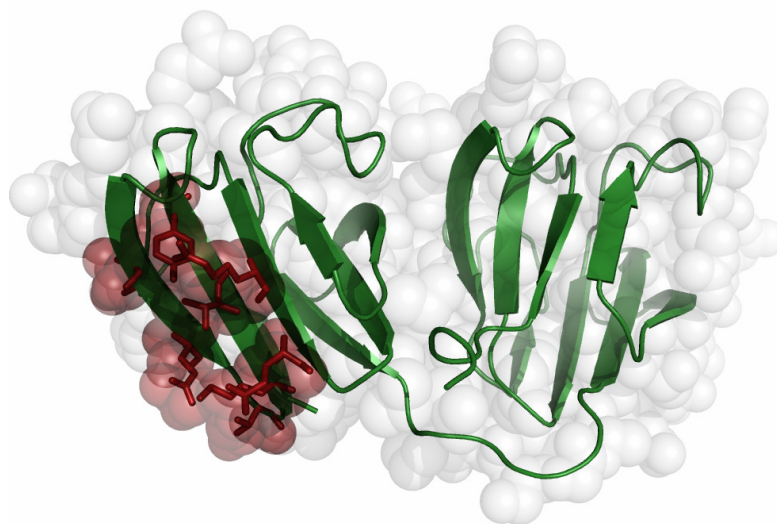


**Figure 5.** Representation of the human  $\gamma$ B-crystallin structure with randomized amino acids and the accessible binding surface area. The eight selected amino acid positions (*i.e.* Lys2, Thr4, Tyr6, Ser15, Glu17, Thr19, Arg36, Glu38) located within the N-terminal domain of human  $\gamma$ B-crystallin (shown as cartoon representation) are highlighted in red with their original side chains. The binding site comprises 6% of the total surface of the protein (Ebersbach *et al.*, 2007). The figure was generated using PyMOL (<http://pymol.org>) and PDB code 2JDF.

The  $\gamma$ B-crystallin library has already been used for the phage display selection of first-generation Affilin molecules against different targets such as human IgG Fc fragment, proNGF or steroid hormones estradiol and testosterone (Ebersbach *et al.*, 2007). The isolated Affilin variants revealed micromolar to nanomolar target affinities and high level of thermodynamic stability. As shown by crystallographic analysis, the isolated Affilin molecules preserved the overall structure and domain arrangement of the parental  $\gamma$ B-crystallin scaffold (Ebersbach *et al.*, 2007). The application of Affilin molecules as ligands for affinity purification has already been demonstrated (Fiedler *et al.*, 2006), whereas other applications remain to be shown.

#### 1.4 Selection of binding proteins by phage display

The isolation of protein variants exhibiting desired binding properties from large libraries requires methodologies that allow the evaluation of all members of the repertoire simultaneously in a biological screening assay. This can be achieved by various *in vitro* display technologies such as phage display, ribosome display, mRNA display or cell surface display (Wittrup, 2001; Lipovsek & Pluckthun, 2004; Paschke, 2006). The concept on which all display technologies are based requires a physical linkage between the phenotype (*i.e.* target-binding behavior) and the encoding genotype.

The display of protein library on filamentous phage is by far the most commonly used selection technology (reviewed in Hoogenboom & Chames, 2000; Paschke, 2006; for a general scheme see Fig. 6). The filamentous bacteriophages contain a single-stranded DNA (ssDNA) genome and are capable of infecting *E. coli* cells. The phage coat is composed of five different proteins, *i.e.* pIII, pVI, pVII, pVIII and pIX. The pIII protein, which is the most commonly used coat protein for display, is located at the tip of the phage (3 - 5 copies) and is necessary for the phage infectivity (Russel, 1991; Karlsson *et al.*, 2003). The filamentous phages are produced in bacterial periplasm and subsequently secreted from infected cells without cell lysis (Clackson & Lowman, 2004).

To generate a phage display library, randomized DNA sequences are inserted into an appropriate phagemid vector as a C-terminal fusion to the pIII protein. The phagemid encodes also the N-terminal leader sequence to direct pIII-fusion proteins into the bacterial periplasm. In addition to the standard plasmid origin of replication, the phagemid carries the M13 phage replication origin which allows production of single-stranded phagemid DNA (Hoogenboom *et al.*, 1991; Viti *et al.*, 2000).

To produce recombinant phage particles, *E. coli* host cells harboring phagemids are infected with the helper phage such as M13KO7 in a process called phage rescue (Barbass *et al.*, 2001).

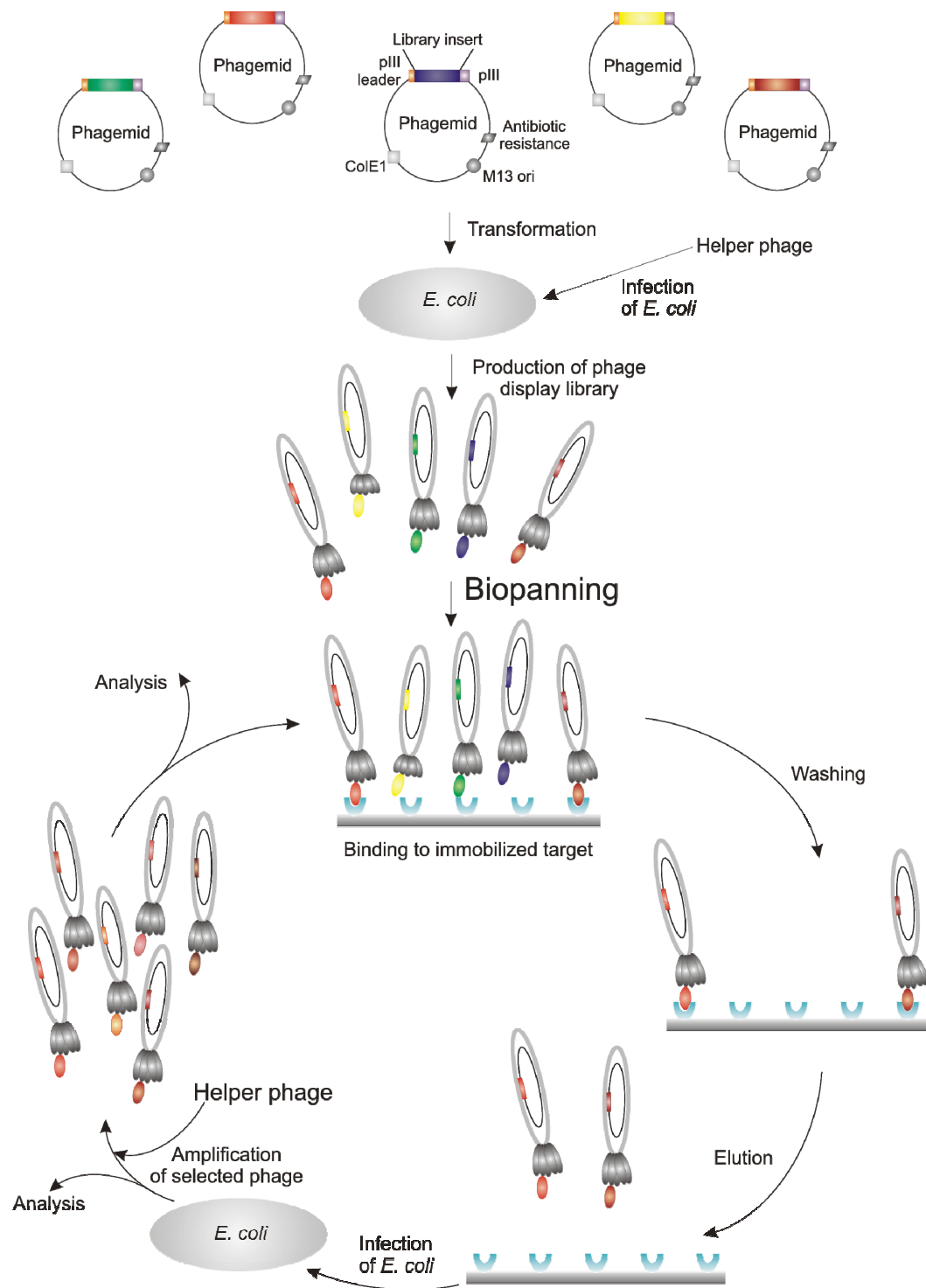


**Figure 6.** Schematic overview of the phage display selection. The DNA library is inserted between the pIII leader sequence and the pIII protein (45 kDa) of the filamentous bacteriophage in the phagemid vector. The phagemid vector contains M13 and *E. coli* origins of replication. To produce phage particles *E. coli* cells harboring phagemids are infected with a helper phage such as M13KO7. The helper phage provides genes required for replication of ssDNA and phage assembly. A mutation in the M13KO7 genome reduces replication and packaging of helper phage DNA and ensures the preferential packaging of phagemid DNA. During panning procedure, the recombinant phage particles are incubated with the target molecule immobilized on a solid support. Following washing of unbound phages, target-specific phages are eluted, re-infected to *E. coli* and used for additional panning rounds for further enrichment of target-binding clones.

Following infection, bacterial cells express phage-encoded structural and nonstructural proteins required for replication of ssDNA and phage assembly as well as the pIII-fusion protein from the phagemid. Due to the less efficient incorporation of the phagemid-encoded pIII-fusion constructs, the phage particles display an average of less than one copy of the recombinant pIII-fusion protein on their tips in addition to the wild-type pIII protein expressed from the phage genome (Azzazy & Highsmith, 2002; Kramer & Wunderli-Allenspach, 2003). As the M13KO7 helper phage carries a genetic mutation reducing the efficiency of replication and packaging of the helper phage genome, the phage particles produced from this infection preferentially contain the phagemid DNA encoding displayed fusion construct (Vieira & Messing, 1987). This establishes a linkage between the displayed protein variant and its gene ensuring that phages produced and released from the same bacteria are identical (Paschke, 2006).

In a typical selection approach, usually referred to as biopanning, the recombinant phage particles purified from the culture supernatant are allowed to bind to the target molecule immobilized on a solid support. In the next step, the non-binding phages are removed by washing and retained phages are eluted and amplified by reinfection of *E. coli* cells. The target-enriched phage population can then be subjected to the next rounds of biopanning. As a genotype-phenotype coupling occurs within each phage particle, clones with desired binding properties can be finally identified and individually analyzed (Barbass *et al.*, 2001).

In addition to the standard procedure described above, several modifications of the selection strategy are possible (Hoogenboom, 2002; Clackson & Lowman, 2004). They exploit the extraordinary stability of phage particles against a variety of conditions such as extremes in pH, treatment with denaturants, nucleases or proteolytic enzymes. This enables the selection of protein variants with certain desired properties such as stable folding (Forrer *et al.*, 1999; Bai & Feng, 2004), enhanced thermal stability (Chakravarty *et al.*, 2000) or improved enzyme function (Atwell & Wells, 1999; Heinis *et al.*, 2001).

### **1.5 Human papillomavirus E7 protein as a model target for the generation of intracellular Affilin molecules**

The human papillomavirus (HPV) E7 protein represents a promising target for the development of therapeutic strategies against HPV-associated tumors (zur Hausen, 2002). Due to the lack of homology between viral and cellular proteins, the E7 protein provides also a suitable model system for evaluation of different strategies aiming at inhibition of intracellular targets (Nauenburg *et al.*, 2001; Kamio *et al.*, 2004; Accardi *et al.*, 2005).

### 1.5.1 Human papillomaviruses and associated diseases

Human papillomaviruses infect the epithelial cells of skin and mucosa. They can cause a variety of diseases including benign skin and genital warts, cervical epithelial neoplasia as well as invasive cervical carcinoma (zur Hausen, 2000).

From over 100 different HPV types identified so far, approximately half infect the genital tract. Based on the association with benign or malignant lesions, these viruses are classified into low-risk or high-risk groups (de Villiers *et al.*, 2004). From several high-risk HPVs associated with genital malignancy, the HPV types 16 and 18 account for about 70% of all cervical cancer cases worldwide (de Villiers *et al.*, 2004; Cogliano *et al.*, 2005). The same high-risk HPV types also seem to be associated with the etiology of a subset of head and neck cancers (Gillison & Shah, 2001; Hennessey *et al.*, 2009).

Cervical cancer, being the second most common cause of the cancer mortality among women worldwide (Parkin *et al.*, 2005), has received much attention over the past decades as a serious public health problem. Extensive research studies have led to the successful development of two prophylactic vaccines based on the recombinant virus-like particles assembled from the L1 major capsid protein of certain HPV types (Harper *et al.*, 2006; Siddiqui & Perry, 2006). In addition to the prophylactic vaccines, many therapeutic approaches are under current investigation to treat established HPV infections as well as HPV-associated tumors (Bernard, 2004; Speck & Tyring, 2006).

### 1.5.2 Genomic organization of human papillomaviruses

All papillomaviruses share a common genetic structure, which comprises double-stranded circular DNA of approximately 8000 base pairs (Zheng & Baker, 2006; Fig. 7). The HPV genome contains eight open-reading frames (ORFs) divided into two functional groups, *i.e.* early (E) genes (E1, E2, E4, E5, E6, and E7) and late (L) genes (L1 and L2).

The E1 and E2 ORFs encode proteins that play important roles in the viral genome replication (Chiang *et al.*, 1992); E2 acts also as the main regulator of the viral gene transcription (McBride *et al.*, 1991; Demeret *et al.*, 1997). The E4 protein facilitates the virus assembly and release (Roberts *et al.*, 1994), whereas the E5 protein functions as an activator of unscheduled proliferation of HPV-infected cells (Fehrmann *et al.*, 2003). The E6 and E7 proteins cooperate, each with a separate role, to alter the activity of several cell cycle regulators in order to create an environment favorable for viral replication (reviewed in zur Hausen, 2000 and Munger *et al.*, 2004). In addition to significant alterations of cell cycle regulation and apoptosis, expression of these two viral proteins induces phenotypic changes in host cells such as abnormal centrosome number, aberrant mitotic spindle pole formation, and genomic instability (Duensing *et al.*, 2000; Duensing & Munger, 2004).

The L region encodes major (L1) and minor (L2) structural proteins that assemble pentameric capsomers forming icosahedral capsid around the viral genome (Modis *et al.*, 2002; Finnen *et al.*, 2003).

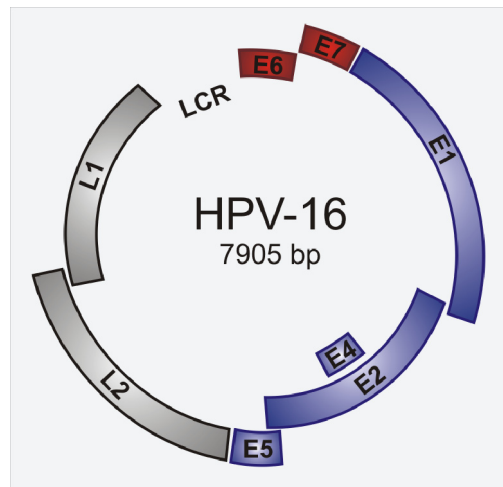


**Figure 7.** Schematic representation of the HPV-16 DNA genome. The HPV genome comprises eight ORFs encoding so-called early proteins, *i.e.* E1, E2 and E4 to E7 as well as late proteins, *i.e.* L1 and L2. The long control region (LCR) is a non-coding region that contains the origin of viral replication, binding sites for the viral-coded E1 and E2 proteins as well as multiple transcriptional-regulatory motifs (Lewis *et al.*, 1999). Modified from Munger *et al.*, 2004.

### 1.5.3 Viral life cycle

A characteristic feature of the papillomavirus life cycle is that it entirely relies on host enzymes and nucleotide pool for viral replication, except for virus-encoded E1 and E2 proteins, which are necessary for modulation of the viral DNA replication and the regulation of transcription of early genes (Munger *et al.*, 2004; Zheng & Baker, 2006).

The HPV infects exclusively keratinocytes in the proliferating basal layer of stratified squamous epithelia, presumably at the sites of injury (zur Hausen, 2000). Following virus entry, the HPV genome is established in the nucleus of host cells as low copy number episomes that replicate in the synchrony with cellular DNA replication (Thomas *et al.*, 1999). During this stage of the viral life cycle, the early viral proteins facilitate stable maintenance of episomes and contribute to the enhanced proliferation and expansion of HPV-infected cells within the epithelium (zur Hausen, 2002; Fehrmann & Laimins, 2003). As the epithelial cells undergo their normal life cycle, some daughter cells become detached from the basal layer, progress upward in epidermis, exit the cell cycle and undergo terminal differentiation (Fuchs, 1993). In contrast, the HPV-infected cells, when reaching the suprabasal layer of the epithelium, undergo differentiation but remain active in the cell cycle (Cheng *et al.*, 1995; Spitkovsky *et al.*, 1996; Fehrmann & Laimins, 2003). In these terminally differentiated cells

the productive stage of the HPV life cycle occurs, *i.e.* the viral genome is amplified to a high copy number, capsid proteins L1 and L2 are synthesized and the progeny virions are assembled and subsequently released (Stubenrauch & Laimins, 1999; Longworth & Laimins, 2004). As carcinogenesis progresses, the HPV genome frequently integrates into the human genome (el Awady *et al.*, 1987). Following genome integration, the expression of viral E6 and E7 genes is consistently maintained, whereas other portions of the viral DNA are often deleted or their expression is disturbed (Romanczuk & Howley, 1992).

#### 1.5.4 Human papillomavirus E7 protein

##### 1.5.4.1 Biological activities and cellular targets of the E7 protein

The human papillomavirus E7 protein has multiple activities that contribute to cellular transformation and are important during the viral life cycle (reviewed in McLaughlin-Drubin & Munger, 2009; Tab. 2).

**Table 2.** Cellular targets of the E7 protein.

Cellular target	Reference
Retinoblastoma tumor suppressor protein (pRb)	(Dyson <i>et al.</i> , 1989; Munger <i>et al.</i> , 1989)
pRb-related pocket proteins p107 and p130	(Dyson <i>et al.</i> , 1992; Collins <i>et al.</i> , 2005)
Cyclin A/CDK2 and cyclin E/CDK2 complexes	(He <i>et al.</i> , 2003; Nguyen & Munger, 2008)
Cyclin-dependent kinase inhibitor p21	(Helt <i>et al.</i> , 2002)
Cyclin-dependent kinase inhibitor p27	(Zerfass-Thome <i>et al.</i> , 1996)
AP-1 family of transcription factors	(Antinore <i>et al.</i> , 1996; Nead <i>et al.</i> , 1998)
Transcriptional coactivator p300	(Bernat <i>et al.</i> , 2003)
FHL2 transcriptional coactivator	(Campo-Fernandez <i>et al.</i> , 2007)
pCAF acetyltransferase	(Avvakumov <i>et al.</i> , 2003)
TATA-binding protein (TBP)	(Phillips & Vousden, 1997)
Pyruvate kinase type M2	(Zwerschke <i>et al.</i> , 1999)
Mi2 $\beta$ (histone deacetylase complex)	(Brehm <i>et al.</i> , 1999)
S4 subunit of the 26 S proteasome	(Berezutskaya & Bagchi, 1997)
Human DnaJ protein (hTid-1)	(Schilling <i>et al.</i> , 1998)
p48	(Barnard & McMillan, 1999)
Interferon regulatory factor (IRF)-1	(Park <i>et al.</i> , 2000)
Ski interacting protein (Skip)	(Prathapam <i>et al.</i> , 2001)
M phase phosphoprotein 2 (MPP2)	(Luscher-Firzlaff <i>et al.</i> , 1999)
Insulin-like growth factor binding protein 3 (IGFBP-3)	(Mannhardt <i>et al.</i> , 2000)
$\alpha$ -glucosidase	(Zwerschke <i>et al.</i> , 2000)
TBP-associated factor 110 (TAFII110)	(Mazzarelli <i>et al.</i> , 1995)
$\gamma$ -tubulin	(Nguyen <i>et al.</i> , 2007)
F-actin	(Rey <i>et al.</i> , 2000)
Retinoblastoma protein-associated factor p600	(Huh <i>et al.</i> , 2005)
E2F6 transcription factor	(McLaughlin-Drubin <i>et al.</i> , 2008)
Nuclear mitotic apparatus protein 1 (NuMA)	(Nguyen & Munger, 2009)

The most recognized function of E7 is its ability to bind and alter the biological activity of the retinoblastoma tumor suppressor protein (pRb) (Dyson *et al.*, 1989; Munger *et al.*, 1989). The pRb protein represents a structurally and functionally related family of proteins known as retinoblastoma protein family or pocket protein family, which includes also other members, *i.e.* p107 and p130 (Cobrinik, 2005). These proteins control the transition from the G<sub>1</sub> to the S phase of the cell cycle, cellular differentiation and apoptosis. Their deregulation through various mechanisms such as gene alteration or functional inactivation has been described in the majority of human cancers (Malumbres & Barbacid, 2001).

The pRb protein exerts its growth-suppressive effect through the ability to regulate the activity of E2F transcription factors (reviewed in Nevins *et al.*, 1997). Under normal conditions, the formation of pRb/E2F complexes actively represses the transcriptional activities of E2F thereby restricting the S phase entry (Fig. 8A). The phosphorylation of pRb at the late G<sub>1</sub> phase catalyzed by cyclin-dependent kinases (CDKs) disrupts the pRb/E2F complexes and results in the activation of transcription of genes required for DNA synthesis and S phase entry (Fig. 8B; Frolov & Dyson, 2004).

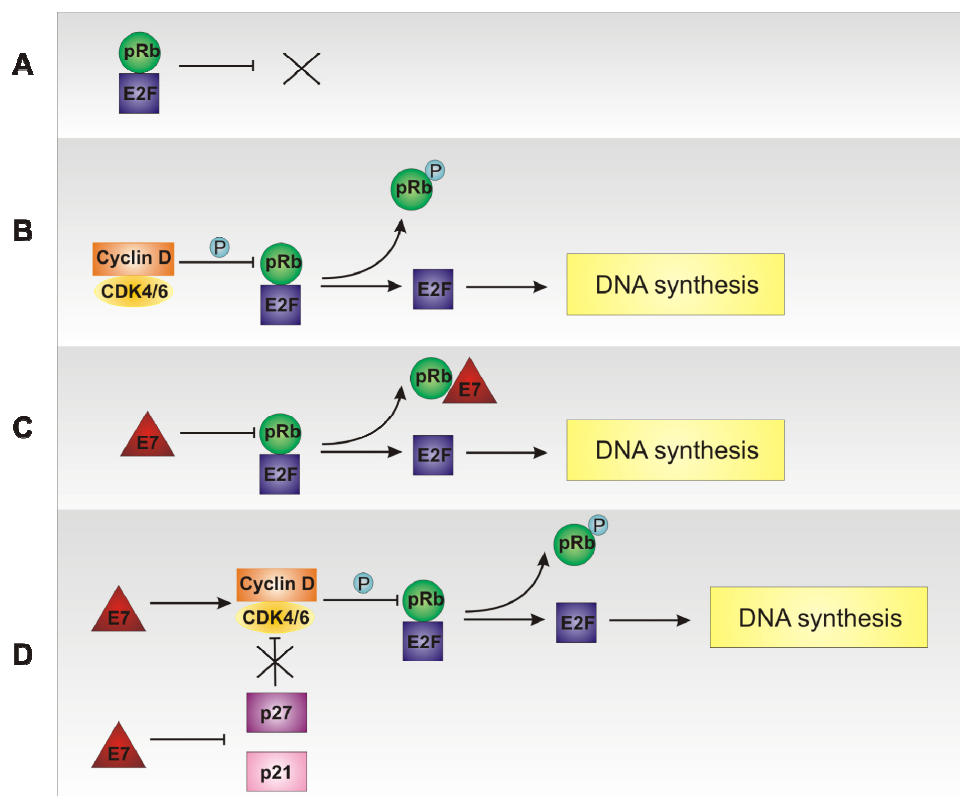


**Figure 8.** The E7 protein encodes the main transforming activity of the human papillomavirus and regulates various components of the cell cycle. See text for details.

In HPV-infected cells, the binding of E7 to pRb results in the misregulated release of E2F transcription factors and inappropriate cell cycle progression (Fig. 8C; Munger *et al.*, 2001). Following destabilization of pRb/E2F complexes, the pRb protein is degraded



As shown by structure analysis, the CR3 domain of E7 assembles a roughly globular and obligate dimer, which contains two zinc atoms, each coordinated by four Cys residues of a subunit (Fig. 10). The monomer exhibits a flattened shape with a  $\beta 1\beta 2\alpha 1\beta 3\alpha 2$  topology (Liu *et al.*, 2006; Ohlenschlager *et al.*, 2006). The formation of an intermolecular two-stranded antiparallel  $\beta$ -sheet between  $\beta 2$  and  $\beta 3$  strands of opposing subunits as well as the interaction between the  $\alpha 1$  helices of each subunit are responsible for the dimer formation (Ohlenschlager *et al.*, 2006).

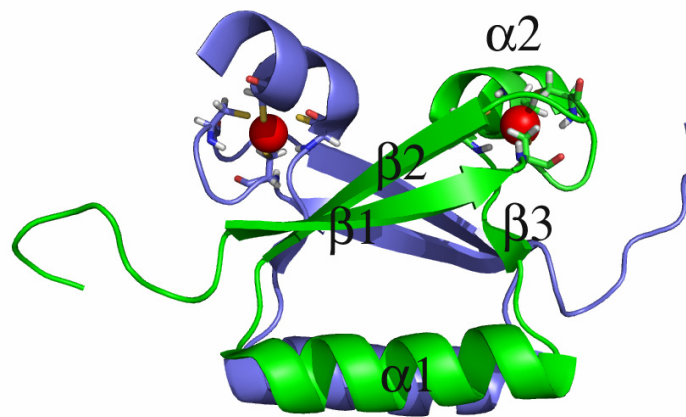


**Figure 10.** Schematic structure of the HPV-45 E7 CR3 homodimer (amino acids 55 - 106, PDB code 2F8B). The protomers of the dimer are colored in blue and green; bound zinc atoms are displayed as red balls and their Cys ligands in a stick mode. Each subunit of the E7 CR3 dimer is composed of two  $\beta$ -strands ( $\beta 1$  and  $\beta 2$ ) forming an antiparallel twisted  $\beta$ -sheet followed by  $\alpha$ -helix 1 ( $\alpha 1$ ),  $\beta$ -sheet 3 ( $\beta 3$ ) and another  $\alpha$ -helix ( $\alpha 2$ ). The interaction between  $\beta 2$  and  $\beta 3$  strands of opposing subunits as well as the interaction of  $\alpha 1$  helices of each subunit contribute to the dimer formation. The N-terminal CR1 and CR2 domains of E7 are unstructured and flexible in solution (Ohlenschlager *et al.*, 2006). The figure was generated using PyMOL (<http://pymol.org>).

Despite of numerous studies demonstrating dimerization as well as oligomerization of E7 (Chinami *et al.*, 1994; Clemens *et al.*, 1995), there is no compelling evidence that the protein exists as a dimer and/or oligomer *in vivo* (McLaughlin-Drubin & Munger, 2009).

Although the E7 sequence does not possess a classical basic nuclear localization signal, the E7 protein has been observed to localize predominantly within the nucleus of cervical cancer cells (Greenfield *et al.*, 1991; Guccione *et al.*, 2002) but also of recombinant mammalian and yeast cells (Sato *et al.*, 1989; Tommasino *et al.*, 1990). This observation is supported by multiple nuclear functions of E7 such as association with the members of the pRb family, transactivation of E2F-regulated genes and interaction with a large number of nuclear factors, such as the AP-1 family of transcription factors (Antinore *et al.*, 1996) or the TATA-binding protein (Phillips & Vousden, 1997). In addition, some reports have

shown that E7 can be detected in the cytoplasm of eukaryotic cells as its interactions with F-actin (Rey *et al.*, 2000), M2 pyruvate kinase (Zwerschke *et al.*, 1999) or  $\alpha$ -glucosidase (Zwerschke *et al.*, 2000) could be observed.

## 1.6 Options for delivery of therapeutic proteins into mammalian cells

An efficient technique for delivery of biologically active proteins across the cell membrane would have potential implications for studies on cellular processes, as well as for the development of new protein-based drug entities. Thus, over the past two decades several methods have been tested for their utility for protein transduction. The techniques initially used for this purpose include microinjection (Rui *et al.*, 2002; Theiss & Meller, 2002), electroporation (Nolkrantz *et al.*, 2002; Eksioglu-Demiralp *et al.*, 2003) and cationic lipids (Zelphati *et al.*, 2001; van der Gun *et al.*, 2007). These methods, however, yielded low transduction efficiencies and caused significant cellular toxicity.

A promising approach to overcome these limitations has emerged with the observation that certain proteins translocate spontaneously through the plasma membrane when incubated exogenously with cells (Frankel & Pabo, 1988; Green & Loewenstein, 1988; Joliot *et al.*, 1991). Subsequently, several highly basic sequences named cell-penetrating peptides (CPPs) or protein transduction domains (PTDs) responsible for this property have been identified (reviewed in Gupta *et al.*, 2005; Vives *et al.*, 2008). Well known examples of CPPs include the penetratin peptide derived from the Antennapedia homeodomain protein of *Drosophila* (Derossi *et al.*, 1994), the Tat peptide originated from the human immunodeficiency virus 1 (HIV-1) transactivator of transcription (Tat) protein (Vives *et al.*, 1997) and the structural protein VP22 of Herpes simplex virus type 1 (HSV-1) (Elliott & O'Hare, 1997).

One of the most extensively studied CPPs is the Tat peptide (reviewed in Brooks *et al.*, 2005). The fragment GRKKRRQRRRPPQ comprising amino acids 49 - 57 of the Tat protein has been identified as a minimal domain sufficient for membrane translocation (Park *et al.*, 2002). This cluster of basic amino acid residues corresponds also to the presumed nuclear localization signal (NLS) of Tat (Ruben *et al.*, 1989; Vives *et al.*, 1997).

The Tat peptide has been shown to mediate transduction of a large variety of chemically or genetically linked cargoes with no apparent size restriction to this process. Some examples of entities efficiently delivered by the Tat peptide include antisense oligonucleotides (Astrib-Fisher *et al.*, 2000), siRNA (Meade & Dowdy, 2007), DNA (Ignatovich *et al.*, 2003; Rudolph *et al.*, 2003), proteins (Peitz *et al.*, 2002; Wadia & Dowdy, 2005), liposomes (Torchilin *et al.*, 2003), radioactive metal complexes (Polyakov *et al.*, 2000) and magnetic nanoparticles (Lewin *et al.*, 2000).

In contrast to previously used techniques, the Tat-mediated protein transduction has been shown to achieve 100% efficiency in a variety of cells with no apparent cellular toxicity (Barka *et al.*, 2000; Wadia & Dowdy, 2005). Within the cell, transduced entities have been localized to the cytoplasm and/or nucleus (reviewed in Gupta *et al.*, 2005; Brooks *et al.*, 2005; Wadia & Dowdy, 2005).

Despite of numerous studies demonstrating the efficient delivery of various molecules into cells, the Tat-mediated transduction has become an object of considerable controversy in the literature. The initial reports on the uptake mechanism of Tat provided an evidence for the direct penetration across the cell membrane (Vives *et al.*, 1997; Futaki *et al.*, 2001). The transduction was shown to be effective at both 37°C and 4°C also in the presence of metabolic inhibitors, indicating an energy-independent fashion of the uptake (Futaki *et al.*, 2001; Torchilin *et al.*, 2001). Later it was found that, following initial ionic cell-surface interaction, the Tat peptide is internalized through endocytosis although different endocytic pathways have been proposed, *i.e.* caveolar endocytosis (Ferrari *et al.*, 2003; Fittipaldi *et al.*, 2003), clathrin-mediated endocytosis (Vendeville *et al.*, 2004; Richard *et al.*, 2005) and macropinocytosis (Nakase *et al.*, 2004; Kaplan *et al.*, 2005). The possibility of simultaneous employment of multiple endocytic pathways has also been suggested (Duchardt *et al.*, 2007; Nakase *et al.*, 2008). In addition to the endocytosis-mediated uptake, the spontaneous translocation of the Tat peptide across the lipid membrane through transient pores has also been described (Herce & Garcia, 2007).

The controversies regarding the Tat entry have also been associated with overestimation of the uptake resulting from the inability of experimental procedures to discriminate between membrane-associated and internalized cargos (reviewed in Brooks *et al.*, 2005). Even though, several studies have demonstrated specific biological activities of Tat-conjugated proteins suggesting a functional delivery of intact Tat-constructs into the cytoplasm and/or nucleus. The examples to illustrate this aspect are observations of induction of apoptosis following Tat-mediated uptake of the HIV protease-activated caspase-3 into HIV-positive cells (Vocero-Akbani *et al.*, 1999), antitumor effect of the adaptor protein phospholipase C- $\gamma$ 1 inhibitor fused to the Tat peptide in breast cancer cells (Katterle *et al.*, 2004), inhibition of adversely activated cell apoptosis by the caspase-8 inhibitor FLIP-Tat protein (Krautwald *et al.*, 2004) or stimulation of osteoblast differentiation by calcineurin A $\alpha$  protein fused to Tat (Dolgilevich *et al.*, 2002). Moreover, the Tat peptide has been shown to deliver functional proteins *in vivo*. In a study conducted in mice, intraperitoneal injection of the  $\beta$ -galactosidase-Tat fusion protein resulted in its internalization into various organs, including brain (Schwarze *et al.*, 1999).

## 1.7 Aim of the study

Affilin molecules represent a novel class of alternative binding proteins, which exploit side chains of the rigid  $\beta$ -sheet structure of the human  $\gamma$ B-crystallin for molecular recognition. As the intrinsic stability of the  $\gamma$ B-crystallin does not rely on the presence of disulfide bonds, this scaffold was considered as an optimal candidate for the generation of intracellular binding reagents. Thus, the main purpose of this study was to evaluate the applicability of the  $\gamma$ B-crystallin scaffold for intracellular use. As a model intracellular target, the human papillomavirus E7 protein implicated in the development of cervical cancer was chosen.

In more detail, the specific aims of this thesis were:

1. Preparation of the HPV-16 E7 protein from recombinant *E. coli* cells as a prerequisite for the phage display selection of anti-E7 Affilin molecules.
2. Phage display selection of anti-E7 Affilin molecules from a  $\gamma$ B-crystallin library, preparation and characterization of anti-E7 clones.
3. Investigation of the feasibility of the Tat peptide derived from the HIV-1 Tat protein for intracellular delivery of Affilin molecules.
4. Validation of efficacy and specificity of anti-E7 Affilin molecules in a cellular model by examination of the effect of their transient expression on the proliferation and apoptosis of target cells.

## 2. Materials and Methods

### 2.1 Materials

#### 2.1.1 Bacterial strains

<i>E. coli</i> strain	Genotype	Source
XL1-Blue	<i>recA1, endA1, gyrA96, thi-1, hsdR17, supE44, relA1, lac</i> [F' <i>proAB, lacIqZM15, Tn10, (Tet<sup>r</sup>)</i> ]	Stratagene, La Jolla, USA
NovaBlue(DE3)	<i>endA1, hsdR17, r<sub>K12</sub><sup>-</sup>m<sub>K12</sub><sup>+</sup>, supE44, thi-1, recA1, gyrA96, relA1, lac</i> [F' <i>proAB, lacIqZM15, Tn10 (Tet<sup>r</sup>)</i> ] (DE3- $\lambda$ clst857, <i>ind1, Sam7, nin5, lacUV5-T7</i> gene 1)	Novagen, Darmstadt, Germany
BL21(DE3)	B, F <sup>-</sup> , <i>ompT, gal, [dcm], [lon], hsdSB(rB-mB<sup>-</sup>), gal<math>\lambda</math>(DE3)</i>	Stratagene, La Jolla, USA
BL21-CodonPlus (DE3)-RIL	B, F <sup>-</sup> , <i>ompT, hsdS(r<sub>B</sub><sup>-</sup> m<sub>B</sub><sup>-</sup>), dcm<sup>+</sup>, Tet<sup>r</sup> gal<math>\lambda</math>(DE3), endA, Hte [argU, ileY, leuW, Cam<sup>r</sup>]</i>	Stratagene, La Jolla, USA
BL21(DE3)pLysS	B, F <sup>-</sup> , <i>dcm, ompT, hsdS(r<sub>B</sub><sup>-</sup> m<sub>B</sub><sup>-</sup>), gal<math>\lambda</math>(DE3), [pLysS Cam<sup>r</sup>]</i>	Stratagene, La Jolla, USA

#### 2.1.2 Eukaryotic cells

Cell line	Description	Source
NIH/3T3	Mouse Swiss NIH embryo cell line established from a NIH Swiss mouse embryo, adherent	LGC Standards, Wesel, Germany; ATCC No. CRL-1658
NIH/3T3-E7	Derivative of the NIH/3T3 cell line, constitutively expresses the HPV-16 E7 protein (Edmonds & Vousden, 1989), adherent	W. Zwerschke, the Medical University Innsbruck, Innsbruck, Austria
Ca Ski	Human cervical epidermoid carcinoma, contains an integrated human papillomavirus type 16 genome (HPV-16) in about 600 copies per cell as well as sequences related to HPV-18, adherent	European Collection of Cell Cultures, Wiltshire, UK, ECACC No. 87020501
C-33 A	Human cervical carcinoma, negative for human papillomavirus DNA and RNA, adherent	LGC Standards, Wesel, Germany; ATCC No. HTB-31
HEK-293	Human kidney cell line transformed with adenovirus 5, constitutively expresses the E1A protein (Graham <i>et al.</i> , 1977), adherent	LGC Standards, Wesel, Germany; ATCC No. CRL-1573

#### 2.1.3 Phage

Phage	Characteristics	Source
M13KO7 Helper Phage	M13 derivative which carries Met40Ile mutation in the gene II, the origin of replication from p15A and the kanamycin resistance gene from Tn903 (Vieira & Messing, 1987)	Invitrogen, Karlsruhe, Germany

## 2.1.4 Vectors

Vector	Use/Characteristics	Origin/Reference
pGEM-T Vector System I	Cloning of PCR products	Promega, Mannheim, Germany
pCANTAB-CR20	pCANTAB 5 E phagemid vector harboring a human $\gamma$ B-crystallin library, used for phage display selection of Affilin molecules	Scil Proteins GmbH (Fiedler & Rudolph, 2001)
pET-20b(+)	Bacterial expression vector containing a C-terminal His <sub>6</sub> -tag	Novagen, Darmstadt, Germany
pcDNA3.1-E7	pcDNA3.1-based vector encoding the HPV-16 E7 protein (Chen <i>et al.</i> , 2000). Used for PCR amplification of the E7 gene	Paterson, Y., University of Pennsylvania School of Medicine, Philadelphia, USA
pET20-E7	pET-20b(+) derivative encoding HPV-16 E7 protein	This study
pET20-E7opt	pET-20b(+) derivative containing optimized HPV-16 E7 sequence	This study
pEGFP-N1	Mammalian expression vector encoding the red-shifted variant of GFP, used for PCR amplification of the EGFP gene	Clontech-Takara Bio Europe, Saint-Germain-en-Laye, France
pET20-EGFP	pET-20b(+) derivative encoding EGFP	This study
pET20-D1 pET20-D4 pET20-E9* pET20-GBC	Constructs based on the modified pET-20b(+) vector in which the <i>Nde</i> I restriction site was mutated to <i>Nco</i> I. They encode Affilin variants or $\gamma$ B-crystallin (GBC) C-terminally fused to the His <sub>6</sub> -tag	This study, except for the modification of the pET-20b(+) vector which was performed by H. Ebersbach, Scil Proteins GmbH
pET20-D1(Ser2,4)	pET20-D1-based construct containing Affilin D1 with Cys2,4 to Ser2,4 mutations	This study
pET20-nTat-A1*-EGFP	pET-20b(+) vector encoding the N-terminal Tat peptide followed by Affilin SPC-1-A1, EGFP and His <sub>6</sub> -tag	This study; A1* corresponds to SPC-1-A1 (Ebersbach <i>et al.</i> , 2007)
pET20-KpnHind	Modified pET-20b(+) vector with <i>Kpn</i> I and <i>Hind</i> III restriction sites downstream of the His <sub>6</sub> -tag	This study
pET20-cTat	pET20-KpnHind vector containing Tat peptide sequence cloned into <i>Kpn</i> I and <i>Hind</i> III restriction sites	This study
pET20-D1-cTat pET20-D4-cTat pET20-E9*-cTat pET20T-GBC-cTat	Constructs based on pET20-cTat encoding Affilin molecules or $\gamma$ B-crystallin (GBC) followed by the C-terminal His <sub>6</sub> -tag and Tat peptide	This study; E9* corresponds to SPC-7-E9 (Ebersbach <i>et al.</i> , 2007)
pCMV/myc/nuc	Mammalian expression vector containing a C-terminal nuclear localization signal from the SV40 large T antigen and a c-myc epitope tag	Invitrogen, Karlsruhe, Germany
pCMV-D1 pCMV-D4 pCMV-GBC	pCMV/myc/nuc vectors encoding Affilin D1, D4 or $\gamma$ B-crystallin (GBC)	This study

### 2.1.5 Oligonucleotides

The DNA oligonucleotides were supplied from MWG-Biotech (Ebersberg, Germany). Sequencing primers were labeled at the 5' end with infrared dyes (IRDye 700 or IRDye 800).

Oligonucleotide	Sequence (5' → 3')	Use
<i>Tat-1</i>	GATCCATATGGGCCGCAAAAACG CCGCCAGCGCCGC	Annealing of both oligonucleotides encoding Tat peptide prior to insertion into the pET20-nTat-A1*-EGFP construct
<i>Tat-2</i>	GGATCCATGGCTGCGGCCGGCG CGGCGCTGGCGGCG	
<i>Tat-3</i>	CGGGTACCGGCCGCAAAAACG CGCCAGCGCCGC	Annealing of both oligonucleotides encoding Tat peptide prior to insertion into the pET20-cTat construct
<i>Tat-4</i>	GGCGCAAGCTTCTGCGGCCGGCG GCGGCGCTGGCGGCG	
<i>pET-His-mut1</i>	GAGCACCACCACCACCACCG CGGTACCAAGCTTTAAGATCCGGC TGC	Modification of the pET-20b(+) vector by site-directed mutagenesis (see 2.2.1.10)
<i>pET-His-mut2</i>	GCAGCCGGATCTTAAAGCTTGTA CCGCCGTGGTGGTGGTGGTGGT CTC	
<i>T7_promoter</i> <i>T7_terminator</i>	TAATACGACTCACTATAGGG GCTAGTTATTGCTCAGCGG	PCR amplification of genes from pET-20b(+)-based vectors
<i>ggbSfil-fwd</i>	GTTCTTTCTATGCGGCCAGCCG GCCATGGG	PCR amplification, cloning of the $\gamma$ B-crystallin library from pCANTAB-CR20
<i>hgcXhoI-rev</i>	GCTTCTCGAGGTACAAATCCAAT GAC	
<i>D1-Cys/Ser-fwd</i>	GATATACCCATGGGCTCTATCTCTT TCGGTGAAGACCG	PCR amplification, generation of the D1-Ser2,4 mutant
<i>ggbBstEII-rev</i>	CGCAGGAAGTACTGGTGACCCTG GTAGTTCG	
<i>E7-1-fwd</i>	GCATATGCATGGAGATACACCTAC ATTG	PCR amplification of the E7 gene from the pcDNA3.1-E7 vector. Primers <i>E7-1-fwd</i> and <i>E7-2-rev</i> : E7 wild-type; <i>E7-3-fwd</i> and <i>E7-2-rev</i> : optimized E7 gene
<i>E7-2-rev</i>	GCCTCGAGTGTTTCTGAGAACAG ATGG	
<i>E7-3-fwd</i>	GATATACATATGCACGGAGATACA CCAACATTGCATG	
<i>pET_Prom_long</i>	GCGAAATTAATACGACTCACTATA GGGAG	Sequencing of constructs based on the pET-20b(+) vector
<i>pET_Term</i>	GCTAGTTATTGCTCAGCGGTGGC	
<i>pCantab</i>	CCATGATTACGCCAAGCTTTGGAG CC	Sequencing of constructs based on the pCANTAB phagemid

### 2.1.6 Chemicals

All chemicals used in this study were purchased from Carl Roth GmbH & Co (Karlsruhe, Germany), Sigma-Aldrich Chemie (München, Germany) or Calbiochem (Schwalbach, Germany) unless stated otherwise.

### 2.1.7 Enzymes

Enzyme	Purchased from
Taq DNA polymerase	Promega, Mannheim, Germany
Shrimp alkaline phosphatase	
T4-DNA ligase	
Restriction enzymes	
Benzonase nuclease	Merck KGaA, Darmstadt, Germany
Lysozyme from egg white	
Chymotrypsin	Sigma-Aldrich Chemie, München, Germany
0.25% (w/v) Trypsin-EDTA	Invitrogen, Karlsruhe, Germany

### 2.1.8 Proteins

Protein	Source
EGFP-His <sub>6</sub>	This study
BSA	Carl Roth GmbH & Co (Karlsruhe, Germany)
HSA	
Retinoblastoma protein (pRb)	QED Bioscience, San Diego, USA
Immunoglobulin G Fc fragment	R&D Systems, Wiesbaden-Nordenstadt, Germany
Tumor necrosis factor $\alpha$	ProSpec-Tany TechnoGene, Rehovot, Israel
Amyloglucosidase	Sigma-Aldrich Chemie, München, Germany
Trypsin inhibitor	
Ubiquitin	Scil Proteins, Halle, Germany
Melanoma inhibitory activity protein	
Nerve growth factor $\beta$	

### 2.1.9 Antibodies

Antigen	Origin	Conjugate	Use	Purchased from
$\gamma$ B-crystallin	Mouse, clone 98.4.1, MK	-	Western blotting 1:500	Biogenes, Berlin, Germany
$\gamma$ B-crystallin	Mouse, clone 98.4.1, MK	horseradish peroxidase	ELISA 1:1000	
HIV-1 Tat	Mouse	-	Western blotting 1:500	Quattromed HTI Laborid, Tartu, Estonia
HPV-16 E7	Mouse	-	ELISA 1:2000 Western blotting 1:1000	Biodesign International, Saco, USA
BrdU	Rat	-	Immunofluorescence 1:100	Abcam, Cambridge, United Kingdom
mouse IgG	Donkey	Cy3	Immunofluorescence 1:500	Dianova, Hamburg, Germany
rat IgG	Goat	Alexa Fluor 488	Immunofluorescence 1:500	Invitrogen, Karlsruhe, Germany
mouse IgG	Rabbit	horseradish peroxidase	ELISA 1:10 000 Western blotting 1:50 000	Sigma-Aldrich Chemie, München, Germany

### 2.1.10 Kits and standards

Kit or standard	Purchased from
1 kbp and 100 bp DNA ladder	New England Biolabs, Schwalbach, Germany
Pre-stained Protein Marker, Broad Range	
LMW-SDS Marker Kit	Amersham Biosciences Europe, Freiburg, Germany
ECL Western Blotting Detection Reagent	
Gel Filtration Calibration Kits (LMW and HMW)	
Bio-Rad Protein Assay Kit	Bio-Rad Laboratories, München, Germany
TMB Plus Substrate Solution	Kem-En-Tec Diagnostic, Copenhagen, Denmark
Amine Coupling Kit	Biacore International, Uppsala, Sweden
CycleReader Auto DNA Sequencing Kit	Fermentas, St. Leon-Rot, Germany
BugBuster 10x Protein Extraction Reagent	Novagen, Darmstadt, Germany
Quickchange Site-directed Mutagenesis Kit	Stratagene, La Jolla, USA
Ni-NTA Superflow 96 BioRobot Kit	Qiagen, Hilden, Germany
QIAprep Spin Miniprep Kit	
QIAGEN Plasmid Maxi Kit	
Qiaquick Gel Extraction Kit	
MinElute PCR Purification Kit	
QIAquick Nucleotide Removal Kit	
MinElute Reaction Cleanup Kit	
Effectene Transfection Reagent	
Prosep-Remtox	Millipore, Schwalbach, Germany
<i>Limulus</i> amoebocyte lysate test	Associates of Cape Cod, Falmouth, USA
Cell Line Nucleofector Kit R	Amaxa, Köln, Germany
<i>In Situ</i> Cell Death Detection Kit Fluorescein	Roche Diagnostics, Mannheim, Germany

### 2.1.11 Buffers and solutions

#### Chromatography buffers

Immobilized metal-ion affinity chromatography	
NPI-20	50 mM NaH <sub>2</sub> PO <sub>4</sub> , 300 mM NaCl, 20 mM imidazole, pH 8.0
NPI-500	50 mM NaH <sub>2</sub> PO <sub>4</sub> , 300 mM NaCl, 500 mM imidazole, pH 8.0
Anion-exchange chromatography	
Q-1	10 mM HEPES, 50 mM NaCl, 10 µM ZnCl <sub>2</sub> , pH 7.6
Q-2	10 mM HEPES, 1 M NaCl, 10 µM ZnCl <sub>2</sub> , pH 7.6
Cation-exchange chromatography	
SP-1	10 mM HEPES, 50 mM NaCl, pH 7.4
SP-2	10 mM HEPES, 1 M NaCl, pH 7.4
Size-exclusion chromatography	
SE-1	10 mM HEPES, 150 mM NaCl, 10 µM ZnCl <sub>2</sub> , pH 7.6
Analytical size-exclusion chromatography	
ASE-1	100 mM NaH <sub>2</sub> PO <sub>4</sub> , 300 mM NaCl, pH 6.0
Reversed-phase chromatography	
RP-1	water, 0.1% (v/v) trifluoroacetic acid
RP-2	acetonitrile, 0.1% (v/v) trifluoroacetic acid

**Other buffers and solutions**

PBS	8 mM Na <sub>2</sub> HPO <sub>4</sub> , 2 mM KH <sub>2</sub> PO <sub>4</sub> , 2.7 mM KCl, 137 mM NaCl, pH 7.3
PBS-T	PBS, 0.1% (v/v) Tween 20
HBS 2x	50 mM HEPES, 280 mM NaCl, 10 mM KCl, 12 mM glucose, 1.5 mM Na <sub>2</sub> HPO <sub>4</sub> , pH 7.1
TAE	20 mM Tris-HCl, 40 mM acetic acid, 2 mM EDTA, pH 8.5
DNA loading buffer 6x	15% (v/v) Ficoll 400, 30 mM EDTA, 0.06% (w/v) bromophenol blue, 1% (w/v) SDS
TBE	44.5 mM Tris-HCl, 44.5 mM boric acid, 1 mM EDTA, pH 8.3
Annealing buffer 10x	100 mM Tris-HCl, 1 M NaCl, 10 mM EDTA, pH 8.0
Resolving polyacrylamide buffer	3 M Tris-HCl, 0.4% (w/v) SDS, pH 8.0
Stacking polyacrylamide buffer	500 mM Tris-HCl, 0.4% (w/v) SDS, pH 6.8
SDS-PAGE loading buffer 5x	40% (v/v) glycerol, 250 mM Tris-HCl, 0.5% (w/v) SDS, 0.6% (w/v) bromophenol blue, 5% (v/v) 2-mercaptoethanol, pH 8.0
SDS-PAGE electrophoresis buffer	50 mM Tris-HCl, 200 mM glycine, 0.1% (w/v) SDS, pH 8.0
Coomassie staining solution	40% (v/v) ethanol, 10% (v/v) acetic acid, 0.1% (w/v) Coomassie Brilliant Blue R250
Destaining buffer	10% (v/v) ethanol, 10% (v/v) acetic acid
Western blotting transfer buffer	20 mM Tris-HCl, 150 mM glycine, 0.05% (w/v) SDS, 20% (v/v) methanol
Ponceau S solution	0.1% (w/v) Ponceau S, 5% acetic acid
Lysis buffer for mammalian cells	50 mM Tris-HCl, 2% (w/v) SDS, 10% (v/v) glycerol, 1 mM PMSF, pH 6.8
Mowiol mounting medium	4.8 g Mowiol 4-88, 12 g glycerol, 12 ml H <sub>2</sub> O, 24 ml 0.2 M Tris-HCl, pH 8.5
Biacore running buffer	10 mM HEPES, 150 mM NaCl, 3 mM EDTA, 0.005% (v/v) Surfactant P20, pH 7.4

**2.1.12 Media and antibiotics for cultivation of *E. coli***

All reagents for preparation of media for cultivation of *E. coli* were purchased from Becton Dickinson, Heidelberg, Germany, whereas antibiotics were purchased from Sigma-Aldrich Chemie, München, Germany.

<b>Medium</b>	<b>Composition (1 l)</b>
Luria-Bertani (LB)	10 g tryptone, 5 g yeast extract, 5 g NaCl
LB-agar	LB medium, 15 g agar
2x YT	17 g tryptone, 10 g yeast extract, 5 g NaCl
SOC	20 g tryptone, 5 g yeast extract, 0.5 g NaCl, 4 g glucose, 2.5 mM KCl, 10 mM MgSO <sub>4</sub> , 10 mM MgCl <sub>2</sub>
SOBAG (16 x 16 cm)	20 g tryptone, 5 g yeast extract, 0.5 g NaCl, 20 g glucose, 10 mM MgCl <sub>2</sub> , 15 g agar, 100 µg/ml ampicillin
<b>Antibiotics</b>	<b>Final concentration</b>
Ampicillin	100 µg/ml
Kanamycin	50 µg/ml
Tetracycline	12.5 µg/ml
Chloramphenicol	30 µg/ml

### 2.1.13 Media for mammalian cell culture

All components of mammalian culture media were purchased from PAA Laboratories, Cölbe, Germany.

Cell line	Medium
NIH/3T3, NIH/3T3-E7, HEK-293	DMEM with 4.5 g/l glucose, 2 mM L-glutamine, 10% (v/v) fetal bovine serum (FBS), 100 U/ml penicillin, 100 µg/ml streptomycin
Ca Ski, C-33 A	RPMI 1640 medium with 2 mM L-glutamine, 1.0 mM sodium pyruvate, 10% (v/v) FBS, 100 U/ml penicillin, 100 µg/ml streptomycin

### 2.1.14 Chromatography columns

Column	Producer
HiTrap Chelating HP 5 ml HiTrap SP Sepharose HP 5 ml HiTrap Q Sepharose HP 5 ml HiLoad 16/60 Superdex G-75	Amersham Biosciences Europe, Freiburg, Germany
TSK-Gel G2000SWXL	Tosoh Bioscience, Stuttgart, Germany
PLRP-S, 250 x 4.6 mm, 5 µm particle size, 300 Å pore size	Polymer Laboratories, Amherst, USA

### 2.1.15 Laboratory equipment

Equipment	Producer
Ultrasonic homogenizer SONOPULS 2200 equipped with sonotrode MS73	Bandelin Electronic, Berlin, Germany
Sunrise absorbance microplate reader	Tecan, Crailsheim, Germany
Biacore 3000 instrument	Biacore International, Uppsala, Sweden
Li-Cor 4200 DNA sequencer	Li-Cor Bioscience, Bad Homburg, Germany
ÅKTA Explorer system	Amersham Biosciences Europe, Freiburg, Germany
Summit HPLC system	Dionex, Idstein, Germany
Nikon Eclipse F600 microscope	Nikon, Düsseldorf, Germany
Cary 300 UV-Vis spectrophotometer	Varian, Darmstadt, Germany
T3 thermocycler	Biometra, Göttingen, Germany
UVstar 15 UV transilluminator	
Centrifuges Avanti J-20, J-25, J-30i	Beckman Coulter, Krefeld, Germany
ELISA washer Columbus	Tecan Deutschland, Crailsheim, Germany
Mini-Protean 3 electrophoresis apparatus Trans-Blot SD semi-dry transfer cell Gel Doc 2000	Bio-Rad Laboratories, München, Germany
MicroPulser electroporator for micro-organisms	
HERAcell incubator Flowbox HERAsafe	Heraeus, Hanau, Germany
Nucleofector device	Amaxa, Köln, Germany

### 2.1.16 Miscellaneous

Miscellaneous	Purchased from
Dialysis tubing with MWCO 3000	Spectrum-Laboratories, Rancho Dominguez, USA
X-ray film	Roche Diagnostics, Mannheim, Germany
Protran nitrocellulose transfer membrane BA 83	Schleicher and Schuell BioScience, Dassel, Germany
96-well microtiter plate, catalog number 260836	Nunc, Wiesbaden, Germany
96-well flat-bottom block	Qiagen, Hilden, Germany
24-well deep well culture plates	
CM5 sensor chip	Biacore International, Uppsala, Sweden
Electroporation cuvettes 0.1 cm	Bio-Rad Laboratories, München, Germany
Sterile syringe filters Millex, pore size 0.20 or 0.45 µm	Millipore, Schwalbach, Germany
MF-Millipore membrane filter	
Amicon Ultra-15 centrifugal filter device with a MWCO of 5000 Da	

## 2.2 Methods

### 2.2.1 Molecular biology

#### 2.2.1.1 Plasmid DNA preparation

The preparations of plasmid DNA were performed with the QIAprep Spin Miniprep Kit (2.1.10) for *E. coli* XL1-Blue cultures of up to 10 ml and the Plasmid Maxi Kit (2.1.10) for culture volumes of 100 ml according to the manufacturer's instructions.

#### 2.2.1.2 Determination of DNA concentration

The concentration and purity of DNA was determined by measuring the absorbance at 260 and 280 nm in a UV-Vis spectrophotometer. The concentration of DNA ( $c$ ) in µg/ml was calculated using equation:

$$c = A_{260} \times f \times sc \quad (1)$$

with  $A_{260}$ : absorbance at 260 nm,  $f$ : dilution factor and  $sc$ : standard coefficient (for dsDNA  $sc = 50$  µg/ml).

Ratio of readings at 260 nm and 280 nm provided an estimate of purity of DNA. Samples with  $A_{260}/A_{280}$  ratio between 1.8 and 2.0 were regarded as high-quality DNA and used for sequencing and transfection experiments.

#### 2.2.1.3 Polymerase chain reaction

The DNA amplification was carried out using the polymerase chain reaction (PCR) with pairs of specific primers (listed in 2.1.5) and a thermostable *Taq* DNA polymerase.

The reaction mix was prepared accordingly:

Component	Final volume	Final concentration
DNA template	variable	250 ng
<i>Taq</i> DNA polymerase 10x reaction buffer	5 $\mu$ l	1x
MgCl <sub>2</sub> solution, 25 mM	3 $\mu$ l	1.5 mM
dNTP, 10 mM each	1 $\mu$ l	0.2 mM each dNTP
Upstream primer, 10 $\mu$ M	1 $\mu$ l	0.5 $\mu$ M
Downstream primer, 10 $\mu$ M	1 $\mu$ l	0.5 $\mu$ M
<i>Taq</i> DNA polymerase (5 U/ $\mu$ l)	0.25 $\mu$ l	1.25 U
Nuclease-free water	to 50 $\mu$ l	

The PCR program included one denaturation step (95°C, 2 min) and 30 repeated cycles consisting of denaturation (95°C, 30 sec), primer annealing (5°C lower than the melting temperature of primers, 30 sec) and DNA synthesis (72°C, 1 min/1000 bp) followed by a final elongation step (72°C, 7 min). The amplified products were purified by the MinElute PCR Purification Kit or the QIAquick Gel Extraction Kit (2.1.10) following the manufacturer's instructions.

#### 2.2.1.4 DNA digestion

The DNA digestion with restriction endonucleases was carried out under conditions specified by the enzyme provider. For analytical purposes, DNA (0.5  $\mu$ g) was digested with 1 U of an appropriate enzyme for 90 min in a reaction volume of 20  $\mu$ l, whereas the preparative digestion was carried out using 5  $\mu$ g of DNA and 5 U of appropriate enzyme in a reaction volume of 50  $\mu$ l. The DNA fragments were separated by agarose gel electrophoresis (see 2.2.1.7) and purified using the QIAquick Gel Extraction Kit (2.1.10).

#### 2.2.1.5 Generation of double-stranded oligonucleotides

In annealing reaction, 100  $\mu$ M of the top strand and bottom strand oligonucleotides (*i.e.* *Tat-1* and *Tat-2* for the generation of the N-terminal Tat construct and *Tat-3* and *Tat-4* for the generation of the C-terminal Tat construct; see 2.1.5) were incubated in 1x annealing buffer (2.1.11) at 95°C for 10 min with subsequent gradual decreasing of the temperature (5°C/5 min) to 20°C. The annealed oligonucleotides were treated with *Taq* DNA polymerase in the presence of dNTPs and appropriate *Taq* DNA polymerase reaction buffer for 30 min at 72°C. For generation of the N-terminal Tat construct, the product of fill-in was directly cloned into pGEM-T vector and the Tat-coding sequence was cut out using the *Nde*I and *Nco*I restriction enzymes and subcloned into precut pET-20b(+) vector. In case of the C-terminal Tat construct, the product of fill-in was digested with *Kpn*I and *Hind*III restriction enzymes and cloned into precut pET20-KpnHind vector (see 2.1.4 and 2.2.1.10).

### 2.2.1.6 Dephosphorylation of DNA

Shrimp alkaline phosphatase was used to remove the terminal 5'-phosphate groups from the DNA in order to prevent fragments from self-ligating in certain cloning strategies. Dephosphorylation was carried out at 37°C for 1 h in the restriction enzyme digest using 1 U of phosphatase per 1 µg of DNA. The enzyme was inactivated by heating at 65°C for 15 min.

### 2.2.1.7 Agarose gel electrophoresis

The agarose gel electrophoresis was used for analysis and preparation of DNA. The DNA samples mixed with DNA loading buffer (2.1.11) were loaded on the agarose gel containing 0.8 - 2% (w/v) agarose in the TAE buffer (2.1.11). The 1 kb and 100 bp DNA ladders (2.1.10) served as standards. Electrophoresis was run at 8 V/cm with TAE as a running buffer. The gel was stained for 20 min in the ethidium bromide solution (1 µg/ml) and DNA was visualized using a UV transilluminator. For imaging and documentation, the Gel Doc 2000 system equipped with the Quantity One 1-D Analysis Software (Bio-Rad Laboratories, München, Germany) was used.

### 2.2.1.8 DNA gel extraction

The DNA fragments obtained after restriction digestion or PCR were purified by agarose gel electrophoresis (2.2.1.7) followed by a gel extraction using the QIAquick Gel Extraction Kit (2.1.10) according to the manufacturer's instructions.

### 2.2.1.9 DNA ligation

The ligation reaction containing approximately 50 ng of the linear vector DNA, 3:1 (insert/vector) molar ratio of the insert DNA, 1 µl of the ligation buffer and 0.5 U of the T4 DNA ligase in 10 µl reaction volume was incubated overnight at 16°C. The reaction mixture was dialyzed against distilled water on a MF-Millipore membrane filter (2.1.16) for 1 h and subsequently used for transformation into *E. coli* XL1-Blue competent cells (see 2.2.2).

For direct cloning of PCR-amplified DNA fragments, pGEMT vector was used (2.1.4), according to the manufacturer's protocol.

### 2.2.1.10 Site-directed mutagenesis

Modification of the pET-20b(+) vector, in which the restriction sites *KpnI* and *HindIII* were introduced downstream of the His<sub>6</sub>-tag along with the elimination of existing TGA stop codon and introduction of a new TGA codon downstream of the *HindIII* restriction site, was performed using the QuickChange Site-directed Mutagenesis Kit (2.1.10) with primers

*pET-His-mut1* and *pET-His-mut2* (2.1.5) according to the manufacturer's protocol. Following digestion of the non-mutated parental DNA template using the enzyme *DpnI*, the modified vector was transformed into *E. coli* XL1-Blue chemically competent cells and after plasmid isolation, the introduced mutations were confirmed by sequencing (see 2.2.1.11).

#### 2.2.1.11 DNA sequencing

The DNA sequencing was performed according to the dideoxy chain-termination method (Sanger *et al.*, 1977; Sambrook & Russell, 2001) using the CycleReader Auto DNA Sequencing Kit (2.1.10) and IRDye 700- or 800-labeled primers (2.1.5) as described in the manual of the kit provider. The gel electrophoresis was carried out on a Li-Cor DNA sequencer with TBE as a running buffer (2.1.11). The sequences were analyzed using the Li-Cor e-Seq DNA sequencing software (Li-Cor Bioscience, Bad Homburg, Germany).

### 2.2.2 Transformation of *E. coli* cells

#### 2.2.2.1 Chemically competent *E. coli* cells

For preparation of chemically competent *E. coli* cells, 5 ml of the overnight culture obtained from a single colony was inoculated in 500 ml of LB medium (2.1.12). The cells were grown at 37°C with shaking at 220 rpm until the absorbance at 600 nm ( $OD_{600}$ ) reached ~0.5. Following centrifugation (4000 x *g*, 4°C, 10 min), the cell pellet was resuspended in 300 ml of the ice-cold 0.1 M  $CaCl_2$  solution and incubated in an ice-water bath for 1 h. After centrifugation (4000 x *g*, 4°C, 10 min), the cell pellet was resuspended in 15 ml of the ice-cold 0.1 M  $CaCl_2$  solution and 500 µl of dimethylsulfoxide (DMSO) was added. After incubation for 15 min, DMSO was added for a second time and the cells were frozen in 200 µl aliquots at -80°C.

Prior transformation, an aliquot of cells was thawed on ice and incubated for 30 min with ~100 ng of plasmid DNA. After heat shock at 42°C for 90 sec, the cells were placed on ice for 2 min and then transferred to 1 ml of the SOC medium (2.1.12). Following 1 h incubation at 37°C with shaking at 220 rpm, transformed cells were plated on the LB agar plate containing appropriate antibiotics and incubated overnight at 37°C.

#### 2.2.2.2 Electrocompetent *E. coli* cells

For preparation of electrocompetent *E. coli* cells, 4 ml of the overnight culture obtained from a single colony was inoculated in 400 ml of LB medium (2.1.12). The cells were grown at 37°C with shaking at 220 rpm until the  $OD_{600}$  reached ~0.5. The cells were harvested by centrifugation (4000 x *g*, 4°C, 10 min) and subsequently washed in 400, 200 and 40 ml

of the ice-cold 10% (v/v) glycerol. The cell pellet was resuspended in 600  $\mu$ l of 10% (v/v) glycerol and 40  $\mu$ l aliquots were frozen at  $-80^{\circ}\text{C}$ .

For transformation of ligated DNA, an aliquot of cells was thawed on ice and 2  $\mu$ l of the ligation mixture (2.2.1.9) was added. Thereafter, the mixture was transferred to the pre-chilled 0.1 cm electroporation cuvette and an electrical pulse of 25  $\mu$ F capacitance, 1.7 kV and 200  $\Omega$  resistance was applied. The cells were resuspended in 1 ml of the SOC medium (2.1.12) and incubated at  $37^{\circ}\text{C}$  for 1 h with shaking at 220 rpm. The cells were plated on the LB agar plate containing appropriate antibiotics. The plate was incubated overnight at  $37^{\circ}\text{C}$ .

### 2.2.3 Phage display selection of anti-E7 Affilin molecules

#### Phage rescue

To prepare the phage particles that display the library of  $\gamma$ B-crystallin variants, an aliquot of *E. coli* XL1-Blue cells containing the phagemid pCANTAB-CR20 (see 2.1.4 and 3.2) was inoculated in 1 l of 2x YT medium supplemented with 2% (w/v) glucose and ampicillin. The cells were grown at  $37^{\circ}\text{C}$  with shaking at 220 rpm. When the  $\text{OD}_{600}$  of culture reached  $\sim 0.4$ , the cells were infected with the M13KO7 helper phage at a phage to cell ratio of 20:1. Following incubation of cells for 1 h with gentle shaking at 50 rpm, the cell suspension was centrifuged at 1000  $\times g$  for 10 min. To produce phage particles, infected cells were resuspended in a glucose-deficient 2x YT medium containing ampicillin, kanamycin and 8 mM reduced glutathione and grown overnight at  $28^{\circ}\text{C}$  with shaking at 220 rpm. The cell suspension was then centrifuged (15 000  $\times g$ , 30 min,  $4^{\circ}\text{C}$ ) and supernatant was filtered through a syringe filter with a 0.45  $\mu\text{m}$  pore size. The phage particles were precipitated from the supernatant by adding 200 ml of PEG/NaCl solution (20% (w/v) of polyethyleneglycol (PEG 6000), 2.5 M NaCl) and incubation on ice for 1 h. Following centrifugation (15 000  $\times g$ , 30 min,  $4^{\circ}\text{C}$ ), the phage pellet was resuspended in 2 ml of PBS.

The infectivity titer of the phage stock was determined by colony count. For this purpose, the serial dilutions of the phage stock were prepared and used for infection of log-phase *E. coli* XL1-Blue cells. Following incubation at  $37^{\circ}\text{C}$  for 30 min, the infected cells were plated onto the LB agar plates with ampicillin and incubated overnight at  $37^{\circ}\text{C}$ . The plates having approximately 100 - 500 colonies were selected for colony counting. The number of colonies multiplied by the reciprocal of the dilution factor for the selected plate provided the phage titer in colony forming units (cfu) per ml.

#### Biopanning

Prior to selection, the phage library stock was incubated with 2 ml of 6% (w/v) BSA in PBS for 30 min at RT. Thereafter, the phages were added into 12 wells of the 96-well microtiter

plate (100  $\mu$ l/well) immobilized with the E7 target protein and incubated for 1 h at RT with gentle rocking. The E7 immobilization was carried out beforehand by incubation of the E7 protein solution (10  $\mu$ g/ml, 100  $\mu$ l/well, overnight, 4°C), blocking of the plate with 3% (w/v) BSA in PBS (300  $\mu$ l/well) for 2 h at 37°C and washing with PBS.

In order to remove unbound phage, the plate was washed according to washing conditions listed in Tab. 3. Phage particles that remained bound were eluted by 100 mM triethylamine, pH 10.0 (100  $\mu$ l/well, 10 min, RT). The eluted phages were collected and pH of solution was neutralized with 0.8 ml of 1M Tris-HCl, pH 7.4. Subsequently, the phage particles were used for infection of *E. coli* XL1-Blue cells (20 ml, OD<sub>600</sub> ~0.4). The culture was incubated for 30 min at 37°C with shaking at 50 rpm.

The plate after elution with triethylamine was washed with PBS and *E. coli* XL1-Blue cells (100  $\mu$ l/well, OD<sub>600</sub> ~0.4) were added to the wells in order to rescue retained phages. The plate was incubated for 30 min at 37°C with gentle rocking. Infected *E. coli* cells were collected from the plate and combined with bacteria obtained from infection with triethylamine-eluted phage. The cells were pelleted by centrifugation (4500 x *g*, 15 min), resuspended in 1 ml of 2x YT medium and plated on SOBAG plates. Following incubation of plates overnight at 37°C, the cells were scraped using 10 ml of 2x YT medium and frozen at -80°C in 20% (v/v) glycerol. The bacterial stocks were then used for further selection rounds by repeating the steps of the phage rescue and biopanning with increased stringency of washing conditions with every selection round (washing conditions presented in Tab. 3).

**Table 3.** Washing conditions in conventional phage display selection.

Round	Washing conditions
1	3x PBS, 3x PBS-T
2	5x PBS, 5x PBS-T, 3x 3% (w/v) BSA in PBS (5 min), 1x PBS
3	8x PBS, 8x PBS-T, 3x 3% (w/v) BSA in PBS (5 min), 2x 6% (w/v) skimmed milk in PBS (5 min), 1x EGFP-His <sub>6</sub> (60 $\mu$ g/ml) in PBS (5 min), 1x PBS
4	10x PBS, 10x PBS-T, 4x 3% (w/v) BSA in PBS (5 min), 4x 6% (w/v) skimmed milk in PBS (5 min), 1x EGFP-His <sub>6</sub> (60 $\mu$ g/ml) in PBS (5 min), 1x E7 in PBS (10 $\mu$ g/ml) (1 min), 1x PBS

The number of input phages for each selection round as well as the output of biopanning were determined by colony count and are presented in Tab. 5 (section 3.2.1.1).

### Selection by phage display with proteolysis

In proteolysis-based phage display approach, the pool of phagemids obtained from the first round of conventional selection was used as an input. Following preparation of the phage library stock by PEG/NaCl precipitation, the phage particles were incubated with the chymotrypsin enzyme (10 U/ml) in 50 mM Tris-HCl buffer, pH 7.4 containing

100 mM NaCl and 2 mM CaCl<sub>2</sub> for 10 min at RT. The chymotrypsin stock (400 U/ml) was prepared immediately before use in cold 1 mM HCl. After incubation, the enzyme was inhibited by addition of phenylmethanesulfonylfluorid (PMSF) to the final concentration of 1 mM. The phages were incubated with 6% (w/v) BSA in PBS for 30 min at RT and subjected to the biopanning as described previously. The washing of unbound phages was carried out as described in Tab. 4. The phage infectivity after chymotrypsin treatment was monitored by colony count. The number of phages used in each selection round as well as the output of biopanning are presented in Tab. 8 (section 3.2.2.1).

**Table 4.** Washing conditions in proteolysis-based phage display selection.

Round	Washing conditions
1	3x PBS, 3 x PBS-T, 3x 3% (w/v) BSA (5 min), 1x PBS
2	5x PBS, 5x PBS-T, 2x 3% (w/v) BSA in PBS (5 min), 1x 6% (w/v) skimmed milk in PBS (5 min), 2x EGFP-His <sub>6</sub> (60 µg/ml) in PBS (5 min), 1x PBS

### Analysis of individual clones

For analysis of individual clones, the DNA pool encoding E7-enriched clones after indicated selection round was subcloned from the phagemid pCANTAB-CR20 into pET-20b(+) vector using primers *ggbSfil-fwd* and *hgcXhol-rev* (2.1.5). In each case, 96 individual clones were picked and the proteins were expressed using *E. coli* NovaBlue(DE3) cells in 24-well format. For preparation of overnight cultures, single colonies were inoculated in 1 ml of 2x YT medium containing ampicillin in the 96-well flat-bottom blocks and incubated overnight at 37°C with shaking at 220 rpm. The overnight cultures (100 µl/well) were inoculated in 4 ml of 2x YT medium in the 24-well deep well culture plates and incubated at 37°C with shaking at 220 rpm until OD<sub>600</sub> reached 0.5 - 0.8. The protein expression was induced with isopropyl β-D-1-thiogalactopyranoside (IPTG) at a final concentration of 1 mM and the cultures were grown overnight at 28°C. The cells were harvested by centrifugation (5 min, 1500 x g) and lysed using BugBuster 10x Protein Extraction Reagent according to the manufacturer's recommendations. Protein purification under native conditions from crude cell lysates was carried out using the Ni-NTA Superflow 96 BioRobot Kit (2.1.10) on the vacuum manifold as described in the manual of the kit provider.

The protein samples were analyzed by reducing SDS-polyacrylamide gel electrophoresis (SDS-PAGE) (see 2.2.6.2). The purified proteins were also screened for E7 binding by enzyme-linked immunosorbent assay (ELISA) in a 96-well format (see 2.2.6.4). The DNA sequences of positive clones were verified as described in 2.2.1.11.

## 2.2.4 Protein expression using recombinant *E. coli*

### Small-scale protein expression

Small-scale expression trials were performed to identify the optimal conditions for soluble and high-level expression of each recombinant protein. For this purpose, various *E. coli* expression strains (2.1.1) were transformed with corresponding plasmids (2.1.4) and overnight cultures were prepared from a single transformed colony. Next day, the cultures were diluted 1:50 in 20 ml of medium (LB or 2x YT) containing appropriate antibiotics. The cultures were grown at 37°C with shaking at 220 rpm until OD<sub>600</sub> values from 0.6 to 1.4 were reached. The protein expression was induced with IPTG at a final concentration ranging from 0.1 to 1 mM. The cultures were further grown at temperatures from 25°C to 37°C for 1 to 16 h. The cells were harvested by centrifugation (5 min, 1500 x *g*) and suspended in BugBuster 10x Protein Extraction Reagent. The clarified extracts were used for protein purification under native conditions using the Ni-NTA Superflow 96 BioRobot Kit (2.1.10) on the vacuum manifold according to the manufacturer's recommendations.

The samples collected before induction, at hourly intervals after induction of protein expression, crude cell lysates and samples after purification were analyzed by reducing SDS-PAGE (see 2.2.6.2). The purified proteins were also analyzed for target binding in an ELISA (see 2.2.6.4).

### Large-scale protein expression

For large scale expression of HPV-16 E7 protein, the overnight culture was prepared from the freshly transformed *E. coli* BL21(DE3)pLysS cells harboring pET20-E7 or pET20-E7opt vectors. Expression was carried out in 1.5 l of 2x YT medium containing ampicillin and chloramphenicol. Following induction of expression at OD<sub>600</sub> ~0.6 by addition of IPTG to a final concentration of 1 mM and supplementation of the medium with zinc using ZnCl<sub>2</sub> to a final concentration of 10 μM, the cells were grown for additional 4 h at 30°C. The cell suspension was centrifuged at 6000 x *g* for 30 min at 4°C and the cell pellet was stored at -20°C until used for protein purification (see 2.2.5).

Affilin variants, wild-type γB-crystallin, EGFP-His<sub>6</sub> and Tat-fusions thereof were expressed from the corresponding pET-20b(+)-derived vectors (see 2.1.4). For expression of Affilin variants containing amber stop codons, *E. coli* NovaBlue(DE3) cells were used. In other cases *E. coli* CodonPlus(DE3)-RIL strain was used. The overnight cultures obtained from a single colony were diluted 1:50 in 1.5 l of 2x YT medium containing ampicillin and grown at 37°C with shaking at 220 rpm. The induction of expression with IPTG at a final concentration of 1 mM was performed when OD<sub>600</sub> of cultures reached ~0.6 for all proteins and ~1.3 for D1-Tat. The cultures were grown at the temperature of 30°C for all proteins,

and 25°C for D1-Tat variant. Following induction period (6 h for all proteins and 16 h for D1-Tat protein), the cell pellets were collected by centrifugation (6000 x *g*, 30 min, 4°C) and stored at -20°C until used for protein purification (see 2.2.5).

## 2.2.5 Protein purification and chromatographic analysis

### Protein purification

For protein purification, frozen bacterial cell pellets were thawed on ice for 30 min and resuspended in 30 ml of NPI-20 buffer (2.1.11) containing 1 mM PMSF. The cells were lysed by addition of lysozyme to a final concentration of 0.5 mg/ml. Following incubation of the bacterial cell suspension on ice for 30 min, the DNA was degraded by addition of benzonase nuclease (2.1.7) at a concentration of 25 U/ml in the presence of 10 mM MgCl<sub>2</sub>. Sonication was done using the ultrasonic homogenizer SONOPULS 2200 equipped with the sonotrode MS73 (five cycles, 25% of sonication power for 15 sec with 1 min delay between pulses). Following centrifugation (30 000 x *g*, 30 min, 4°C), the soluble protein fraction was applied onto a HiTrap Chelating HP 5 ml immobilized metal-ion affinity chromatography (IMAC) column charged with Ni<sup>2+</sup> and equilibrated with the buffer NPI-20 (2.1.11). The proteins were eluted with a linear imidazole gradient of 15 column volumes from 20 to 500 mM using buffer NPI-500 (2.1.11).

For purification of the E7 protein, the pooled protein fractions from IMAC column were dialyzed overnight at 4°C in dialysis tubing (MWCO 3000) against buffer Q-1 (2.1.11). Thereafter, the protein sample was loaded onto a HiTrap Q Sepharose HP 5 ml anion-exchange chromatography column. The E7 protein was eluted with a linear NaCl gradient of 20 column volumes from 300 mM to 1 M using buffer Q-2 (2.1.11). The peak fractions containing E7 were pooled and subsequently dialyzed overnight at 4°C against buffer Q-1. The protein was concentrated to approximately 1 mg/ml using an Amicon Ultra-15 centrifugal filter device (MWCO 5000) and applied onto a HiLoad 16/60 Superdex G-75 size-exclusion chromatography column. The E7 protein was eluted from the column in the SE-1 buffer (2.1.11). The column was calibrated with proteins from Gel Filtration LMW and HMW Calibration Kits, *i.e.* ribonuclease A (13.7 kDa), ovalbumin (43 kDa), aldolase (158 kDa) and thyroglobulin (669 kDa).

For purification of Affilin-Tat variants and  $\gamma$ B-crystallin-Tat, the pooled protein fractions from IMAC column were dialyzed against buffer SP-1 (2.1.11) and applied to a HiTrap SP HP 1 ml cation-exchange chromatography column. Protein elution was accomplished by linear NaCl gradient (20 column volumes) using SP-2 buffer (2.1.11). The collected protein fractions were dialyzed overnight at 4°C against buffer SP-1.

The protein samples were stored at 4°C for short-term use or at -80°C for prolonged storage. To prevent the formation of nonnative disulfide bonds in Affilin variants,  $\beta$ -mercaptoethanol

at a final concentration of 5 mM was added to all buffers used for purification and protein storage.

All purification steps were controlled by the ÄKTA Explorer system and carried out at RT. The protein elution was monitored by measuring the absorbance at 280 nm and additionally at 230 nm for the E7 protein.

To eliminate the endotoxin contamination from protein samples, the Affilin-Tat preparations used for cell culture studies were incubated with Prosep-Remtox beads according to manufacturer's instructions. Following removal of Prosep-Remtox beads, the level of endotoxins in protein samples was estimated by the *Limulus* amoebocyte lysate test (2.1.10) as recommended by the manufacturer.

### **Analytical high-performance liquid chromatography**

For size-exclusion high-performance liquid chromatography (HPLC) analysis, protein samples (approximately 10 µg) were injected onto a TSKGel SW<sub>XL</sub>2000 column. The chromatography was run in ASE-1 buffer (2.1.11) at a flow rate of 1 ml/min. The calibration of the column was performed with proteins from the Gel Filtration LMW Calibration Kit, *i.e.* ribonuclease A (13.7 kDa), carbonic anhydrase (29 kDa), ovalbumin (43 kDa) and conalbumin (75 kDa).

For reversed-phase HPLC analysis, the protein samples (approximately 20 µg) were injected on a PLRP-S column equilibrated with the RP-1 buffer (2.1.11). The protein was eluted using a linear gradient from 30% to 60% of buffer RP-2 (2.1.11) over a period of 30 min at a flow rate of 1 ml/min.

The HPLC was controlled by a Dionex Summit HPLC system and carried out at 25°C. During protein analysis, the absorbance at 280 nm was detected.

## **2.2.6 Protein characterization**

### **2.2.6.1 Quantification of protein concentration**

#### **Ultraviolet/Visible (UV/Vis) Spectroscopy**

The concentration of proteins purified from large-scale expression experiments was determined by measuring the absorbance at 280 nm. The concentration was calculated using equation derived from the Beer-Lambert law (Pace *et al.*, 1995):

$$A = \epsilon \times c \times l \quad (2)$$

with *A*: absorption,  $\epsilon$ : molar extinction coefficient, *c*: molar concentration and *l*: cell path length

The molar extinction coefficient was calculated using ProtParam tool available at <http://www.expasy.org>.

### **Bradford Assay**

In other cases, the protein concentration was determined by method developed by Bradford (Bradford, 1976) using the Bio-Rad Protein Assay Kit (2.1.10) according to the manufacturer's recommendations. As a protein standard, BSA at a concentration of 0.2 to 0.9 mg/ml was used.

#### **2.2.6.2 SDS-PAGE**

The SDS-PAGE was performed according to Laemmli (Laemmli, 1970) in 15 % SDS-polyacrylamide gels. Protein samples were mixed with the SDS-PAGE loading buffer (2.1.11), incubated at the temperature of 95°C for 5 min and loaded on the gel assembled in a Mini-Protean 3 electrophoresis apparatus. Electrophoresis was run at 200 V for 45 min in the SDS-PAGE electrophoresis buffer (2.1.11). The LMW-SDS Marker Kit (2.1.10) served as a molecular weight standard. The gels were either stained in the Coomassie staining solution (2.1.11) followed by incubation in destaining solution (2.1.11) or blotted onto nitrocellulose transfer membrane (see 2.2.6.3).

#### **2.2.6.3 Western blotting**

For Western blotting, proteins resolved on the polyacrylamide gel were transferred onto the Protran nitrocellulose transfer membrane in a semi-dry blotting apparatus (0.8 mA per cm<sup>2</sup> of the gel, 2 h) with Western blotting transfer buffer (2.1.11). Protein transfer was confirmed by staining of the membrane with Ponceau S solution (2.1.11). The membrane was rinsed with water and blocked in 5% (w/v) skimmed milk in PBS-T for 1 h at RT. Subsequently, the membrane was incubated with appropriate primary antibody (see 2.1.9) overnight at 4°C or for 2 h at RT. After washing three times for 10 min with PBS-T, the membrane was incubated with an anti-mouse IgG horseradish peroxidase-conjugated antibody (2.1.9) for 1 h at RT. Finally, the membrane was washed three times with PBS-T for 15 min followed by one brief wash with PBS. Detection of protein bands was performed using the ECL Western Blotting Detection Reagent (2.1.10) as recommended by the manufacturer.

#### **2.2.6.4 ELISA**

The ELISA was performed for determination of apparent dissociation constants of E7-pRb and Affilin-E7 interactions as well as for screening of anti-E7 Affilin molecules after phage display selection (2.2.3). In each case, the target and control proteins (2 µg/ml, 100 µl/well) were immobilized on the 96-well microtiter plate overnight at 4°C. The plate was washed three times with 400 µl of PBS-T, blocked with 3% (w/v) BSA in PBS-T (37°C, 2 h) and subsequently washed with PBS-T.

For affinity determination, sequentially diluted purified protein fractions were applied to the wells at concentrations indicated in the corresponding figures. For specificity analysis of D1-Tat and D4-Tat Affilin variants, the amount of 300 nM of each protein was used in the assay. In case of screening of anti-E7 clones, the volume of 100  $\mu$ l of each purified protein variant was applied to the wells with immobilized target protein.

In each case, the proteins were incubated for 1 h at 37°C and thereafter the wells were washed three times with PBS-T. Bound proteins were detected with specific antibodies. For detection of E7, an anti-HPV-16 E7 antibody was used followed by a secondary detection step with an anti-mouse IgG horseradish peroxidase-conjugated antibody (2.1.9). Affilin variants were detected with horseradish peroxidase-conjugated anti- $\gamma$ B-crystallin antibody (2.1.9). All antibodies were incubated for 1 h at 37°C. After washing with PBS-T for three times and once with PBS, the ELISA was developed using the TMB Plus substrate solution (50  $\mu$ l/well). The reaction was stopped by addition of 0.2 M H<sub>2</sub>SO<sub>4</sub> (50  $\mu$ l/well) and absorbance was measured at 450 nm ( $A_{450}$ ) with 620 nm as a reference using a Sunrise absorbance microplate reader. The measured  $A_{450}$  values were considered as a direct reflection of the amount of protein of interest bound to the immobilized target molecule. For determination of apparent dissociation constant ( $K_d$ ), the  $A_{450}$  values were plotted against the protein concentration using SigmaPlot 2000 software. The  $K_d$  values were calculated using equation derived from the law of mass action (Raghava & Agrewala, 1994; Voss & Skerra, 1997):

$$A = (A_{max} \times c) / (K_d + c) \quad (3)$$

with  $A$ : measured absorbance at 450 nm after reference subtraction,  $A_{max}$ : signal for saturated binding,  $c$ : protein concentration,  $K_d$ : apparent dissociation constant.

#### 2.2.6.5 Surface plasmon resonance

The surface plasmon resonance (SPR) analysis of protein-protein interactions was performed on a Biacore 3000 instrument. The target proteins were covalently linked to the dextran matrix of a CM5 sensor chip using the Amine Coupling Kit (2.1.10) according to instructions of the manufacturer. The pRb protein was immobilized to ~3600 resonance units (RU) by injection of 35  $\mu$ l of pRb solution (10  $\mu$ g/ml, dialyzed overnight against 50 mM MES buffer, pH 6.0). To immobilize E7, the protein was dialyzed overnight against 100 mM sodium acetate buffer, pH 4.3 and 35  $\mu$ l of the 50  $\mu$ g/ml solution was injected resulting in an immobilization level of ~5800 RU. To correct for non-specific binding and bulk refractive-index change, a blank flow-cell channel activated with NHS/EDC and blocked with ethanolamine was used as a negative control. All steps of the immobilization procedure were performed at a flow rate of 5  $\mu$ l/min.

To analyze the E7-pRb interaction, the E7 protein was diluted in the Biacore running buffer (2.1.11) in a concentration series from 900 to 225 nM in twofold dilution steps. For analysis of Affilin binding to E7, Affilin molecules were applied in a series of twofold dilutions ranging from 600 to 37 nM for D1-Tat and 1.4  $\mu$ M to 87 nM for D4-Tat. The binding interactions were measured at 25°C at a flow rate of 30  $\mu$ l/min. Regeneration of the matrix was performed with stripping solution (1 M KCl) applied for 30 sec at a flow rate of 30  $\mu$ l/min.

The sensorgrams subtracted from a blank flow-cell channel were analyzed using the BIAevaluation 3.1 software (Biacore International, Uppsala, Sweden).

## **2.2.7 Cell biology**

### **2.2.7.1 Mammalian cell propagation**

The mammalian cells (see 2.1.2) were grown as monolayers in culture media (2.1.13) in a 37°C incubator with 5% CO<sub>2</sub>. Upon reaching 70-90% confluence, the cells were washed with PBS and detached from the culture dish surface by a 0.25% (w/v) trypsin-EDTA solution (2.1.7). Following incubation at 37°C (approximately 5 - 10 min), the cells were resuspended in a fresh culture medium and dispensed into new culture flasks or wells.

### **2.2.7.2 Tat-mediated internalization of Affilin molecules into mammalian cells**

For investigation of Tat-mediated Affilin internalization, the NIH/3T3 or NIH/3T3-E7 cells were plated at a density of  $4 \times 10^5$  cells/well in 6-well cell culture plates (for Western blotting) and  $6 \times 10^4$  cells/well in 24-well cell culture plates containing glass coverslips (for immunofluorescence microscopy). Next day, the culture medium was replaced with a fresh medium containing Affilin-Tat fusion proteins at a final concentration of 0.01 - 10  $\mu$ M. After incubation for indicated time intervals (see 3.3.4), the cells were washed five times with PBS to remove extracellular protein. Immunofluorescence analysis was performed as described in 2.2.7.4. For Western blot analysis, the cells were lysed using lysis buffer (2.1.11), centrifuged at 13 000  $\times g$  for 10 min at RT and for each sample an equal amount of cell lysate (20  $\mu$ l) was mixed with the SDS-PAGE loading buffer (2.1.11) and applied onto a 15% SDS-polyacrylamide gel. Western blotting with an anti- $\gamma$ B-crystallin antibody was performed as described in 2.2.6.3.

For determination of intracellular protein stability, the cells were plated at  $2 \times 10^5$  cells/well in 6-well plates. Next day, the cells were treated with the E9\*-Tat protein at a final concentration of 1  $\mu$ M for 3 h, washed 5 times with fresh culture medium to remove extracellular protein and incubated for indicated time intervals (see 3.3.4). The total cell lysates were prepared as described previously and equal amounts of cell lysates (20  $\mu$ l) for each sample were analyzed by Western blotting (2.2.6.3).

When indicated, the cells following incubation with Affilin-Tat fusion proteins were washed three times with PBS, incubated with 0.25% (w/v) trypsin-EDTA for 10 min at 37°C, replated at the same cell density and allowed to attach to the culture dish surface for approximately 3 h before analysis. Western blotting and immunofluorescence studies were performed as described above.

### 2.2.7.3 Transfection of mammalian cells

The calcium phosphate method (Graham & van der Eb, 1973; Wigler *et al.*, 1977) was used to transfect NIH/3T3-E7, C-33 A and HEK-293 cell lines for transient expression of Affilin molecules and  $\gamma$ B-crystallin from corresponding mammalian expression vectors (2.1.4). Briefly, the cells were plated the day before transfection in 24-well cell culture plates containing glass coverslips at a density resulting in 50-70% confluent monolayers. Three hours prior to transfection, the culture medium was replaced with a fresh medium. For each well, the DNA-calcium phosphate co-precipitates were prepared by mixing 2  $\mu$ g of the vector DNA with  $\text{CaCl}_2$  at a final concentration of 125 mM in 1x HBS buffer (2.1.11) in a volume of 40  $\mu$ l. The precipitates were allowed to form for 20 min at RT and subsequently added to the cell culture medium (40  $\mu$ l/well). The cells were exposed to the precipitates for 6 h and thereafter the glycerol shock was performed. For this purpose, the cells were treated with 15% (v/v) glycerol in 1x HBS buffer for 2 min. After removal of the glycerol by adding fresh medium, aspiration of the mixture and replacement with a fresh medium, transfected cells were incubated under standard culture conditions for specified time prior to analysis.

Transient transfection of Ca Ski cells with vectors encoding Affilin molecules and  $\gamma$ B-crystallin (2.1.4) was performed using Effectene transfection reagent with 1:25 ratio of DNA to Effectene reagent according to the manufacturer's instructions. Due to observed cytotoxicity, the Effectene-DNA complexes were removed from the cells after 6 h of the incubation time.

Transfection of NIH/3T3 cells was carried out using Nucleofector II device according to the manufacturer's recommendations. For each sample, the amount of  $1 \times 10^6$  cells was resuspended in the Cell Line Nucleofector Kit R solution (2.1.10) and the cells were transfected with 3  $\mu$ g of the plasmid DNA (2.1.4) using program U-30.

In each case, the efficiency of transfection was verified by immunofluorescence staining with an anti- $\gamma$ B-crystallin antibody (see 2.2.7.4).

### 2.2.7.4 Immunofluorescence microscopy

Cells grown on glass coverslips were washed with PBS and fixed with either 100% methanol (10 min, -20°C) or 4% (w/v) paraformaldehyde (PFA) in PBS (20 min, RT).

The methanol-fixed cells were re-hydrated with PBS (10 min, RT). The cellular membranes were permeabilized with 0.5% (v/v) Triton X-100 in PBS (10 min, RT). The non-specific binding sites were blocked with 3% (w/v) skimmed milk in PBS (30 min, RT). For staining of Affilin molecules or wild-type  $\gamma$ B-crystallin, the cells were probed with an anti- $\gamma$ B-crystallin antibody (2.1.9) for 1 h at 37°C followed by staining with Cy3-conjugated anti-mouse IgG antibody (2.1.9) for 1 h at RT. The counter staining was performed by incubation of cells with 4',6-diamidino-2-phenylindole (DAPI) at a final concentration of 1  $\mu$ g/ml (10 min, RT). The coverslips were mounted on microscope slides using the Mowiol mounting medium (2.1.11). Images were taken with a Nikon Eclipse F600 microscope equipped with a CCD camera and Lucia GF software (Nikon, Düsseldorf, Germany).

#### **2.2.7.5 Bromodeoxyuridine incorporation assay**

For analysis of cellular proliferation, the transfected cells were incubated with BrdU at a final concentration of 10  $\mu$ M for the last 4 h (NIH/3T3, NIH/3T3-E7, HEK-293) and 10 h (Ca Ski, C-33 A) of the 48 h post-transfection period. Thereafter, the cells were washed three times with PBS, fixed with 4% (w/v) PFA in PBS and labeled with an anti-human- $\gamma$ B-crystallin antibody as described previously (2.2.7.4). Following post-fixation with 4% (w/v) PFA in PBS for 20 min at RT, the DNA was denatured with 4 M HCl for 10 min. The cells were subsequently washed three times for 10 min using PBS containing 1% (w/v) BSA and 0.1% (v/v) Triton X-100. BrdU was detected by an anti-BrdU antibody (2.1.9) incubated for 8 h at RT followed by staining with an Alexa Fluor 488-conjugated anti-rat IgG antibody (2.1.9) for 1 h at RT. The cellular DNA was stained with DAPI as described in 2.2.7.4.

For each independent experiment conducted in triplicate, at least 500 cells expressing indicated Affilin molecules or  $\gamma$ B-crystallin were analyzed and the number of BrdU-positive cells among them was counted. Statistical analysis was carried out using the Student's *t*-test with SigmaStat statistical software. The probability (*P*) values are given in the corresponding figures. Images were taken with a Nikon Eclipse F600 microscope equipped with a CCD camera and Lucia GF software (Nikon, Düsseldorf, Germany).

#### **2.2.7.6 Analysis of apoptosis**

Apoptosis was detected at 72 h post-transfection with the *In Situ* Cell Death Detection Kit Fluorescein (2.1.10) following the manufacturer's instructions. Images were taken with a Nikon Eclipse F600 microscope equipped with a CCD camera and Lucia GF software (Nikon, Düsseldorf, Germany).

### 3. Results

#### 3.1 Recombinant production of the HPV-16 E7 protein

In order to achieve an efficient selection of binding molecules by phage display, target protein is required in a sufficient quantity and quality. The following section describes expression of the HPV-16 E7 protein using recombinant *E. coli* cells as well as its purification and biophysical characterization.

##### 3.1.1 Cloning, expression and purification of the HPV-16 E7 protein

The gene encoding the HPV-16 E7 protein was amplified from a pcDNA3.1-E7 vector (2.1.4) by PCR and cloned into the bacterial expression vector pET-20b(+) carrying the C-terminal His<sub>6</sub>-tag. The resulting plasmid is referred to as pET-20-E7.

In small-scale expression experiments using different *E. coli* strains (*i.e.* BL21(DE3), BL21-CodonPlus(DE3)-RIL, or BL21(DE3)pLysS) carrying the pET-20-E7 vector as well as various growth conditions, the E7 protein was found to be expressed at a very low level, detectable only after Western blot analysis with a corresponding anti-E7 antibody (data not shown).

The analysis of the E7 gene revealed that the His2 and Gly3 triplets form an alternative ATG start codon (Fig. 11). It was hypothesized that recombinant *E. coli* cells could use this codon for the initiation of the translation machinery resulting in the expression of a short peptide and premature termination of translation.

	1		25		50											
<b>E7</b>	<u>ATGCA</u> <b>T</b> GGAGATACAC <b>C</b> <u>T</u> ACATTGCATGAATATATGTTAGATTTGCAACC															
	M	H	G	D	T	P	T	L	H	E	Y	M	L	D	L	Q
		M	E	I	H	L	H	C	M	N	I	C	STOP			
<b>E7opt</b>	<u>ATGCA</u> <b>C</b> GGAGATACAC <b>C</b> <u>T</u> ACATTGCATGAATATATGTTAGATTTGCAACC															

**Figure 11.** Optimization of the E7 gene. The DNA sequence of the E7 gene was obtained from the GenBank database (accession no. AF486352) and confirmed by sequencing. The ATG start codon of the E7 gene and an alternative ATG codon are underlined. The amino acid sequence of the HPV-16 E7 protein (positions 1 to 15) and the incorrect product of the alternative translation initiation are indicated by single-letter amino acid code. Mutations introduced into the E7 gene are highlighted in red in both unmodified and optimized (E7opt) E7 gene.

To eliminate the possibility of the alternative translation initiation, the introduction of a silent mutation to the codon for His2 was proposed (Fig. 11). In an attempt to further optimize the E7 gene, the ProteoExpert web-based service ([www.proteoexpert.com](http://www.proteoexpert.com)) was used.

The ProteoExpert was originally designed by Roche Applied Sciences in order to optimize the expression templates for protein synthesis in the cell-free Rapid Translation System. In this program, the sequence mutations in the first codons of the translated region that are expected to result in a substantial increase in the protein yield are identified according to an algorithm based on the theoretical analysis of over 700 mRNA sequences and experimental data obtained by expressing the corresponding proteins.

As an output of the calculation, the ProteoExpert bioinformatics service provided 10 variants of the E7-coding sequence (Fig. 12). The silent mutation in the His2 codon was proposed for six sequence variants. As the silent mutation in the codon for Pro6 occurred in seven proposed sequences, this codon was also selected for E7 gene optimization.

The optimized E7-coding sequence (referred to as E7opt) containing two silent mutations in His2 and Pro6 codons was generated by PCR. The DNA sequence of the E7opt gene was verified by sequencing (2.2.1.11).

	1	20
<b>E7 wild-type</b>	ATGCATGGAGATACACCTACA	
<b>E7-1</b>	ATGCA <b>C</b> GGAGATACAC <b>C</b> AACA	
<b>E7-2</b>	ATGCA <b>C</b> GGAGATACACCTACA	
<b>E7-3</b>	ATGCA <b>C</b> GGAGACACAC <b>C</b> AACA	
<b>E7-4</b>	ATGCATGGAGATACAC <b>C</b> AAC <b>G</b>	
<b>E7-5</b>	ATGCATGGAGATACAC <b>C</b> AACA	
<b>E7-6</b>	ATGCA <b>C</b> GGAGATAC <b>C</b> CAACA	
<b>E7-7</b>	ATGCATGGAGATACAC <b>C</b> AA <b>C</b> T	
<b>E7-8</b>	ATGCATGGAGATACACCTAC <b>G</b>	
<b>E7-9</b>	ATGCA <b>C</b> GGAGACACACCTACA	
<b>E7-10</b>	ATGCA <b>C</b> GGAGATACAC <b>C</b> AA <b>C</b> T	

**Figure 12.** Sequence variants of the E7 gene provided by the ProteoExpert web-based service application ([www.proteoexpert.com](http://www.proteoexpert.com)). Mutated bases are highlighted in red.

Following small-scale expression test, a significant increase of the expression level was observed for the optimized E7 construct (data not shown). In order to establish optimal expression and growth conditions, several parameters such as composition of the culture medium, cell density at the induction time, IPTG concentration, expression temperature and duration of the induction were evaluated for their influence on the soluble protein yield (data not shown). Finally, the E7 protein was produced by induction of *E. coli* BL21(DE3)pLysS cells harboring the pET-20-E7opt vector at OD<sub>600</sub> ~0.6 with 1 mM IPTG followed by expression at 30°C for 4 h. The cell extracts from expression cultures were examined by SDS-PAGE under reducing conditions. As shown in Fig. 13 (lanes 3, 4 and 5), the recombinant E7 protein accounted for approximately 30% of the total protein with almost equal distribution between soluble and insoluble fractions.

The E7 protein from the soluble fraction was first purified using immobilized metal-ion affinity chromatography (IMAC) under native conditions. This step was followed by separation on anion-exchange and size-exclusion chromatography columns. From this procedure, the amount of approximately 30 mg of the E7 protein was obtained per 1 l of shake flask bacterial culture.

Based on the SDS-PAGE analysis under reducing conditions, the purity of the protein preparation was estimated to be greater than 90% (Fig. 13, lane 8, arrow). An additional band at ~28 kDa seen in the purified protein fraction possibly represented the E7 dimer resistant to the conditions of SDS-PAGE. This band was detected by corresponding anti-E7 antibody in Western blot analysis (shown in section 3.1.2.1).

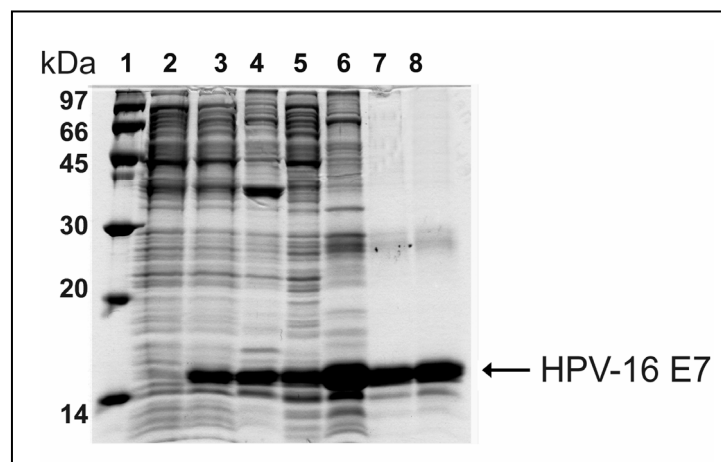


**Figure 13.** Analysis of the recombinant production of the HPV-16 E7 protein by reducing SDS-PAGE. The protein samples were resolved in a 15% polyacrylamide gel and stained with Coomassie Brilliant Blue. Lane 1, low molecular weight protein markers (kDa); lane 2, cell extract from non-induced culture; lane 3, cell extract from induced culture; lane 4, insoluble protein fraction; lane 5, soluble protein fraction; lane 6, peak fraction after IMAC; lane 7, peak fraction after anion-exchange chromatography; lane 8, peak fraction after size-exclusion chromatography.

The molecular weight of the E7-His<sub>6</sub> fusion protein deduced from its amino acid sequence is ~12 kDa. As shown in Fig. 13, the recombinant HPV-16 E7 protein migrated to a position corresponding to a molecular mass of ~16 kDa.

Such unusual electrophoretic behavior has already been observed for chemically synthesized E7 (Rawls *et al.*, 1990) as well as for E7 protein expressed in *E. coli* (Moro & Hernandez, 1996), yeast (Tommasino *et al.*, 1990), baculovirus (Stacey *et al.*, 1993), cervical cancer cells (Smotkin & Wettstein, 1986) and cell-free system (Roggenbuck *et al.*, 1991). The aberrant electrophoretic migration of E7 on polyacrylamide gels has been attributed to the high content of acidic amino acid residues (Armstrong & Roman, 1993). This phenomenon has also been ascribed to the high stability of the E7 protein structure

which is expected to be resistant to the combined effects of high temperature and SDS (Heck *et al.*, 1992; Alonso *et al.*, 2002).

In size-exclusion chromatography on a HiLoad 16/60 Superdex G-75 column, the E7 protein eluted as one major peak at a volume corresponding to protein species with a molecular weight of approximately 700 kDa (Fig. 14). Considering the molecular weight of the E7-His<sub>6</sub> monomer (~12 kDa), this indicated that the E7 protein existed as a soluble higher-order oligomer.

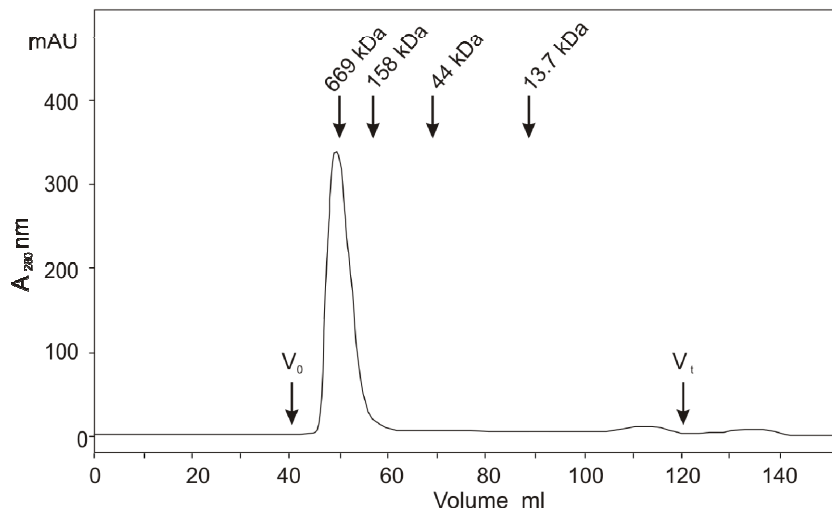


**Figure 14.** Elution profile of the E7 protein from a HiLoad 16/60 Superdex G 75 size-exclusion chromatography column. The E7 protein was eluted from the column in the SE-1 buffer (2.1.11). The column was calibrated using ribonuclease A (13.7 kDa), ovalbumin (43 kDa), aldolase (158 kDa) and thyroglobulin (669 kDa). Arrows indicate the void ( $V_0$ ) and total ( $V_t$ ) column volume as well as the elution volumes of molecular mass standards (molecular mass in kDa given above the arrow).

This result is consistent with previous studies, in which the recombinant E7 protein was observed to form dimers, tetramers and oligomers (Chinami *et al.*, 1994; Clements *et al.*, 2000; Alonso *et al.*, 2004).

The mechanism of E7 oligomerization has not been fully disclosed yet. The E7 dimer formation has been proposed to occur through the intermolecular interaction between a unique zinc-binding fold of two E7 monomers (McIntyre *et al.*, 1993; Ohlenschlager *et al.*, 2006). The coordinated zinc ions are not directly involved in the E7 dimer formation, though they are essential for this process by the means of maintaining the folded state of the zinc-binding CR3 domain (Ohlenschlager *et al.*, 2006). However, as described by Alonso *et al.*, the E7 oligomers have been observed to assemble in the absence of zinc ions. As a non-specific chelating agent (EDTA) was used in this study, the authors suggested that other metals than zinc may be involved in the E7 oligomer assembly (Alonso *et al.*, 2004). In the present study, zinc was added to the buffers used for E7 purification and metal

chelators were omitted from these buffers. Nevertheless, as the mechanism of E7 oligomerization is not fully defined, these measures were insufficient to prevent the formation of E7 oligomers.

### 3.1.2 Biophysical characterization of the HPV-16 E7 protein

#### 3.1.2.1 Western blot analysis

The Western blot analysis of protein samples from expression and purification of the E7 protein with an anti-E7 antibody demonstrated multiple reactive bands: one predominant band at ~16 kDa corresponding to the E7 monomer (Fig. 15, arrow) and two additional bands at ~28 and 40 kDa. These bands may represent various oligomeric assemblies of the E7 protein persistent under conditions of the reducing SDS-PAGE and Western blotting.

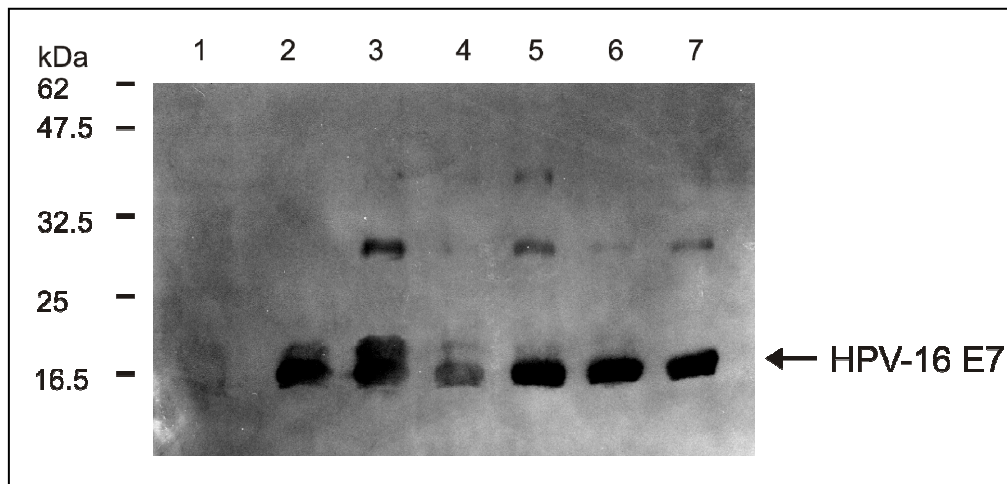


**Figure 15.** Western blot analysis of recombinant HPV-16 E7 protein. Lane 1, cell extract from non-induced culture; lane 2, cell extract from induced culture; lane 3, insoluble protein fraction; lane 4, soluble protein fraction; lane 5, peak fraction after IMAC; lane 6, peak fraction after anion-exchange chromatography; lane 7, peak fraction after size-exclusion chromatography.

#### 3.1.2.2 Binding of the HPV-16 E7 protein to pRb

The binding of the recombinant E7 protein to the full-length retinoblastoma protein was investigated by concentration-dependent enzyme-linked immunosorbent assay (ELISA) and surface plasmon resonance (SPR).

In ELISA experiment, the recombinant pRb protein was directly coated onto the wells of a 96-well microtiter plate and sequentially diluted E7 protein bound to it was detected by an anti-E7 antibody and an anti-mouse IgG horseradish peroxidase-conjugated antibody in a chromogenic reaction.

As shown in Fig. 16, the E7 protein was capable of pRb binding in a dose dependent fashion with saturation at the E7 protein concentration of approximately 300 nM. Using nonlinear regression analysis (2.2.6.4), the apparent dissociation constant ( $K_d$ ) value of the E7-pRb interaction was determined as approximately 20 nM.

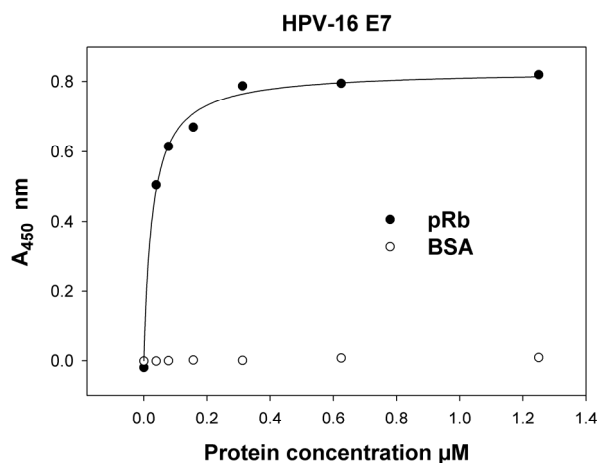


**Figure 16.** Determination of the apparent dissociation constant ( $K_d$ ) of the E7-pRb binding using ELISA. The pRb (target) and BSA (control) were immobilized on wells of the microtiter plate and purified E7 protein was applied in a dilution series. Bound E7 protein was detected by an anti-E7 antibody and an anti-mouse IgG horseradish peroxidase-conjugated antibody in a chromogenic reaction. The absorbance was measured at 450 nm ( $A_{450}$ ) with 620 nm as a reference. The curve represents the nonlinear fit of the data to equation 3 (2.2.6.4). The calculated  $K_d$  was ~20 nM.

The SPR analysis of the E7-pRb interaction was performed on a Biacore 3000 instrument. The Biacore technology utilizes the SPR optical phenomenon for monitoring the macromolecular interactions between injected analyte and immobilized biomolecule in real time. During the measurements, changes in the refractive index at the surface of a sensor chip are detected (Jason-Moller *et al.*, 2006; Piliarik *et al.*, 2009).

In the set-up employed in this study, the recombinant pRb protein was covalently immobilized onto a CM5 sensor chip by amine coupling (2.2.6.5) to approximately 3600 resonance units (RU).

Two independent experiments for serial E7 concentrations ranging from 250 to 900 nM applied over the same regenerated surface were performed. The sensorgrams subtracted from a blank flow-cell channel (Fig. 17) were analyzed using the BIAevaluation 3.1 software. During the measurements, a reduction of the ligand binding activity visible as both a decrease of the signal at the same analyte concentration after every cycle (see Fig. 17) and as a negative base-line drift was observed. Although different regeneration conditions were tested, it was not possible to regenerate the pRb binding surface without loss of the ligand binding activity. The loss of pRb binding activity precluded the calculation of the apparent dissociation constant from the equilibrium titration measurements.

The evaluation of the surface plasmon resonance data revealed that the interpretation according to the 1:1 Langmuir model ( $A + B \leftrightarrow AB$  with  $A$ : analyte, defined as a molecule in solution and  $B$ : immobilized ligand), bivalent analyte model ( $A + B \leftrightarrow AB$ ; second step:  $AB + B \leftrightarrow ABB$ ) or heterogeneous analyte model ( $A1 + B \leftrightarrow A1B$ ;  $A2 + B \leftrightarrow A2B$ ) was not applicable. In addition to the instability of the pRb protein, the complex interaction between pRb and the oligomeric E7 protein may cause difficulties with the SPR data evaluation. In general, the investigation of binding between the multivalent protein and the ligand immobilized on a biosensor chip is difficult due to the nonconformity of the data with the model on which the quantitative analysis is based (Kalinin *et al.*, 1995; Nieba *et al.*, 1996). To avoid the influence of the analyte multivalency on the SPR measurements, the multivalent molecule should be immobilized on the biosensor chip. However, due to limited availability and instability, the pRb protein could not be used as an analyte in this study. Thus, the evaluation of kinetics and affinity of the E7-pRb interaction based on SPR data could not be accomplished. Nevertheless, the response curves recorded during SPR measurements (Fig. 17) showed that recombinant E7 protein is able to bind to immobilized pRb.

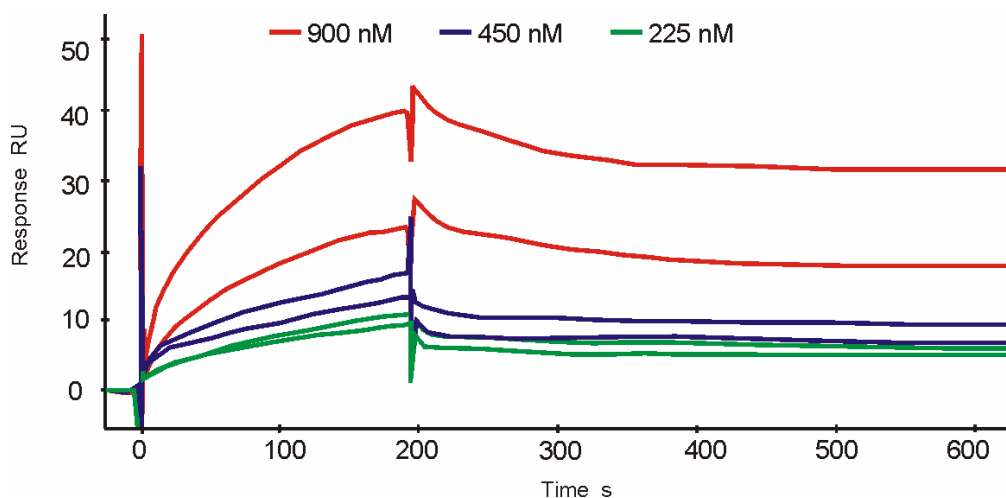


**Figure 17.** Surface plasmon resonance analysis of the binding of E7 to the pRb protein immobilized on a CM5 biosensor chip. The concentrations of E7 protein used were: 900 nM, 450 nM and 225 nM. Two injections were performed for each protein concentration. The binding analysis was performed at a flow rate of 30  $\mu\text{l}/\text{min}$ .

Taken together, the E7 protein was prepared from the recombinant *E. coli* cells in a purity sufficient for performing the selection of anti-E7 Affilin molecules (for phage display selection a protein purity of >90% is usually required; Fung, 2004). The biological activity of the recombinant E7 protein was shown by its ability to bind to pRb in ELISA and SPR experiment.

### 3.2 Phage display selection of anti-E7 Affilin molecules from a $\gamma$ B-crystallin library

The  $\gamma$ B-crystallin library used in this study for the selection of anti-E7 Affilin clones was provided by Scil Proteins GmbH (Fiedler & Rudolph, 2001; Ebersbach *et al.*, 2007). The library is composed of randomized  $\gamma$ B-crystallin sequences cloned upstream of the gene III in the pCANTAB 5 E phagemid vector. A schematic representation of the recombinant pCANTAB-CR20 construct is shown in Fig. 18.

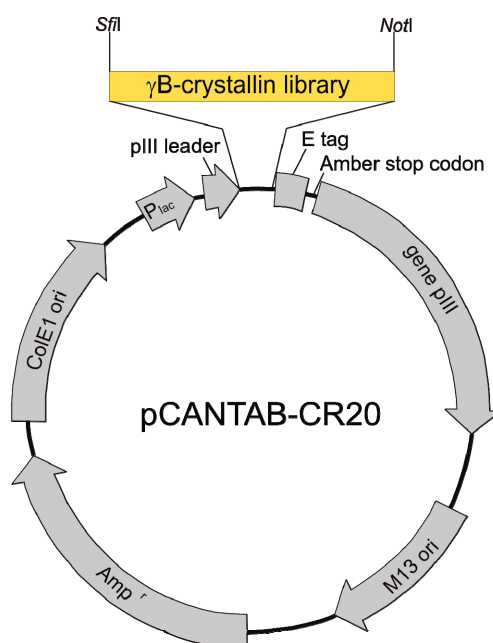


**Figure 18.** Schematic representation of the phagemid pCANTAB-CR20. The  $\gamma$ B-crystallin genetic library was inserted between the pIII leader and the gene encoding the pIII protein using *SfiI* and *NotI* restriction sites. The recombinant pCANTAB-CR20 vector contains also the lac promoter/operator element (lacP), a peptide tag (E-tag) followed by the amber translational stop codon which permits the expression of the library members as a fusion with pIII in the amber suppressor host strain. In addition, the vector carries the M13 and bacterial origins of replication (M13 and ColE1, respectively) and the antibiotic resistance marker (the gene for  $\beta$ -lactamase providing resistance to ampicillin).

The phage display selection of anti-E7 Affilin molecules from the corresponding library is presented in the following sections.

#### 3.2.1 Conventional phage display selection of anti-E7 Affilin molecules

##### 3.2.1.1 Affinity selection

The phage particles displaying the members of a  $\gamma$ B-crystallin library were propagated and precipitated according to the protocol described in the Materials and Methods (2.2.3).

For selection of anti-E7 Affilin molecules, the phage particles were incubated with recombinant HPV-16 E7 protein immobilized on the surface of a 96-well microtiter plate. The unspecific phages were washed out by several washing steps (see 2.2.3). Bound phages were eluted by incubation with triethylamine at pH 10.0. Following neutralization of the eluent, phage particles were used to infect *E. coli* XL1-Blue cells. Phages that retained after the triethylamine elution were allowed to directly infect *E. coli* XL1-Blue cells and were subsequently combined with triethylamine-eluted phages. Following amplification of target-enriched phage particles, further rounds of selection were performed. With each round, the stringency of selection was increased by additional washing steps (for details see 2.2.3). As the recombinant E7 protein carries a His<sub>6</sub>-tag, incubation with a non-related His<sub>6</sub>-tagged protein (EGFP-His<sub>6</sub>) was included in the washing protocol in order to exclude potential His<sub>6</sub>-tag-binding Affilin variants.

The phage titers from each selection round are summarized in Tab. 5. The enrichment of binding clones was achieved up to the third selection round, since the amount of phages recovered in the fourth round was lower in comparison to the previous rounds. Thus, the pool of Affilin variants from the third selection round was used for screening of individual anti-E7 clones.

**Table 5.** Output of different biopanning rounds in cfu/ml.

Selection round	Input phage, cfu/ml	Amount of eluted phage particles, cfu/ml
1	10 <sup>10</sup>	1 x 10 <sup>6</sup>
2	10 <sup>11</sup>	3 x 10 <sup>6</sup>
3	10 <sup>12</sup>	4 x 10 <sup>6</sup>
4	10 <sup>12</sup>	1 x 10 <sup>6</sup>

### 3.2.1.2 Analysis of individual clones by ELISA

To eliminate any dependence of the target binding on the pIII-fusion format, the DNA pool encoding selected E7 binders from the third biopanning round was amplified by PCR from the pCANTAB-CR20 phagemid and subcloned into the cytoplasmic expression vector pET-20b(+) carrying the C-terminal His<sub>6</sub>-tag. To identify specific anti-E7 Affilin molecules, 96 randomly picked clones were pre-screened with regard to their target binding and specificity by ELISA. For this purpose, the proteins were expressed in *E. coli* NovaBlue(DE3) cells in 24-well deep well culture plates and purified under native conditions using IMAC in a microtiter plate format. The purified proteins were probed for binding to the immobilized E7 target protein and BSA as a control.

From 96 individual Affilin variants, 32 clones gave significant signals with  $A_{450} > 0.5$  (Fig. 19) and showed specific binding to the E7 target protein as compared to the binding to BSA

(ratio: E7/BSA binding >5). Only a small number of clones showed unspecific binding to the E7 protein (ratio: E7/BSA binding  $\leq$ 1).

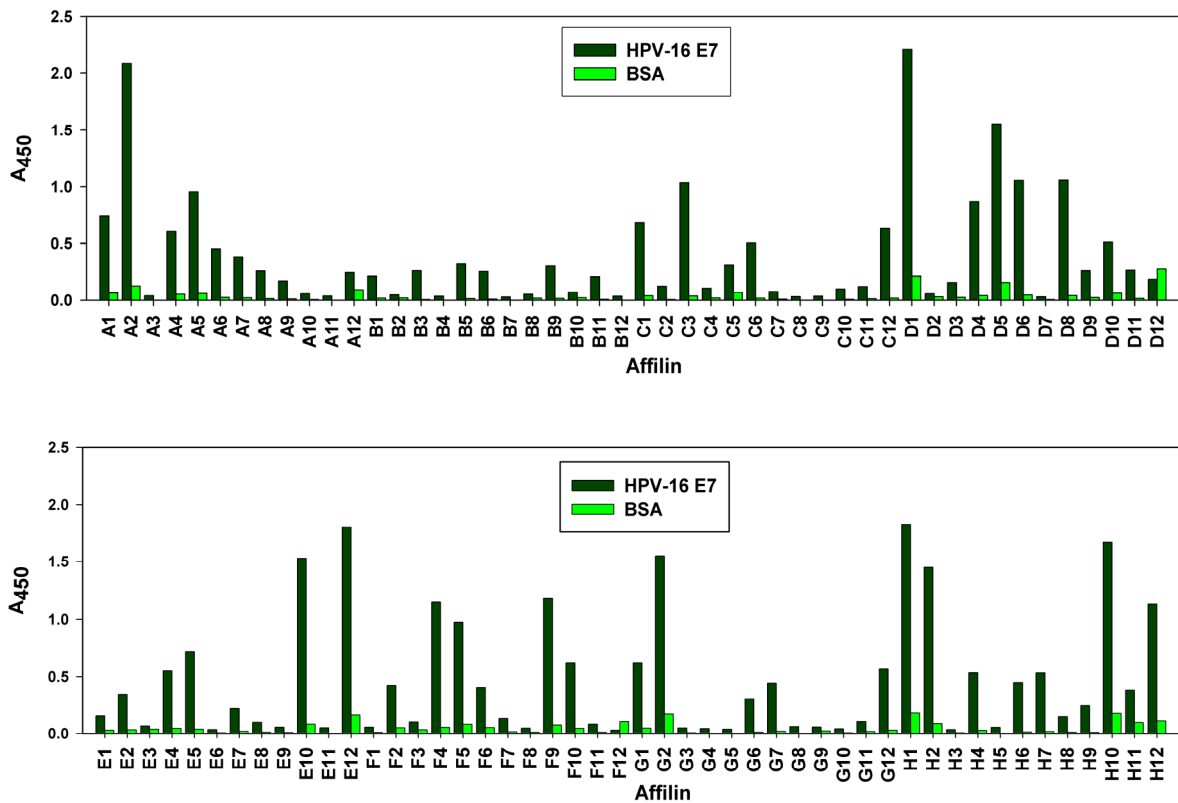


**Figure 19.** Identification of E7-specific Affilin variants in the ELISA screening. The 96 randomly picked clones from the third round of biopanning against E7 protein were expressed and purified as described in 2.2.3. The proteins were applied to the wells of a microtiter plate coated with recombinant E7 target protein or BSA. Bound Affilin molecules were detected by an anti- $\gamma$ B-crystallin antibody conjugated to horseradish peroxidase in a chromogenic reaction. The absorption values at 450 nm are shown.

Based on the ELISA screening, 20 clones showing the highest signal were subjected to DNA sequencing.

### 3.2.1.3 Sequence analysis of individual clones

The DNA sequences of 20 clones showing the highest signal in the ELISA screening were determined as described in 2.2.1.11 (Tab. 6 presents the deduced amino acid sequences at corresponding randomized positions).

The sequence analysis showed that 13 of 20 constructs were correct at the DNA level (*i.e.* no frameshift, no TAA or TGA stop codons and correct framework residue codons). Of them, seven clones displayed identical amino acid sequences (*i.e.* clones A2, A5, D6, E10, E12, F9 and G2) with two clones encoded by identical DNA. In addition, two other

clones (*i.e.* D5 and C3) shared a high sequence similarity with seven identical clones as only one (for D5 variant) and two (for C3 variant) amino acid positions were exchanged.

The selection of variants with shared sequences usually suggests the identification of a consensus binding motif characterized by a high target affinity (Barbass *et al.*, 2001). This remained to be verified by determination of dissociation constants of Affilin clones with identical amino acid sequences (see 3.2.1.4).

Most of analyzed variants contained the amber stop codon, which was regarded as Gln due to amber suppression in the *E. coli* host strain used for the propagation of the library and preparation of recombinant clones. The parental wild-type  $\gamma$ B-crystallin sequence was not found among the sequenced clones, only the Arg36 residue was not substituted in case of seven clones with identical amino acid sequences (*i.e.* clones A2, A5, D6, E10, E12, F9 and G2) and clone A1.

**Table 6.** Affilin clones selected after the third round of phage display selection against the E7 protein (deduced amino acid sequences at randomized positions are shown). Yellow boxes highlight hydrophobic amino acid residues (hydropathy index value >0 on the Kyte-Doolittle scale, Kyte & Doolittle, 1982). Basic residues are highlighted in blue and acidic residues in red. The TAG codon was considered as Gln (referred to as Gln\*) due to its suppression in *supE E. coli* strain. The variants with identical amino acid sequence are highlighted in green.

Protein	Randomized position							
	2	4	6	15	17	19	36	38
$\gamma$ B-crystallin	Lys	Thr	Tyr	Ser	Glu	Thr	Arg	Glu
A1	Ser	Val	Ala	Pro	Thr	Gly	Arg	Tyr
A2	Ala	Cys	Ser	Glu	Lys	Leu	Arg	Gln*
A5	Ala	Cys	Ser	Glu	Lys	Leu	Arg	Gln*
C3	Ala	Cys	Ser	Glu	Lys	Leu	Gln	Gly
D1	Cys	Cys	Gly	Ala	Arg	Arg	Lys	Gly
D4	Phe	Met	Thr	Arg	Asp	Gly	Lys	Lys
D5	Ala	Cys	Ser	Glu	Lys	Leu	Met	Gln*
D6	Ala	Cys	Ser	Glu	Lys	Leu	Arg	Gln*
E10	Ala	Cys	Ser	Glu	Lys	Leu	Arg	Gln*
E12	Ala	Cys	Ser	Glu	Lys	Leu	Arg	Gln*
F9	Ala	Cys	Ser	Glu	Lys	Leu	Arg	Gln*
G2	Ala	Cys	Ser	Glu	Lys	Leu	Arg	Gln*
H12	Ala	Val	Gly	Cys	Thr	Ala	Cys	Gln*

When compared to the wild-type  $\gamma$ B-crystallin protein, selected Affilin molecules revealed the presence of several hydrophobic amino acid substitutions, which could mediate the binding to the target protein via hydrophobic interactions. They occurred mainly at positions 2, 4 and 19. In addition, several clones revealed the enrichment of basic amino acid substitutions (expected content of both Arg and Lys residues calculated from the genetic NNK code used for the library construction was one per eight randomized positions), particularly Affilin variants D1 and D4, in which three out of eight amino acids were

substituted for Lys and Arg residues. The variants with identical amino acid sequence contained two basic substitutions within randomized region.

The seven remaining clones from 20 analyzed were not functional at the DNA level. They carried insertions or deletions at the randomized positions 36 and 38 resulting in either +1 or -1 frameshifts followed by non-suppressed stop codons (TGA or TAA in the *E. coli* XL1-Blue strain used). The variants encoded by these sequences were probably not functionally displayed on the phage particles, since they were not in frame with the pIII phage coat protein. However, as the truncated sequences contained Cys residues (*i.e.* Cys18, 22 and 32 present in the  $\gamma$ B-crystallin scaffold), these peptides could be displayed on the phage particles upon forming of disulfide bonds with the pIII protein (McLafferty *et al.*, 1993; Paschke, 2006). Such clones might have been enriched during selection due to enhanced growth rates of *E. coli* cells expressing only short peptide sequences in contrast to bacteria producing the full-length pIII-fusion constructs (Carcamo *et al.*, 1998; Azzazy & Highsmith, 2002).

The SDS-PAGE analysis of purified protein fractions obtained from clones encoded by frameshifted sequences revealed that the full-length proteins were not produced (data not shown). Thus, the positive signals of frameshifted clones in the ELISA screening could derive from truncated polypeptides encoded by these sequences and recognized by an anti- $\gamma$ B-crystallin antibody used in this assay.

The clones with correct DNA sequence were further analyzed regarding their binding affinities. From seven clones with identical amino acid sequence, the clone A5 was chosen as a representative.

#### **3.2.1.4 Affinity determination**

To evaluate the binding affinity of anti-E7 Affilin molecules, the concentration-dependent ELISA experiment was performed. To obtain proteins with higher purity and quantity, the expression of Affilin molecules was scaled up to 1.5 l and carried out in shake flasks. The proteins were purified from the soluble fraction by IMAC on a HiTrap Chelating HP column to > 90% purity. The yield of protein preparation for individual clones under non-optimized conditions varied between 0.6 to 18 mg per 1 l of culture, depending on the expression level and the protein solubility.

To determine binding affinities, protein samples were allowed to bind to the immobilized recombinant HPV-16 E7 protein in the ELISA (2.2.6.4). The specificity was analyzed by comparing the binding of Affilin molecules to the E7 target protein with the binding to BSA. The apparent dissociation constants were determined by nonlinear regression analysis of the binding data according to equation 3 (2.2.6.4).

The Affilin variants D1 and D4 showed the highest affinities with  $K_d$  values calculated to be  $\sim 80$  nM and  $\sim 260$  nM, respectively (the curves representing the nonlinear regression fit are shown in Fig. 20). The remaining variants achieved binding affinities in the micromolar range (Tab. 7). All variants showed specific binding to the E7 target protein as compared to the binding to BSA (for D1 and D4 shown in Fig. 20).

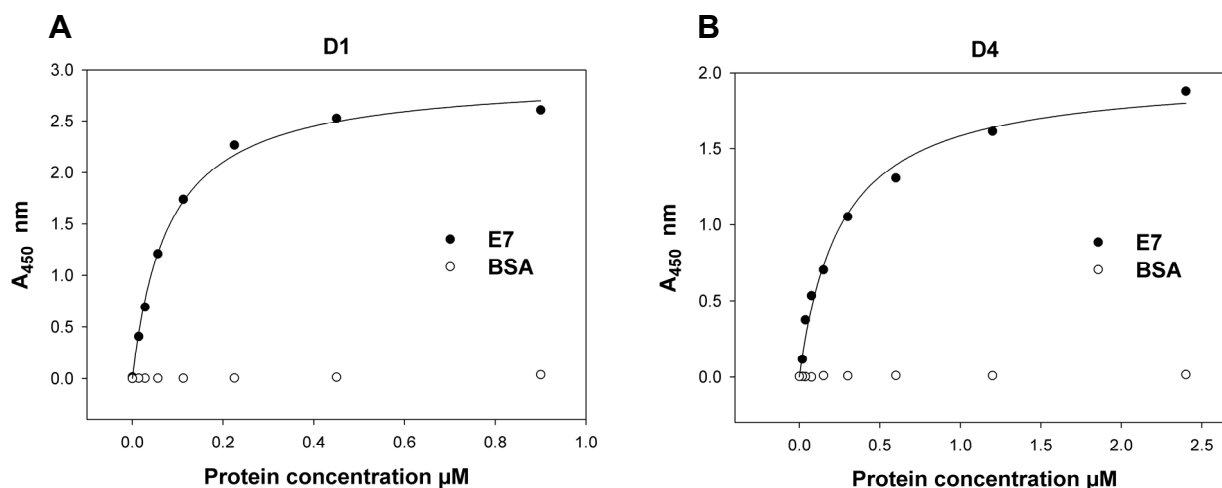


**Figure 20.** Determination of the apparent dissociation constant ( $K_d$ ) of Affilin-E7 binding using ELISA, exemplified for D1 (A) and D4 (B) variants. The HPV-16 E7 (target) and BSA (control) were immobilized on wells of the microtiter plate and purified Affilin molecules were applied in a dilution series. Bound Affilin molecules were detected by an anti- $\gamma$ B-crystallin antibody conjugated to horseradish peroxidase in a chromogenic reaction. The curves represent the nonlinear fit of the data to equation 3 (2.2.6.4). The calculated  $K_d$  values were  $\sim 80$  nM and  $\sim 260$  nM for D1 and D4, respectively.

Surprisingly, the clone A5 which was used as a representative of seven clones carrying identical amino acid substitutions did not show a high affinity toward the E7 target protein ( $K_d$  was determined as  $\sim 5$   $\mu$ M). This finding indicated that the sequence pattern enriched during phage display did not constitute the consensus motif mediating high-affinity E7 binding.

**Table 7.** The binding affinity data obtained from an ELISA for Affilin molecules selected against E7 protein in the conventional phage display selection.

Affilin	$K_d$
A1	2.1 $\mu$ M
A5	5.0 $\mu$ M
C3	14 $\mu$ M
D1	80 nM
D4	260 nM
D5	1.2 $\mu$ M
H12	3.1 $\mu$ M

### 3.2.1.5 Effect of the Cys to Ser exchange on the affinity of Affilin D1

The Affilin variant D1 showing the highest affinity toward E7 protein contained two Cys residues at randomized position 2 and 4, in addition to seven free Cys residues present in the  $\gamma$ B-crystallin scaffold. As Cys residues are considered to be non-favorable amino acid substitutions due to the high reactivity of their thiol side chains at physiological conditions, both Cys residues within randomized region of the D1 variant were replaced with structurally similar Ser residues. For this purpose, the D1-coding sequence was amplified by PCR with primers *D1-Cys/Ser-fwd* and *ggbBstEII-rev* (see 2.1.5 and 2.2.1.2). The introduced mutations were confirmed by sequencing (2.2.1.11) and the D1-Ser2,4 protein was prepared according to the procedure described previously.

The comparison of apparent  $K_d$  values obtained from the ELISA experiment (Fig. 21) revealed a tenfold lower binding affinity of the D1-Ser2,4 mutant ( $K_d \sim 870$  nM) as compared to the native D1 variant ( $K_d \sim 80$  nM).

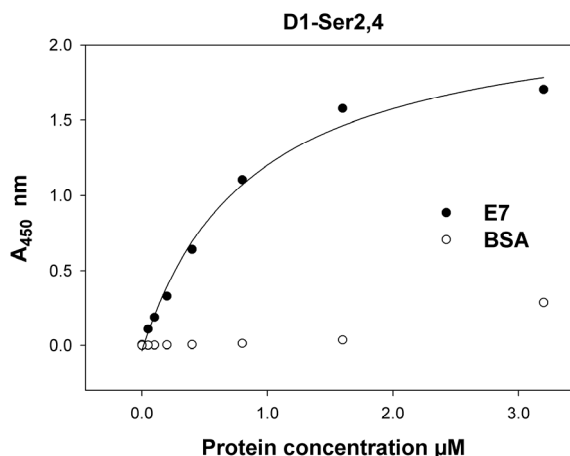


**Figure 21.** Evaluation of the affinity of D1-Ser2,4 mutant to the E7 protein using ELISA. The wells of the microtiter plate were immobilized with HPV-16 E7 (target) and BSA (control) and the purified D1-Ser2,4 mutant was applied in a dilution series. Bound Affilin was detected by an anti- $\gamma$ B-crystallin antibody conjugated to horseradish peroxidase in a chromogenic reaction. The curve represents the nonlinear fit of the data to equation 3 (2.2.6.4). The calculated  $K_d$  was  $\sim 870$  nM.

Although Cys and Ser residues are structurally similar, they differ in polarity - the thiol group of Cys is relatively non-polar compared to the hydroxyl side chain of the Ser residue (Nagano *et al.*, 1999). Thus, by replacing the Cys residues with Ser residues, not only the reactive thiol groups were eliminated but also the hydrophobicity of the the binding region was decreased. This suggests an importance of the hydrophobicity of amino acid residues occurring at the randomized positions for the recognition of the target molecule. Based on these results, the native D1 variant was used in further experiments.

In conclusion, using the conventional phage display approach it was possible to select two Affilin variants, namely D1 and D4, which specifically bound to the E7 target protein with affinities in the nanomolar range. Nevertheless, a number of isolated clones that revealed high signal in the ELISA screening did not exhibit a significant affinity to the E7 protein. Moreover, several clones obtained from this selection approach were encoded by non-functional sequences carrying undesired insertions or substitutions at the randomized positions.

As described in the literature, the phage display selection of recombinant libraries often suffers from enrichment of non-specific and/or low-affinity clones (Fischer *et al.*, 1994; Paschke & Hohne, 2005). In an attempt to eliminate irrelevant clones and to isolate variants with higher affinity to E7, the alternative phage display selection was carried out.

### **3.2.2 Selection of Affilin molecules against the HPV-16 E7 protein by phage display with proteolysis**

In the alternative phage display approach, the library displaying  $\gamma$ B-crystallin variants was first exposed to chymotrypsin before phage particles were subjected to biopanning (2.2.3). The entire concept to use proteases in phage display selection is based on the assumption that unfolded proteins are more sensitive to proteolytic degradation (Imoto *et al.*, 1986). Provided that the filamentous bacteriophage retains the infectivity upon exposure to the site-specific proteases such as trypsin, chymotrypsin or GluC (Sieber *et al.*, 1998), the misfolded variants displayed on the surface of phage particles, which contribute to the non-stoichiometric and/or non-specific binding, should be removed by protease digestion (Pedersen *et al.*, 2002; Bai & Feng, 2004). The disulfide-constrained peptides encoded by frameshifted sequences were also expected to be eliminated by protease treatment.

#### **3.2.2.1 Affinity selection**

For selection of anti-E7 Affilin molecules via the proteolysis-based phage display approach, the pool of phage particles from the first round of selection described in 3.2.1 was used as an input. Following incubation of phage particles with chymotrypsin and chymotrypsin inhibition, the biopanning against E7 target protein was performed as described previously with exception of modified washing conditions used to remove non-binding phages (listed in 2.2.3). As calculated from the titration experiments, the phage infectivity after chymotrypsin treatment was decreased by a factor of 10. For selection, approximately  $10^{11}$  phage particles were used (Tab. 8).

In this approach, the amount of phage particles eluted after every selection round was lower in comparison to the conventional phage display selection (compare Tab. 5 and 8).

The biopanning was stopped after two cycles, since no evidence of further phage enrichment was observed. The specific clones were subjected to analysis.

**Table 8.** Output of different biopanning rounds in cfu/ml.

Selection round	Input phage, cfu/ml	Amount of eluted phage particles, cfu/ml
1 (described in 3.2.1.1)	$10^{10}$	$1 \times 10^6$
2	$10^{11}$	$4 \times 10^4$
3	$10^{11}$	$5 \times 10^5$

### 3.2.2.2 Analysis of individual clones by ELISA

Following two selection rounds with chymotrypsin treatment, the DNA pool encoding selected Affilin variants was subcloned into the pET-20b(+) vector and 96 randomly selected individual clones were pre-screened in ELISA as described for the conventional phage display approach (3.2.1.2). The  $A_{450}$  values are shown in Fig. 22.

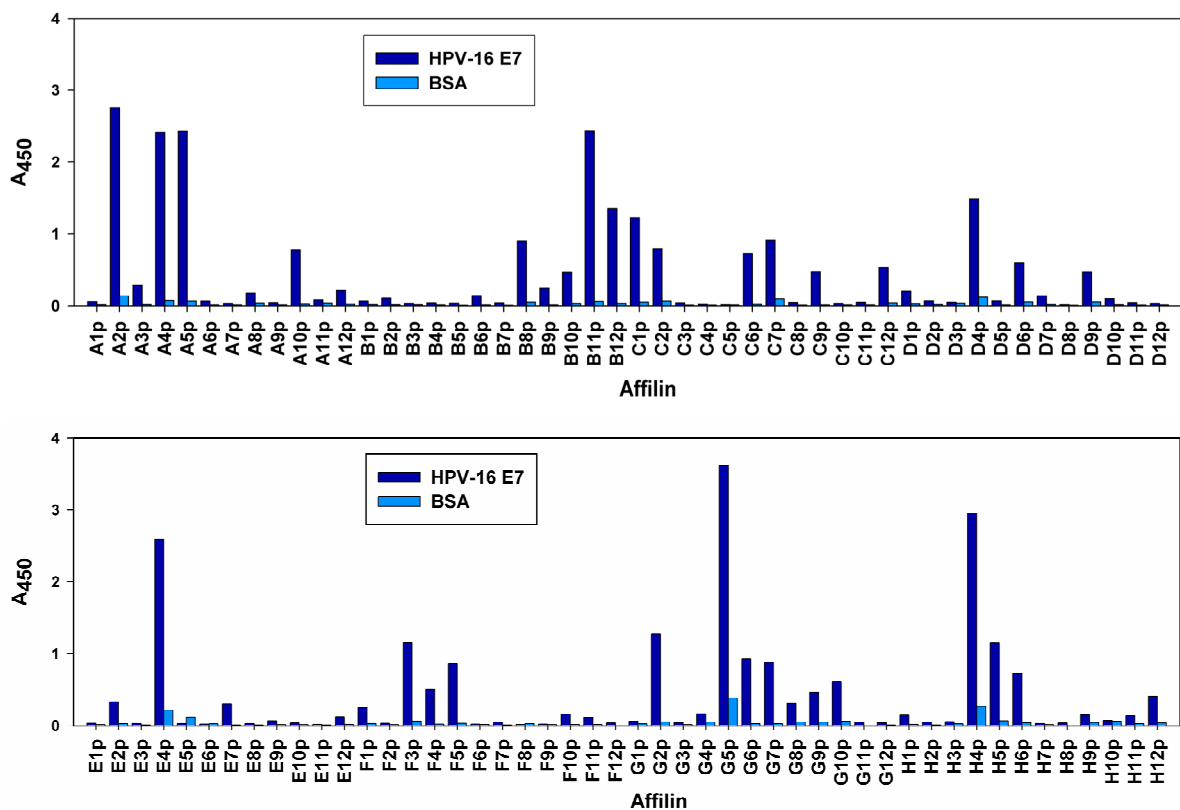


**Figure 22.** Identification of E7-specific Affilin variants obtained from the proteolysis-based phage display approach in the ELISA screening. The 96 randomly picked clones from the third round of biopanning against E7 protein were expressed and purified as described in 2.2.3. The proteins were applied to the wells of a microtiter plate coated with recombinant E7 target protein or BSA. Bound Affilin molecules were detected by an anti- $\gamma$ B-crystallin antibody conjugated to horseradish peroxidase in a chromogenic reaction. The absorption values at 450 nm are shown.

From analyzed clones, 26 showed strong signal ( $A_{450} > 0.5$ ) and revealed specific binding to the E7 target protein (ratio: E7/BSA binding  $> 5$ ). Only a small number of clones were unspecific (*i.e.* E7/BSA binding ratio:  $\leq 1$ ). Based on the ELISA signals, 22 clones were submitted for sequencing.

### 3.2.2.3 Sequence analysis of individual clones

The sequence analysis of 22 ELISA-positive clones revealed 19 clones carrying codon replacements in the anticipated positions. These sequences were clearly different from the wild-type  $\gamma$ B-crystallin scaffold with only few amino acid positions, particularly Arg36, remaining conserved (Tab. 9).

**Table 9.** Affilin clones selected after two rounds of proteolysis-based phage display approach against the HPV-16 E7 protein (deduced amino acid sequences at randomized positions are shown). Yellow boxes highlight hydrophobic amino acid residues (hydropathy index value  $> 0$  on the Kyte-Doolittle scale, Kyte & Doolittle, 1982). Basic residues are highlighted in blue and acidic residues in red. The TAG codon was considered as Gln (referred to as Gln\*) due to its suppression in *supE E. coli* strain. The variants with identical amino acid sequence are highlighted in green.

Protein	Randomized position							
	2	4	6	15	17	19	36	38
$\gamma$ B-crystallin	Lys	Thr	Tyr	Ser	Glu	Thr	Arg	Glu
A4p	Cys	Ser	Ser	Thr	Val	Gly	Arg	Asp
A5p	Val	Phe	Leu	Pro	Ser	Gly	Ala	Arg
A10p	Leu	Phe	Ile	Ala	Ser	Val	Pro	Ser
B8p	Gly	Arg	Cys	Arg	Met	Tyr	Gly	Gln*
B11p	Val	Pro	Leu	Arg	Ile	Arg	Arg	Tyr
B12p	Cys	Ala	Val	Pro	Gly	Ser	Val	Lys
C1p	Ser	Cys	Val	Arg	Trp	Thr	Trp	His
C6p	Cys	Ala	Val	Pro	Gly	Ser	Val	Lys
C7p	Phe	Leu	Leu	Gly	Tyr	His	Gln*	Ile
D4p	Ser	Ala	Val	Gln*	Thr	Gly	Met	Phe
E4p	Cys	Ala	Val	Arg	Lys	Arg	Lys	Arg
F3p	Phe	Ala	Ile	Glu	Lys	Gly	Arg	Gln
F5p	Gly	Arg	Ser	Arg	Met	Glu	Gly	Gln*
G2p	Cys	Tyr	His	Ile	Ile	Gly	Ser	Ser
G5p	Ala	Ala	Cys	Ala	Ala	Gly	Tyr	Cys
G6p	Leu	Ala	Ser	Phe	Arg	Met	Arg	Ile
G7p	Cys	Tyr	Gln*	Arg	Cys	Gln*	Ala	Phe
H4p	Leu	Phe	Arg	Glu	Ser	Gly	Gln*	Arg
H5p	Gly	Met	Tyr	Gly	Glu	Thr	Gln*	Gly

The variants obtained from the proteolysis-based phage display selection exhibited preferences for certain amino acid substitutions similar to that observed for clones obtained from conventional phage display approach (for comparison see Tab. 6 and 9). The hydrophobic amino acid residues occurred frequently and were found at positions 2, 4

and 6. Moreover, seven clones of 19 contained higher than expected content of basic exchanges, *i.e.* more than one Arg or Lys residue as calculated from the genetic NNK code used for the library design. The amber stop codon encoding the Gln residue in the *supE E. coli* strain was found in some clones. Two clones, *i.e.* B12p and C6p were identical at both DNA and protein level.

Of 22 analyzed clones, only three variants were not functional at the DNA level (*i.e.* clones A2p, C2p and H6p) having insertion or deletion of one nucleotide within the randomized NNK triplets. The truncated variants encoded by non-functional sequences could be displayed on the surface of phage particles by disulfide-mediated cross-linking with the pIII phage protein (McLafferty *et al.*, 1993; Paschke, 2006). The reduction of the number of aberrant clones achieved following this selection approach may indicate that these variants were indeed removed from the library pool by the means of chymotrypsin cleavage.

#### 3.2.2.4 Affinity determination

Prior to affinity determination, Affilin variants obtained from proteolysis-based phage display selection were expressed and purified as described previously (3.2.1.2). From two variants with identical amino acid sequence (*i.e.* B12p and C6p) only variant B12p was produced. It was possible to obtain approximately 0.4 to 16 mg of protein from 1 l of shake flask culture for individual clones under non-optimized conditions.

Following determination of the apparent  $K_d$  values from a concentration-dependent ELISA, one clone named G6p was identified to bind the E7 protein with the highest affinity (*i.e.* calculated  $K_d$  value was ~520 nM; Fig. 23).

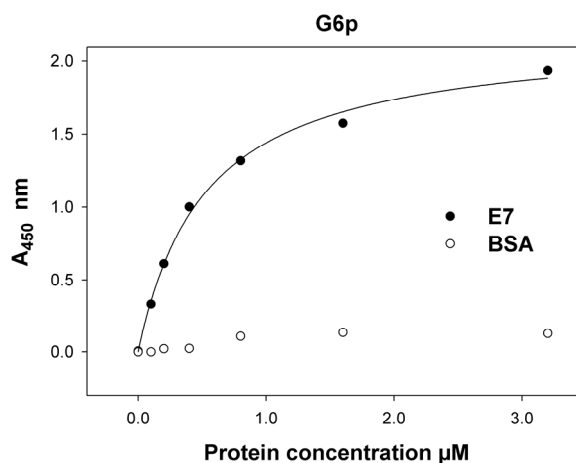


**Figure 23.** Determination of the apparent dissociation constant ( $K_d$ ) of Affilin-E7 binding using ELISA, exemplified for G6p variant selected by proteolysis-based phage display approach. The wells of the microtiter plate were immobilized with HPV-16 E7 (target) and BSA (control) and purified G6p was applied in a dilution series. Bound Affilin variant was detected by an anti- $\gamma$ B-crystallin antibody conjugated to horseradish peroxidase in a chromogenic reaction. The curve represents the nonlinear fit of the data to equation 3 (2.2.6.4). The calculated  $K_d$  was ~520 nM.

The B12p clone representing two identical clones bound the E7 protein with micromolar affinity ( $K_d \sim 6.6 \mu\text{M}$ ). Clones A4p, E4p, G5p and H4p revealed affinities in the low micromolar range (Tab. 10).

**Table 10.** The binding affinity data obtained for anti-E7 Affilin clones selected by proteolysis-based phage display approach. n.d., not determined.

Affilin	$K_d$
A4p	2.3 $\mu\text{M}$
B12p	6.6 $\mu\text{M}$
E4p	5.5 $\mu\text{M}$
G5p	1.1 $\mu\text{M}$
G6p	520 nM
H4p	2.6 $\mu\text{M}$
A5p, A10p, B8p, B11p, C1p, C6p, C7p, D4p, F3p, F5p, G2p, G7p, H5p	n.d.

The remaining clones bound to E7 in a concentration-dependent manner; however, as the binding curves did not reach equilibrium under protein concentrations applied in the assay, the apparent  $K_d$  values for these variants could not be determined. All analyzed variants were specific as only background signals were obtained for binding of these clones to BSA (for the G6p variant shown in Fig. 23).

In conclusion, both phage display approaches were successful yielding Affilin molecules that specifically bound the E7 target protein. The conventional phage display selection allowed identification of variants with the highest affinity ( $\sim 80$  nM and  $\sim 260$  nM  $K_d$  values were achieved for D1 and D4 variants, respectively). When proteolysis was included in the phage display protocol, the number of background clones encoded by frameshifted sequences was decreased as only three such variants were encountered among 22 analyzed clones. Both approaches led to the selection of Affilin variants exhibiting similar preferences for amino acid substitutions, in which the hydrophobic amino acids occurred frequently at certain positions and basic Arg and Lys residues were enriched in some clones. Consequently, the variants D1 and D4 showing the highest affinity to the E7 protein were chosen as primary candidates for further experiments.

### 3.3 Investigation of the Tat-mediated delivery of Affilin molecules

In recent years, cell-penetrating peptides (CPPs) have been widely used as a tool for intracellular delivery of different cargoes (reviewed in Gupta *et al.*, 2005; Wagstaff & Jans, 2006 and Foged & Nielsen, 2008). One of the most extensively studied CPPs is Tat derived from the HIV-1 Tat protein (Lindsay, 2002; Vives *et al.*, 2008). The Tat-conjugated cargoes were reported to translocate across the plasma membrane irrespective of the cell type (Joliot

& Prochiantz, 2004) and to localize to the cytoplasm and/or nucleus of cells (Schwarze *et al.*, 2000). For this reason, Tat-mediated transduction appeared to be a well-suited approach for the intracellular delivery of Affilin molecules. To address this issue, fusion constructs comprising Affilin and Tat peptide were engineered, characterized and tested for their ability to be taken up by mammalian cells.

As the investigation of Tat-mediated Affilin delivery was partially performed before the final selection of anti-E7 Affilin molecules, the non-related Affilin variants SPC-1-A1 and SPC-7-E9 referred to as A1\* and E9\*, respectively, were used in some experiments. The generation of Affilin A1\* and E9\* has been described by Ebersbach *et al.*, 2007.

### 3.3.1 Generation of Affilin-Tat fusion proteins

As the N-terminal domain of Affilin molecules contains a universal binding site, the Tat peptide had to be fused to the C-terminus in order to preserve the binding properties of Affilin molecules. In addition, a His<sub>6</sub>-tag was required to enable convenient purification of Affilin variants by IMAC. To assemble Tat and His<sub>6</sub>-tag at the C-terminus of Affilin molecules, the pET-20b(+) vector was modified in that two additional restriction sites were introduced downstream of the His<sub>6</sub>-tag (see 2.1.4). The annealed oligonucleotides encoding the Tat peptide (amino acids GRKKRRQRRPPQ corresponding to the positions 48 - 60 of the HIV-1 Tat protein) were inserted into the modified pET-20b(+) vector along with the genes encoding Affilin molecules D1 or D4. As the wild-type  $\gamma$ B-crystallin protein was used in all experiments as a control, a fusion construct encoding  $\gamma$ B-crystallin, C-terminal His<sub>6</sub>-tag and Tat peptide was generated as well.

### 3.3.2 Expression and purification of Affilin-Tat fusion proteins and $\gamma$ B-crystallin-Tat

The analysis of expression of Affilin variants D1 and D4 with or without Tat peptide in *E. coli* expression system under standard growth conditions revealed a high expression level that was, however, associated with the formation of insoluble protein aggregates, commonly referred to as inclusion bodies (Baneyx & Mujacic, 2004).

To obtain the native (*i.e.* correctly folded), and hence active form of the protein from inclusion bodies, solubilization followed by refolding can be carried out (Mayer & Buchner, 2004). Alternatively, to increase the fraction of soluble protein in bacterial lysates, strategies involving optimization of expression conditions can be employed (Sorensen & Mortensen, 2005). As soluble expression enables cost-efficient and easy production of proteins, the approach based on determination of optimum conditions for increased levels of soluble Affilin-Tat fusion proteins in recombinant *E. coli* cells was chosen in this study.

### 3.3.2.1 Optimization of the bacterial expression of Affilin-Tat fusion proteins

Due to the presence of several codons within the framework region of Affilin molecules that are rarely used by the *E. coli* host, the BL21-CodonPlus(DE3)-RIL strain which overcomes the codon bias problem was used for the expression of Affilin molecules.

To optimize the soluble expression of Affilin D1-Tat and D4-Tat, several growth and expression parameters were tested. In each case, the amount of soluble protein as well as the E7-binding activity of purified proteins were determined. First, the reduction of the growth temperature after induction was evaluated as a well known technique to limit the *in vivo* aggregation of recombinant proteins (Schein, 1991). It was found that the temperature shift to 25°C following induction increased the amount of soluble D1-Tat protein, whereas the temperature of 30°C was found to be optimal for the D4-Tat variant (data not shown).

The effect of the IPTG concentration on the soluble expression of Affilin-Tat molecules was also examined by using varied IPTG concentrations ranging from 0.1 to 1 mM. The reduction of the IPTG concentration below 1 mM resulted in a drop of the expression level of both Affilin variants (data not shown). However, as an increased amount of soluble protein was not achieved under these expression conditions, the concentration of 1 mM of IPTG was chosen for further experiments.

To determine the optimum cell density for the induction of protein expression, the IPTG at 1 mM final concentration was added to cultures at densities associated with the mid-log phase (*i.e.* OD<sub>600</sub> ~0.6) or the late-log phase (*i.e.* OD<sub>600</sub> ~1.3) for both Affilin variants. In general, the induction of protein expression during the mid-log phase is recommended (Berrow *et al.*, 2006). Surprisingly, induction of D1-Tat expression at the late exponential phase of growth was beneficial for soluble expression of this variant (data not shown). The same effect was not observed for D4-Tat variant and, consequently, this protein was expressed following induction at the mid-log phase.

Finally, the post-induction time was determined in the time course analysis of soluble expression. It was found that the highest productivity of soluble and active proteins was achieved after 16 and 4 h of expression for D1-Tat and D4-Tat variants, respectively (data not shown).

The  $\gamma$ B-crystallin-Tat control protein was expressed in *E. coli* BL21-CodonPlus(DE3)-RIL strain under following cultivation conditions: induction at OD<sub>600</sub> ~0.6 with 1 mM IPTG and 8 h incubation time at 30°C prior to cell harvesting.

Following optimization of expression conditions, Affilin-Tat fusion proteins as well as the  $\gamma$ B-crystallin-Tat were subjected to protein purification.

### 3.3.2.2 Purification of Tat-fused Affilin variants and $\gamma$ B-crystallin-Tat

As the proteins to be used in cell culture experiments require high purity, an additional chromatographic step was included in the protocol for purification of Affilin variants D1, D4 and the wild-type  $\gamma$ B-crystallin fused to the Tat peptide. Following the initial IMAC step, the protein fractions were purified on a HiTrap SP HP cation-exchange chromatography column.

The samples from various stages of protein expression and purification were evaluated by SDS-PAGE under reducing conditions (Fig. 24A, B and C).

The purified protein preparations contained single protein bands with a molecular weight of ~24 kDa, consistent with the predicted molecular weight of the  $\gamma$ B-crystallin-Tat fusion protein (Fig. 24, arrows). As estimated by SDS-PAGE, the protein preparation had a purity of more than 95%.

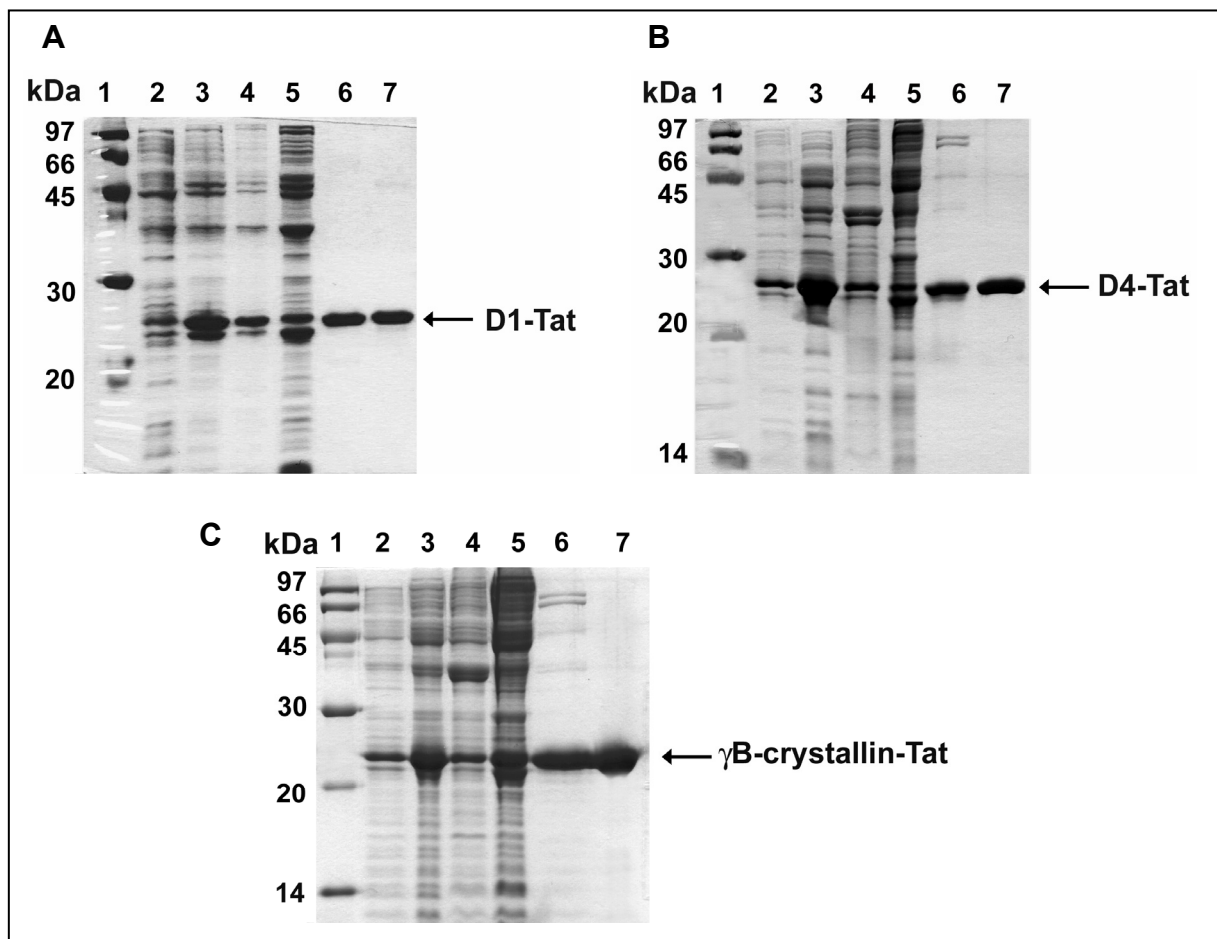


**Figure 24.** SDS-PAGE illustrating the purification of D1-Tat (A), D4-Tat (B) and  $\gamma$ B-crystallin-Tat (C). The proteins were resolved in a 15% reducing SDS-polyacrylamide gel and stained with Coomassie Brilliant Blue. Lane 1, low molecular weight protein marker (kDa); lane 2, cell extract from a non-induced culture; lane 3, cell extract from an induced culture; lane 4, insoluble protein fraction; lane 5, soluble protein fraction; lane 6, peak fraction after IMAC; lane 7, peak fraction after cation-exchange chromatography.

The protein purity determined by high-performance liquid chromatography on a PLRP-S reversed-phase column was in the range of 96 - 98% (for D4-Tat exemplified in Fig. 25).

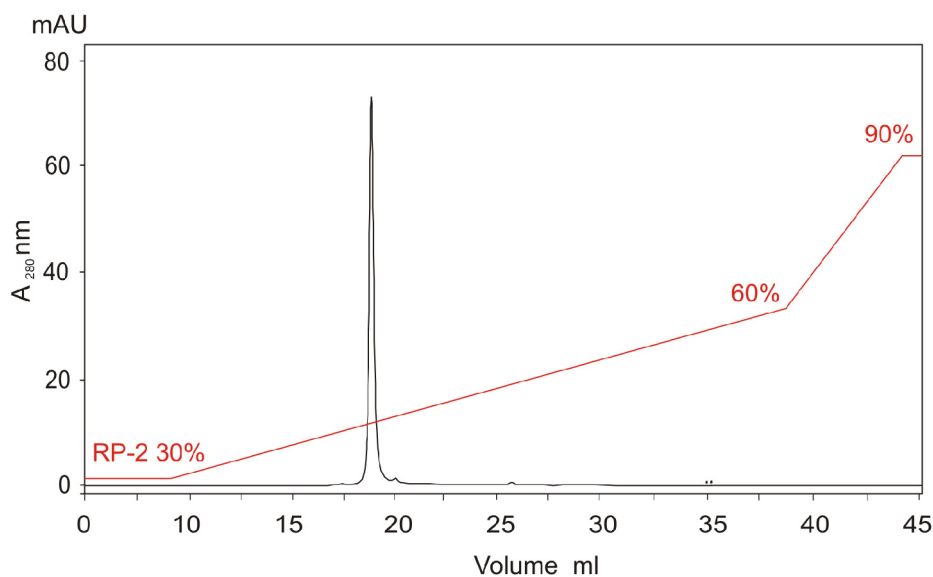


**Figure 25.** Reversed-phase separation used to assess the protein purity, exemplified for D4-Tat. The protein samples were injected on a PLRP-S column at a flow rate of 1 ml/min. As eluents, buffers RP-1 and RP-2 were used (2.1.11). The protein was eluted by a linear gradient from 30% to 60% of RP-2 in 30 min. The protein purity of D4-Tat defined as the amount of protein of interest compared to the sum of impurities was determined to be 98%.

Analytical size-exclusion chromatography on a TSK-Gel G2000SW<sub>XL</sub> column indicated that the anti-E7 Affilin-Tat variants as well as the wild-type  $\gamma$ B-crystallin-Tat were monomeric as only single peaks at the size expected for the monomer were observed (Fig. 26).

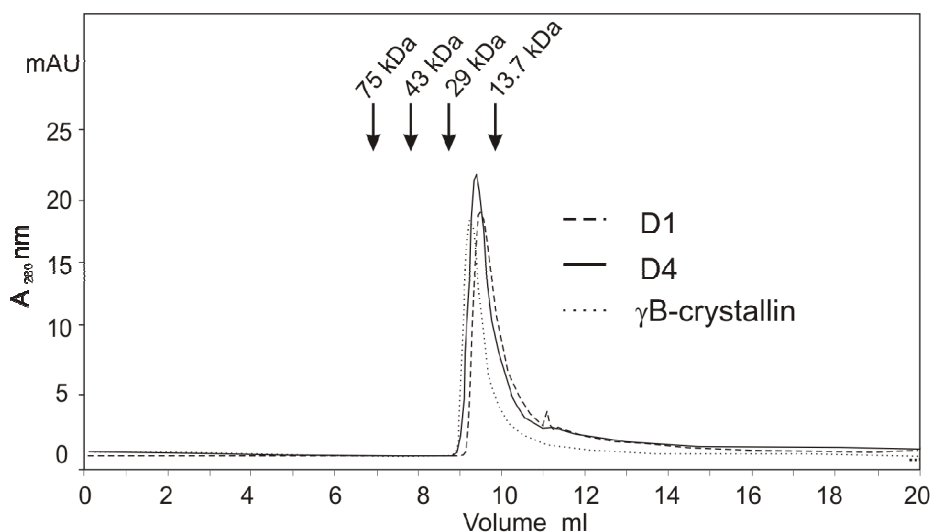


**Figure 26.** Representative elution profiles of D1-Tat, D4-Tat and  $\gamma$ B-crystallin-Tat from a TSKGel SW<sub>XL</sub>2000 analytical size-exclusion chromatography column. The chromatography was run in the ASE-1 buffer (2.1.11) at a flow rate of 1 ml/min. The arrows indicate the elution volumes of molecular mass standards (molecular mass in kDa given above the arrow).

Following optimization of the expression conditions, the yield of protein preparation obtained from 1 l of shake flask culture increased 13-fold (from 0.6 to 8 mg) and 3-fold (from 5 to 15 mg) for D1-Tat and D4-Tat, respectively. For the  $\gamma$ B-crystallin-Tat fusion protein, a significantly higher amount of purified protein was obtained (65 mg per 1 l of shake flask culture) suggesting that the introduced mutations might influence the *in vivo* protein folding in *E. coli* and, consequently, the final protein yield of Affilin molecules.

Lipopolysaccharides, being frequent contaminations of protein preparations obtained from *E. coli* cells, act as endotoxins by means of affecting the growth and function of mammalian cells in culture (Wille *et al.*, 1992; Han *et al.*, 1994). In order to minimize the endotoxin contamination, the protein samples after purification were incubated with Prosep-Remtox glass beads (2.2.5). As analyzed by *Limulus* amoebocyte lysate assay (2.2.5), the level of endotoxins in Affilin samples was below 50 endotoxin units (EU) per mg of protein preparation (1 EU corresponds to  $\sim$ 0.1 ng of endotoxin, Petsch & Anspach, 2000). Since the endotoxin content of less than 200 EU/ml has been shown to have no effect on the growth of several mammalian cell lines (Epstein *et al.*, 1990), it can be concluded that the endotoxin contamination of Affilin samples was below the limit of concern.

### 3.3.3 Characterization of Tat-fused Affilin variants and $\gamma$ B-crystallin-Tat

#### 3.3.3.1 Western blot analysis

To verify the presence of the Tat peptide in fusion constructs, Western blot analysis was performed with an anti-HIV-1 Tat antibody (2.1.9).

Specific signals were obtained corresponding to a molecular weight of  $\sim$ 24 kDa indicating the presence of the Tat peptide in fusion constructs (Fig. 27, lanes 4, 5, 6, arrow). The Affilin variants lacking Tat peptide did not react with an anti-Tat antibody (Fig. 27, lanes 1, 2, 3).

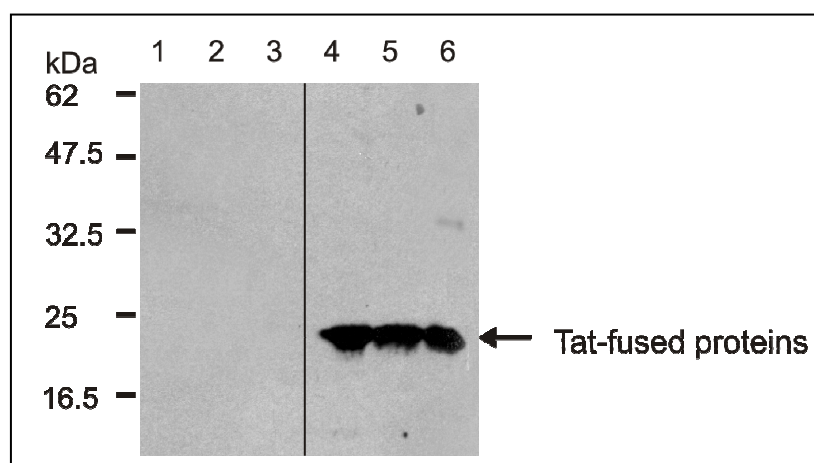


**Figure 27.** Western blot analysis of purified Affilin-Tat fusion proteins. Protein samples (5  $\mu$ g) were transferred to a nitrocellulose membrane and probed with an anti-Tat antibody. Immuno-reactive bands were visualized using ECL detection. Lane 1, D1; lane 2, D4; lane 3,  $\gamma$ B-crystallin; lane 4, D1-Tat; lane 5, D4-Tat; lane 6,  $\gamma$ B-crystallin-Tat.

### 3.3.3.2 Effect of the Tat peptide on the affinity of Affilin variants

To assess the influence of the C-terminal Tat peptide on the affinity of Affilin molecules D1 and D4, a concentration-dependent ELISA was performed. In this experiment, the apparent  $K_d$  values were determined as  $\sim 70$  nM and  $\sim 270$  nM for D1-Tat and D4-Tat, respectively (Fig. 28A and B). As the apparent  $K_d$  values for non-fused D1 and D4 Affilin molecules were in the same range (*i.e.*  $\sim 80$  nM and  $\sim 260$  nM for D1 and D4, respectively), it can be concluded that the C-terminal fusion comprising His<sub>6</sub>-tag and Tat peptide had no effect on the *in vitro* binding affinity of Affilin molecules. The specificity of Affilin-Tat fusion proteins was also retained, as both molecules did not bind to BSA (Fig. 28A and B). As expected, the wild-type  $\gamma$ B-crystallin protein analyzed in a control experiment showed no binding to the E7 target protein and BSA (Fig. 28C).

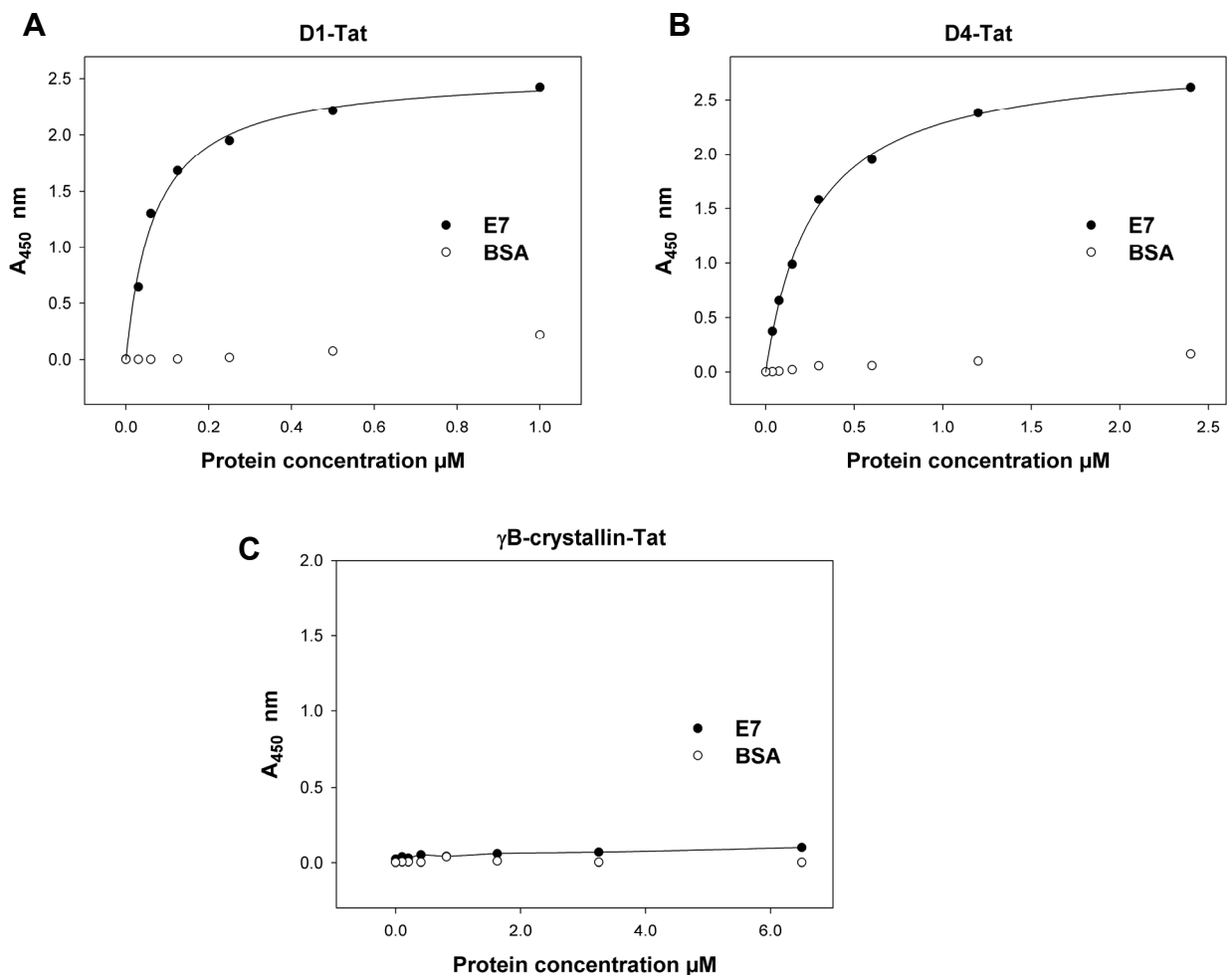


**Figure 28.** Evaluation of the target affinity of D1-Tat (A) and D4-Tat (B) as well as specificity of the  $\gamma$ B-crystallin scaffold (C) by ELISA. The wells of the microtiter plate were immobilized with HPV-16 E7 (target) and BSA (control) and purified Affilin variants and  $\gamma$ B-crystallin fused to the Tat peptide were applied in a dilution series. Proteins were detected by an anti- $\gamma$ B-crystallin antibody conjugated to horseradish peroxidase in a chromogenic reaction. The curves represent the nonlinear fit of the data to equation 3 (2.2.6.4). The calculated  $K_d$  values were  $\sim 70$  nM and  $\sim 270$  nM for D1-Tat and D4-Tat, respectively.

### 3.3.3.3 Binding characteristics of Affilin molecules investigated by surface plasmon resonance

To characterize the binding kinetics of Affilin-E7 interaction, surface plasmon resonance measurements were performed. In these experiments, the E7 protein was covalently linked to a CM5 biosensor chip using amine coupling (2.2.6.5). The achieved level of the ligand immobilization was approximately 5800 RU.

Purified Affilin variants were applied at several concentrations ranging from 37 to 600 nM for D1-Tat and 87 nM to 1.4  $\mu$ M for D4-Tat. The response curves (Fig. 29A and B) were globally fitted to the 1:1 Langmuir binding model using the BIAevaluation 3.1 software. According to this model, the binding sites of the E7 oligomer should behave as separate binding sites upon immobilization on the surface of the CM5 biosensor chip. As the experimental data did not fit to the model, the binding kinetics and affinities of Affilin-E7 interaction could not be determined by this approach.

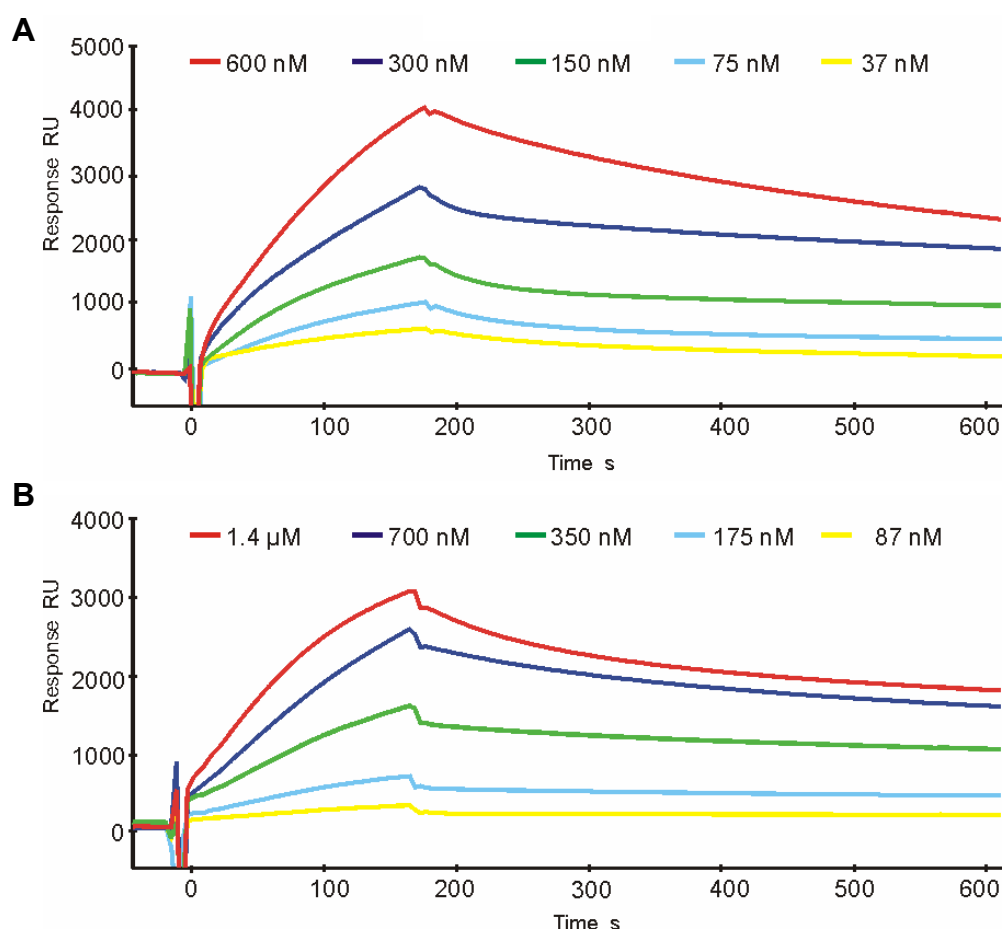


**Figure 29.** Surface plasmon resonance analysis of Affilin-E7 binding. Affilin molecules were applied at concentrations between 37 to 600 nM for D1-Tat (A) and 87 nM to 1.4  $\mu$ M for D4-Tat (B) to a flow cell with immobilized E7. The binding analysis was performed at a flow rate of 30  $\mu$ l/min. The sensorgrams were normalized by the resonance of the channel without E7 protein.

In addition to the kinetic analysis of sensorgrams, affinities can be derived from the analysis of the equilibrium binding experiment, in which the signal responses at the equilibrium for several analyte concentrations are used for calculations. As seen in Fig. 29, the sensorgrams in association phase for several Affilin concentrations showed a relatively steep slope, which did not reach a plateau. The lack of equilibrium state during the association phase precluded the calculation of Affilin-E7 affinities based on equilibrium measurements.

The oligomeric nature of the E7 protein, which probably leads to the heterogeneity of the binding sites on the surface of the biosensor, was considered as a major problem precluding the evaluation of the binding data. In case of a heterogeneous ligand, the binding phase seen on sensorgram reflects the sum of separate binding processes between the analyte and diverse binding sites, which exhibit different rate constants. In order to eliminate the heterogeneity of the E7 protein in SPR measurements, the E7 protein should be prepared in the monomeric form. However, the studies on bacterially expressed HPV-16 E7 show that this protein exists predominantly as a dimer or oligomer in solution depending on the purification procedure (McIntyre *et al.*, 1993; Chinami *et al.*, 1994; Alonso *et al.*, 2004). As demonstrated by sedimentation equilibrium experiments, the E7 protein reaches a monomer-dimer equilibrium with an apparent dissociation constant of approximately 1  $\mu\text{M}$  (Clements *et al.*, 2000).

Although the complex nature of the Affilin-E7 interaction obstructed the calculation of kinetic parameters, the sensorgrams presented in Fig. 29 demonstrated the binding of Affilin molecules to the E7 protein immobilized on a CM5 biosensor chip.

#### **3.3.3.4 Evaluation of the specificity of Affilin variants**

The binding specificity of anti-E7 Affilin molecules was demonstrated previously by using BSA as a control protein in ELISA experiments. To evaluate the specificity further, several unrelated proteins, *i.e.* amyloglucosidase, trypsin inhibitor, BSA, HSA, tumor necrosis factor  $\alpha$ , Fc fragment of the human IgG, melanoma inhibitory activity protein, nerve growth factor, ubiquitin and lysozyme were included in the experiment. These proteins were chosen to span a range of isoelectric point (pI) values from 3.6 (amyloglucosidase) to 11 (lysozyme). The binding data revealed that both Affilin molecules bound specifically to the E7 protein as no significant signal could be detected for other proteins tested, even those exhibiting an acidic pI similar to E7 (Fig. 30).

As expected, the wild-type  $\gamma\text{B}$ -crystallin protein evaluated under identical experimental conditions failed to bind any of the tested proteins (Fig. 30).

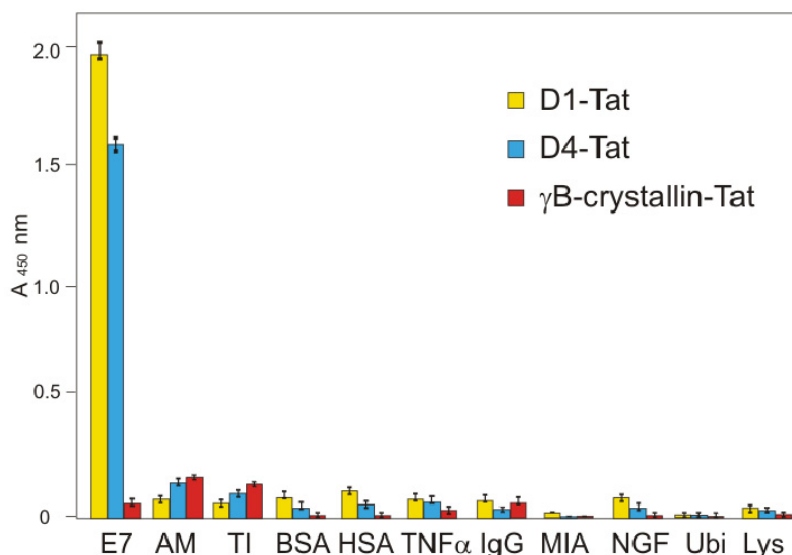


**Figure 30.** Specificity analysis of Affilin molecules and the wild-type  $\gamma$ B-crystallin. The proteins E7, amyloglucosidase (AM), trypsin inhibitor (TI), BSA, HSA, tumor necrosis factor  $\alpha$  (TNF $\alpha$ ), IgG Fc (IgG), melanoma inhibitory activity protein (MIA), nerve growth factor (NGF), ubiquitin (Ubi) and lysozyme (Lys) were immobilized on the wells of a microtiter plate. The Affilin molecules added at a concentration of 300 nM were detected by an anti- $\gamma$ B-crystallin antibody conjugated to horseradish peroxidase. The absorption values at 450 nm as the mean values of samples tested in triplicate are shown.

Following characterization of Affilin molecules fused to the Tat peptide, the proteins were tested for their ability to be taken up by mammalian cells.

### 3.3.4 Analysis of the cellular uptake of Affilin-Tat fusion proteins

To assess the efficiency of Tat-mediated transduction, Western blot analysis of total cell extracts and microscopic observations of cells incubated with Affilin-Tat fusion proteins were carried out.

#### 3.3.4.1 Western blot analysis of the Tat-mediated uptake

The Western blot analysis of Tat-mediated uptake of Affilin molecules was performed before the final selection of anti-E7 Affilin clones using the unrelated E9\* variant (Ebersbach *et al.*, 2007). For the purpose of this study, the construct comprising E9\* and the C-terminal Tat peptide was generated. The protein was expressed in *E. coli* BL21-CodonPlus(DE3)-RIL cells and purified under native conditions as described for other Affilin-Tat fusion proteins. The E9\*-His<sub>6</sub> control protein lacking the Tat peptide was prepared in the same manner.

The Western blot experiments presented in this section included the measurement of time and concentration dependence of protein uptake as well as the analysis of stability of the Affilin-Tat protein within cells. In these experiments, the NIH/3T3 mouse fibroblast cell line was used (2.1.2).

For concentration-dependent assessment, the NIH/3T3 cells were incubated with the E9\*-Tat fusion protein at a concentration ranging from 0.01 to 1  $\mu\text{M}$ . Following a 3 h incubation time, the cells were extensively washed with PBS to remove surface-bound proteins. The total cell lysates were prepared and subjected to Western blotting with an anti- $\gamma\text{B}$ -crystallin antibody (2.1.9).

The Western blot analysis revealed protein bands with predicted size (molecular weight of E9\*-Tat  $\sim 24$  kDa) suggesting an occurrence of the protein internalization (Fig. 31A). At a protein concentration of 0.01  $\mu\text{M}$ , the E9\*-Tat protein was not detected in the cell lysate. For higher protein concentrations, *i.e.* 0.1  $\mu\text{M}$  and 1  $\mu\text{M}$ , the level of protein in cell lysates increased suggesting a concentration-dependent manner of the uptake.

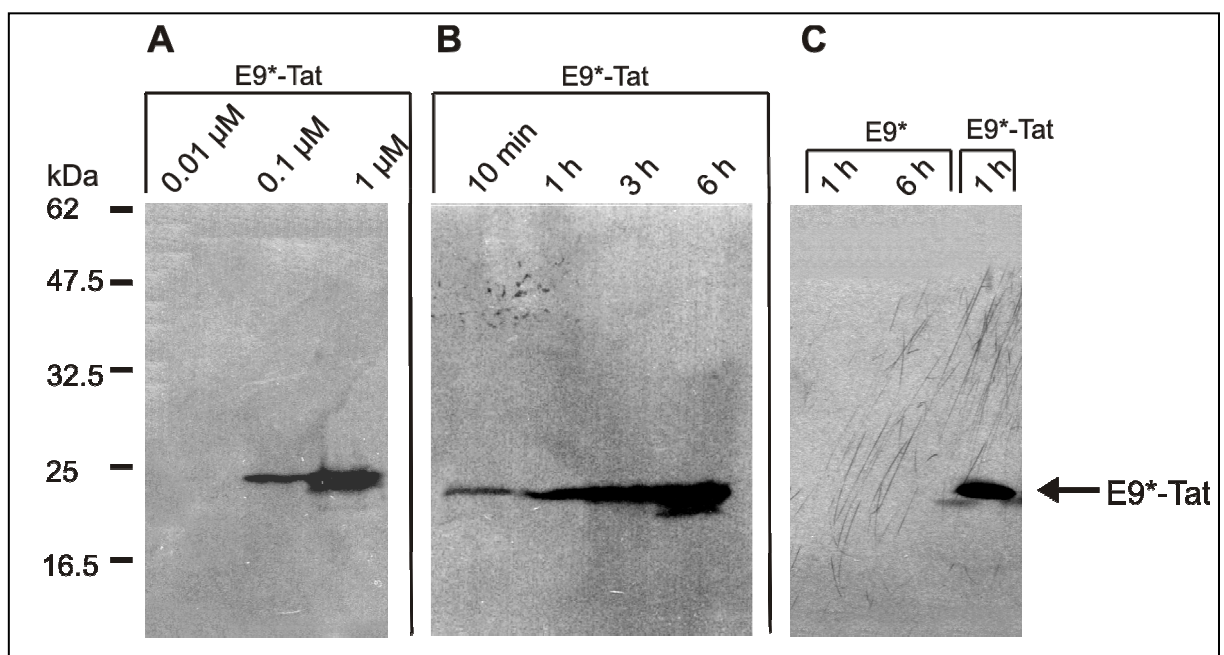


**Figure 31.** Western blot analysis of Tat-mediated protein uptake into the NIH/3T3 cells. (A), The E9\*-Tat protein was added to the cells for 3 h at a concentration of 0.01 to 1  $\mu\text{M}$  (indicated above the figure). (B), The E9\*-Tat protein (1  $\mu\text{M}$ ) was added to the cells for 10 min to 6 h (incubation time indicated above the figure). (C), The E9\* control protein (1  $\mu\text{M}$ ) was added for 1 h and 6 h to the cells whereas the E9\*-Tat protein (1  $\mu\text{M}$ ) was added for 1 h (protein incubation time indicated above the figure). Following extensive washing, the cells were harvested for preparation of total cell lysates. Protein transduction was analyzed by Western blotting with an anti- $\gamma\text{B}$ -crystallin antibody and ECL reagent.

To study the time course of Affilin-Tat internalization, the NIH/3T3 cells were incubated with the E9\*-Tat protein at a final concentration of 1  $\mu\text{M}$  for 10 min to 6 h. Following extensive washing and preparation of total cell lysates at indicated time points, the level of internalized protein was determined by Western blotting with an anti- $\gamma\text{B}$ -crystallin antibody. The intracellular Affilin-Tat fusion protein was detected already after 10 min of protein incubation time suggesting that Tat-mediated transduction is a very rapid process (Fig. 31B).

As the intensity of protein bands visually increased upon protein incubation time, it was assumed that the transduction process was time-dependent (Fig. 31B).

In a control experiment, the NIH/3T3 cells were incubated with the E9\* variant without Tat peptide at a 1  $\mu$ M concentration for 1 h and 6 h and the experiment was performed as described above. As shown in Fig. 31C, the control protein was not detected in protein lysates. The lack of protein internalization in case of the Affilin variant without Tat peptide implied the necessity of the Tat peptide for protein transduction.

To further evaluate Tat-mediated protein delivery, the stability of the E9\*-Tat protein within cells was examined. For this purpose, the NIH/3T3 cells were incubated with E9\*-Tat at a final concentration of 1  $\mu$ M for 6 h. The excess of protein was washed out and the cells were incubated in a fresh medium under standard culture conditions for additional 2 to 48 h. The cell extracts were prepared at indicated time points for Western blot analysis.

As shown in Fig. 32, the transduced E9\*-Tat protein appeared to be degraded in a time-dependent manner. However, the internalized protein was detected within NIH/3T3 cells even for up to 48 h (longer incubation time was not tested) demonstrating a remarkable stability of the internalized protein. This result had an implication for further studies, raising the possibility of investigation of intracellular activity of Affilin molecules for at least up to 48 h following internalization.

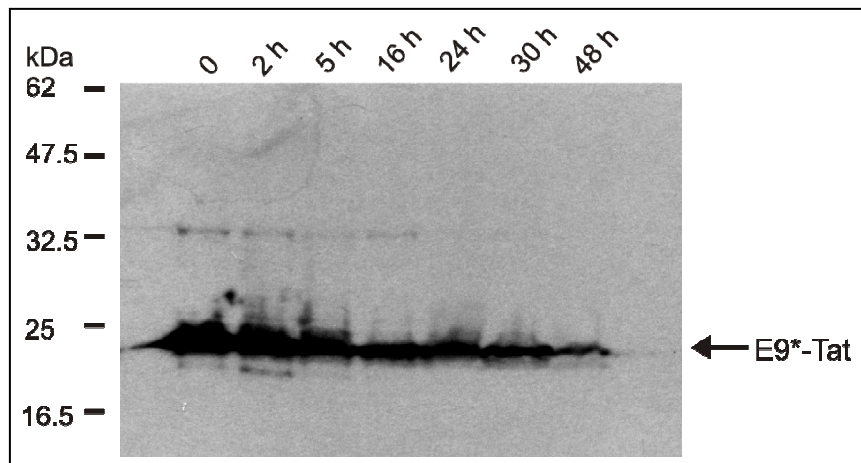


**Figure 32.** Western blot analysis of Tat-mediated protein uptake. The NIH/3T3 cells were pretreated with 1  $\mu$ M of the E9\*-Tat protein for 6 h, extensively washed and incubated in a fresh culture medium for further 2 - 48 h. The total cell lysates were prepared at several time points (indicated above the figure) and the E9\*-Tat protein was detected by Western blotting with an anti- $\gamma$ B-crystallin antibody and ECL reagent.

#### 3.3.4.2 Microscopic examination of the Tat-mediated internalization

The green fluorescent protein (GFP) is a useful tool for monitoring cellular processes in living cells using optical microscopy (Yuste, 2005). In an attempt to enable direct visualization of internalized Affilin-Tat protein in live cells, a fusion construct comprising the N-terminal

Tat peptide followed by an Affilin coupled C-terminally to the enhanced GFP protein (EGFP) (Yang *et al.*, 1996) through a peptide linker (Gly<sub>4</sub>Ser)<sub>2</sub> and His<sub>6</sub>-tag was generated. In this experiment the unrelated Affilin A1\* was tested (Ebersbach *et al.*, 2007).

The Tat-A1\*-EGFP-His<sub>6</sub> fusion protein as well as the control EGFP-His<sub>6</sub> protein without Tat peptide were expressed using *E. coli* BL21(DE3) cells. In contrast to the wild-type EGFP-His<sub>6</sub> protein, the fusion construct containing Affilin A1\* was mostly insoluble. The use of different expression conditions (*i.e.* IPTG concentration, induction duration, culture temperature) did not improve the level of soluble expression (data not shown). The attempts to purify the fusion protein from the soluble fraction yielded a very low protein amount, which was not sufficient for performing the fluorescence microscopic experiments. Thus, due to the problems with obtaining sufficient quantities of protein, an approach based on the use of GFP for detection of Affilin molecules in living cells was discontinued. As an alternative, the indirect immunofluorescence approach was used for determination of the intracellular localization of Tat-fused Affilin molecules. In these experiments, anti-E7 Affilin variants D1-Tat, D4-Tat and  $\gamma$ B-crystallin-Tat were evaluated. The E9\*-His<sub>6</sub> protein lacking Tat peptide was used as a control.

The protein uptake was investigated using a recombinant NIH/3T3 cell line, which constitutively expresses the HPV-16 E7 protein (referred to as NIH/3T3-E7; 2.1.2). The proteins were added directly to the medium of NIH/3T3-E7 cells at various concentrations ranging from 0.1 to 10  $\mu$ M and incubated for 1 h under standard culture conditions. The incubation step was followed by extensive washing of cells with PBS in order to remove membrane-bound proteins. The cells were fixed with methanol and subjected to immunostaining with anti-Tat or anti- $\gamma$ B-crystallin antibodies. Representative pictures of cells incubated with 1  $\mu$ M of indicated Affilin-Tat complexes stained with an anti- $\gamma$ B-crystallin antibody are shown in Fig. 33.

Both Affilin molecules as well as the wild-type  $\gamma$ B-crystallin localized exclusively to the nucleus of NIH/3T3-E7 cells. The same staining pattern was obtained regardless of the antibody used for detection of fusion constructs. The intracellular Affilin molecules as well as  $\gamma$ B-crystallin fused to the Tat peptide could be detected already at a 0.1  $\mu$ M protein concentration although low fluorescence intensity of the staining was observed (data not shown). The protein uptake appeared to be time-dependent as increased fluorescence intensity for longer protein incubation time was observed (data not shown).

In control experiments with the E9\*-His<sub>6</sub> protein lacking the Tat peptide, the cells showed no intracellular fluorescence signal indicating that the protein without the carrier peptide was not able to cross the cell membrane and thus was not present within cells (Fig. 33).

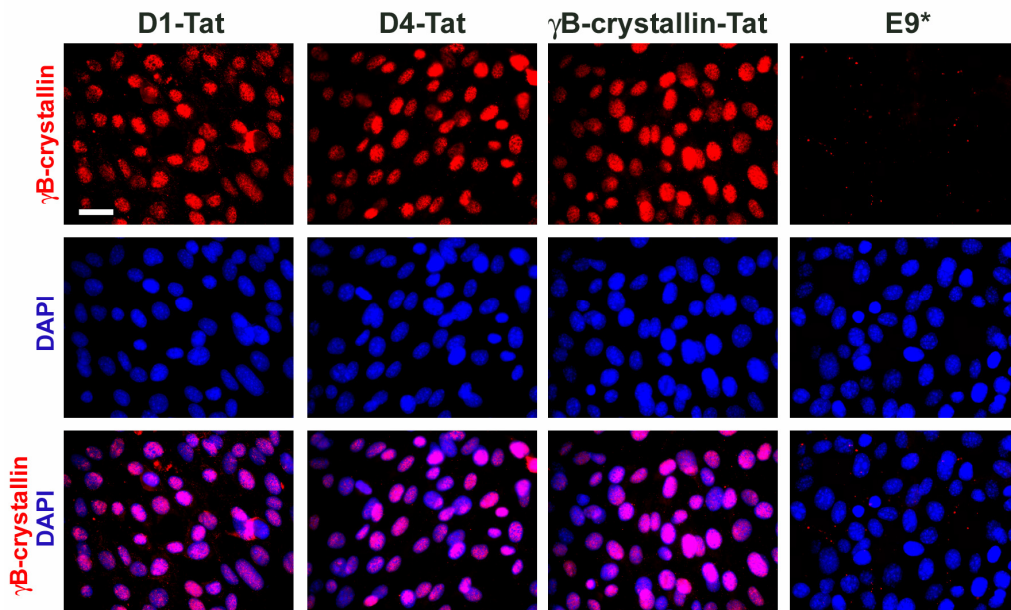


**Figure 33.** Immunofluorescence analysis of Tat-mediated uptake. The NIH/3T3-E7 cells were incubated for 1 h with D1, D4, and  $\gamma$ B-crystallin recombinant proteins fused C-terminally to the Tat peptide at a final concentration of 1  $\mu$ M. As a control, the E9\*-His<sub>6</sub> protein lacking the Tat peptide was used under identical experimental conditions. Following fixation with methanol, the cells were stained with an anti- $\gamma$ B-crystallin antibody (red). The cell nuclei were contrasted with DAPI (blue). The scale bar represents 50  $\mu$ m.

The results from indirect immunofluorescence studies were consistent with those obtained from the Western blot analysis. Both techniques suggested effective, concentration- and time-dependent uptake of Affilin molecules. Based on the immunofluorescence analysis, the internalized proteins were apparently localized in the nucleus of NIH/3T3-E7 cells.

In contrast to numerous studies demonstrating an efficient uptake of functional proteins attached to the Tat peptide (Asada *et al.*, 2002; Makino *et al.*, 2004; Wadia *et al.*, 2004), several reports raised doubts about how, if at all, Tat and other arginine-rich CPPs were able to deliver these molecules for their intracellular activity. Following the finding that fixation, commonly used for preparation of cells for fluorescence microscopy or flow cytometry, caused artifactual redistribution of Tat and other CPPs (Green *et al.*, 2003; Lundberg *et al.*, 2003; Richard *et al.*, 2003), the translocation of Tat has become a topic of an intense discussion in the literature, with sometimes contradictory conclusions being reported (reviewed in Brooks *et al.*, 2005 and Gump & Dowdy, 2007).

The highly cationic nature of Tat and other arginine-rich CPPs has been established as a major reason for the apparent localization of Tat in the nucleus of fixed cells (Brooks *et al.*, 2005; Nakase *et al.*, 2008). Due to the high content of basic residues, the Tat peptide can strongly bind to the negatively charged plasma membrane and is not removed from the cell surface by standard washing conditions. Following fixation, the cell surface-adsorbed peptides as well as peptides present within intracellular vesicles (such as endosomes or macropinosomes) probably leak into the cytosol. The positively charged Tat peptide

is then likely to bind to negatively charged structures within the cell such as nucleic acids, leading to redistribution of Tat during fixation and its apparent accumulation in the nucleus.

Based on these findings, previous experiments showing Affilin-Tat uptake by Western blot and indirect immunofluorescence approaches had to be reevaluated.

To reduce nonspecific migration of proteins upon fixation, a trypsinization step was included in the protocol for immunofluorescence analysis. The trypsin treatment, typically used for detaching the cells from cell culture supports, was expected to remove cell surface-bound Affilin-Tat proteins by digestion of the Tat peptide. To perform this experiment, NIH/3T3-E7 cells were incubated with proteins D1-Tat, D4-Tat and  $\gamma$ B-crystallin-Tat for 3 h, trypsinized, replated at the same cell density and allowed to attach to coverslips before immunofluorescence examination. The staining with an anti- $\gamma$ B-crystallin antibody was carried out using methanol and formaldehyde fixed cells. When trypsin treatment was included in the protocol, the cells did not show any intracellular immunofluorescence signal regardless of the fixation technique used (data not shown).

These results indicated that trypsin treatment removed surface-bound Affilin-Tat fusion proteins, which in previous experiments contributed to the artifactual nuclear staining. However, based on this examination, the internalization of Affilin-Tat could not be ruled out. The small amount of internalized protein present in intracellular vesicles is likely to leak into cytosol during fixation and permeabilization of cell membranes and thus to escape detection by standard immunofluorescence studies.

To verify the presence of Affilin-Tat fusion proteins in cells, Western blotting according to the protocol, which included trypsin digestion of cell membrane-adsorbed proteins prior to analysis, was performed. However, intracellular D1-Tat, D4-Tat and  $\gamma$ B-crystallin-Tat proteins were not detected in cell lysates probed with an anti- $\gamma$ B-crystallin antibody (data not shown). Again in this case, the possibility that a small fraction of protein was internalized but its level was too low to be detected by Western blotting could not be excluded. Nevertheless, such observations rose doubts about whether Affilin-Tat fusion proteins were translocated into the cytoplasm and directed into the nuclear compartment of cells at all.

Since Affilin-Tat molecules strongly adsorb to the cell membrane and endocytosis is likely to be the mechanism of Tat-mediated internalization (Brooks *et al.*, 2005), one could assume that this process took place. However, internalization of the protein into endosomes does not truly mean the intracellular delivery. The proteins internalized by cells via endocytosis remain trapped in the endosomal compartments and are targeted to the late endosomes or lysosomes, where enzymatic degradation and poor cytoplasmic release of intact molecules are anticipated (Melikov & Chernomordik, 2005; Richard *et al.*, 2005; Vives *et al.*, 2008). Thus, the efficient delivery of Affilin molecules into target cells via Tat peptide was considered as rather uncertain. For this reason, further studies on Tat-mediated Affilin

internalization were discontinued. For investigation of intracellular activities of anti-E7 Affilin molecules, transient transfection of target cells with corresponding mammalian expression vectors for expression of Affilin molecules was used.

### 3.4 Intracellular activity of transiently expressed Affilin molecules

Both, E6 and E7 proteins have the capacity to immortalize primary human keratinocytes (Munger *et al.*, 1989; Sedman *et al.*, 1991) and are necessary for the malignant transformation of HPV-positive human cervical cancer cells (von Knebel Doeberitz *et al.*, 1992; von Knebel Doeberitz *et al.*, 1994). These viral genes also possess proliferation-stimulating and transforming activity in a number of cell lines such as rodent NIH/3T3 fibroblasts (Yasumoto *et al.*, 1986; Caldeira *et al.*, 2000).

To examine the potential of anti-E7 Affilin molecules to repress the transforming activity of the E7 protein in the cell, two target cell lines were used, *i.e.* a recombinant NIH/3T3-E7 cell line positive for HPV-16 E7 protein (Edmonds & Vousden, 1989) and a human cervical carcinoma Ca Ski cell line which expresses E6 and E7 proteins from an integrated papillomavirus 16 genome (Yee *et al.*, 1985; Baker *et al.*, 1987).

#### 3.4.1 Transient expression of Affilin molecules in mammalian cells

As E7 is particularly localized to the nucleus of cervical cancer and recombinant cells (Greenfield *et al.*, 1991; Guccione *et al.*, 2002), Affilin molecules were expressed from the pCMV/myc/nuc vector carrying the C-terminal nuclear localization signal (NLS) from the SV40 large T antigen (DPKKKRKV)<sub>3</sub> and a c-myc epitope tag. The basic character of this fusion tag is similar to that of the Tat peptide. As Affilin variants containing the Tat peptide retained their *in vitro* binding properties (3.3.3.2), it was assumed that the NLS-c-myc-tag should not interfere with the E7-binding activity of Affilin variants in the cell as well.

To determine whether the expression of  $\gamma$ B-crystallin-related proteins in cells may in itself affect the cell phenotype, the pCMV/myc/nuc construct encoding the wild-type  $\gamma$ B-crystallin protein was also generated and used in all experiments as a control.

To establish the optimum conditions for mammalian expression of Affilin molecules, several transfection procedures were tested along with the optimization of transfection conditions, *i.e.* amount of transfection agent, DNA concentration and exposure time of transfection agent to cells.

The transfection of the NIH/3T3-E7 cells was achieved by a conventional calcium phosphate transfection procedure (2.2.7.3) with an efficiency estimated to be ~30%. In case of transfection of Ca Ski cells, a cytotoxicity problem was encountered when the calcium

phosphate transfection method or liposome-based transfection reagents were used. In other studies, Ca Ski cells were frequently transfected with recombinant viruses, based on their high transfection efficiency and lack of detectable toxicity (Kamio *et al.*, 2004; Wu *et al.*, 2006; Lagrange *et al.*, 2007). In this study, the Effectene reagent based on the non-liposomal lipid formulation allowed circumventing this problem (2.2.7.3). However, the transfection efficiency of Ca Ski cells using this reagent was relatively low, reaching approximately 5% of all cells. Such transfection efficiency is nevertheless acceptable for performing cell assays on the single-cell level. In addition, single-cell-based assays are particularly suitable for comparing cell lines with different transfection efficiencies, as it was encountered in this study.

The intracellular localization of Affilin variants and the wild-type  $\gamma$ B-crystallin protein in NIH/3T3-E7 and Ca Ski cells was examined by immunostaining using an anti- $\gamma$ B-crystallin antibody and co-staining of nuclei with DAPI. This confirmed the predominant nuclear distribution of proteins within cells. Figure 34 in the following section illustrates the typical expression pattern obtained for Affilin molecules expressed from the pCMV/myc/nuc vector in both target cell lines.

### **3.4.2 Evaluation of the intracellular activity of Affilin molecules**

Numerous studies have demonstrated that E7 inhibition at protein or mRNA level induces growth arrest (Choo *et al.*, 2000; Accardi *et al.*, 2005) or apoptosis (Nauenburg *et al.*, 2001; Jiang & Milner, 2002) in cervical cancer cells. Thus, the intracellular interaction of Affilin molecules with E7 was investigated indirectly by determination of the influence of Affilin expression on the cell proliferation and apoptosis in target cells.

#### **3.4.2.1 Antiproliferative effect of Affilin molecules**

For determination of proliferation rate, the Bromodeoxyuridine incorporation assay was performed (2.2.7.5). Bromodeoxyuridine (BrdU) is a thymidine analog, which becomes incorporated into newly synthesized DNA of replicating cells as a substitute for thymidine. Following pulse-labeling, BrdU is detected immunochemically allowing the assessment of the population of cells which are actively synthesizing DNA (Gratzner, 1982).

In this study, the double immunofluorescence staining was performed for simultaneous detection of BrdU and Affilin in cells. For quantitative purposes, the percentages of BrdU-positive cells were determined at 48 h post-transfection among the population of transfected cells. For each sample, reproducible results were obtained from three independent experiments.

When Affilin D1 and D4 were expressed in NIH/3T3-E7 cells, a significant inhibitory activity on cell proliferation was observed (Fig. 34A). The reduction of the proliferation rate was

in the range of 52% and 37% for Affilin D1 and D4, respectively, as compared to the cells expressing the wild-type  $\gamma$ B-crystallin scaffold (Fig. 34B).

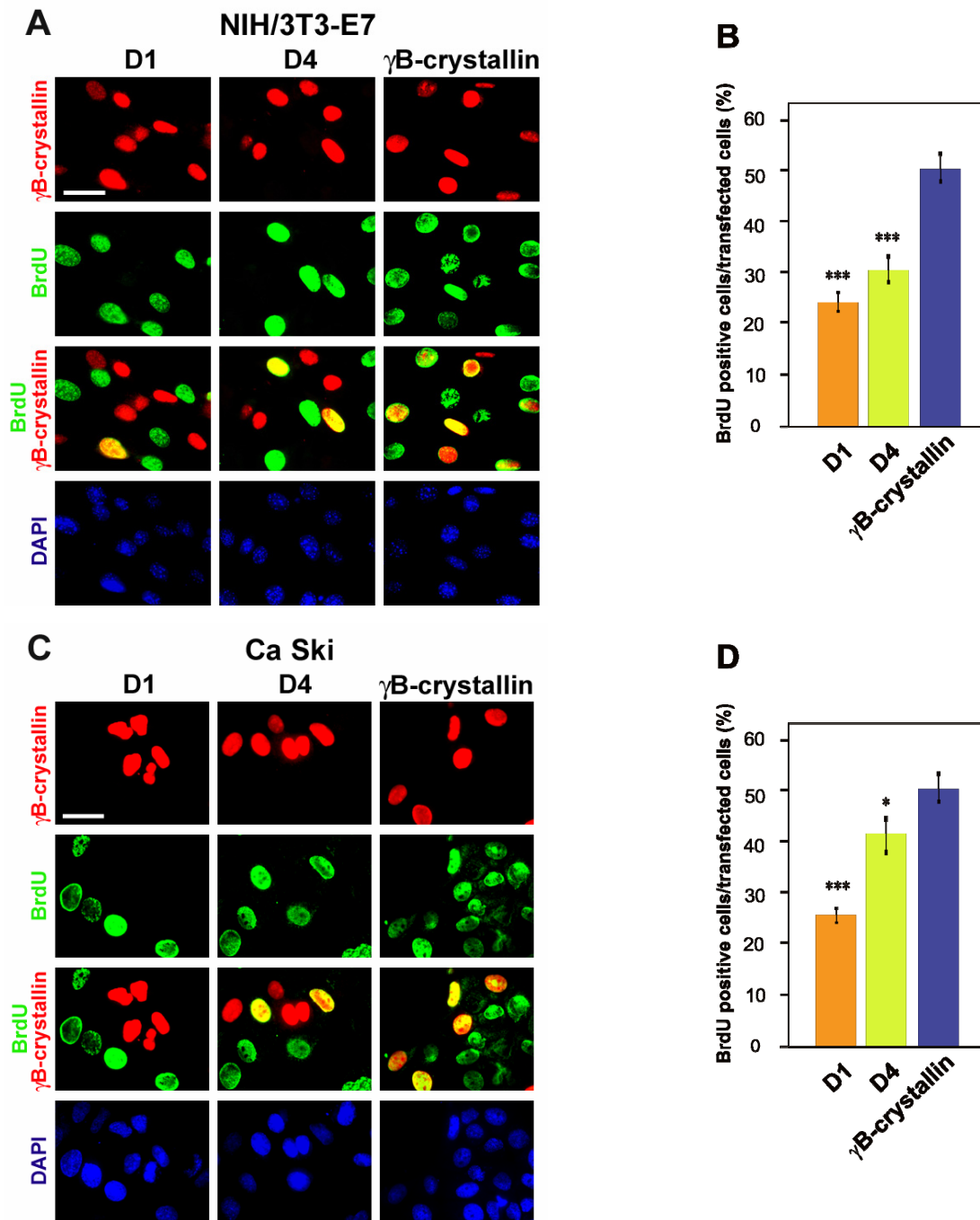
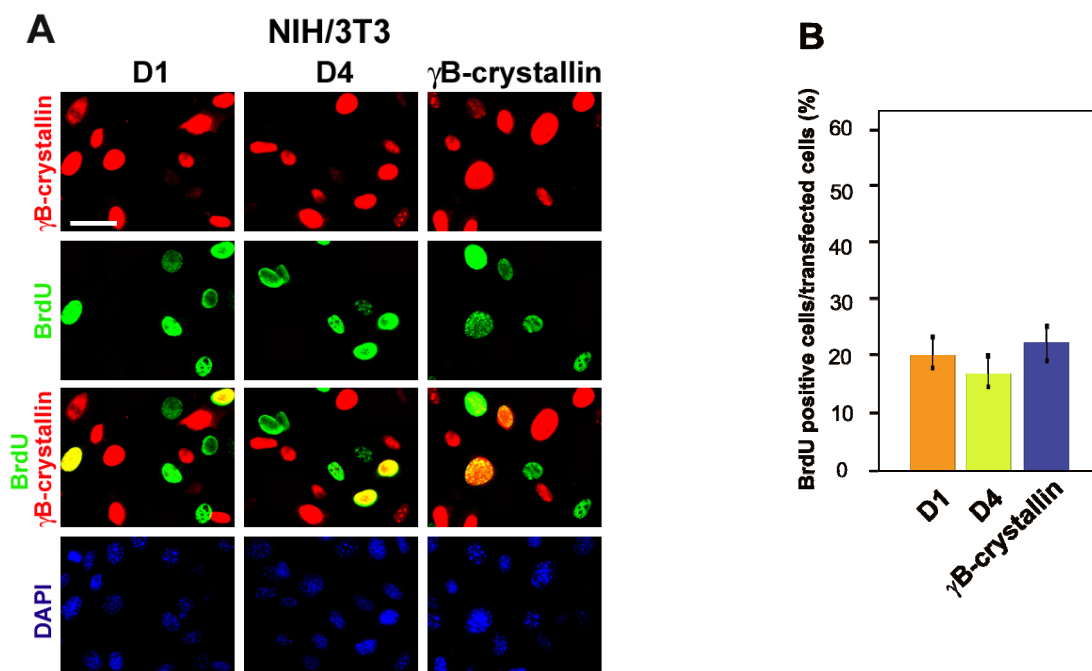


**Figure 34.** Analysis of proliferation of NIH/3T3-E7 (A, B) and Ca Ski (C, D) cells by BrdU incorporation assay. The cells were transiently transfected with vectors for the expression of indicated Affilin molecules or  $\gamma$ B-crystallin. BrdU incorporation was monitored at 48 h post-transfection by staining for BrdU (green). Additionally, the cells were stained for  $\gamma$ B-crystallin (red) and nuclei (DAPI; blue). The percentage of BrdU-positive cells was determined for at least 500 transfected cells counted for each sample. Data were analyzed using the Student's *t*-test where (\*) indicates  $P \leq 0.05$  and (\*\*\*) indicates  $P \leq 0.0005$  as compared to values obtained for cells expressing  $\gamma$ B-crystallin. Error bars indicate the standard deviation of the mean calculated from the three independent experiments. The scale bars represent 50  $\mu$ m.

A similar antiproliferative effect was also observed in Ca Ski cells expressing Affilin D1, whereas the inhibitory activity of the D4 variant was less evident in this cell line (Fig. 34C). The growth inhibition rates were 50% and 16% for Affilin D1 and D4, respectively, as compared to the cells expressing the wild-type  $\gamma$ B-crystallin scaffold (Fig. 34D).

To validate the selectivity of Affilin-induced inhibition of proliferation, the effect of expression of Affilin molecules on the proliferation of cells negative for HPV was examined. The control cell lines were: wild-type NIH/3T3, human cervical carcinoma C-33 A (Yee *et al.*, 1985) and human HEK-293 cell line transformed by introduction of adenovirus 5 DNA (Graham *et al.*, 1977).

The frequency of recombinant expression reached approximately 35%, 30% and 65% for NIH/3T3, C-33 A and HEK-293 cell lines, respectively. For determination of proliferation rate, the cells were analyzed under the same experimental conditions as E7-positive cells. The expression pattern of Affilin molecules and  $\gamma$ B-crystallin in the control cell lines was identical as observed in E7-positive cells (Fig. 35A, C and E). However, the proliferation rate of control cells was essentially unaffected by intracellular expression of Affilin molecules (Fig. 35B, D and F). These results indicated that the cell cycle arrest induced by expression and nuclear targeting of Affilin molecules was restricted exclusively to E7-positive cells. It is noteworthy that the proliferation of HEK-293 cells expressing Affilin molecules remained unchanged. This provided an additional evidence of the specificity of Affilin variants, which did not affect the growth of cells transformed by adenoviral E1A protein sharing certain functional and sequence similarities with E7 proteins from HPV (Chellappan *et al.*, 1992; Lee & Cho, 2002).



See next page for continuation of Fig. 35.

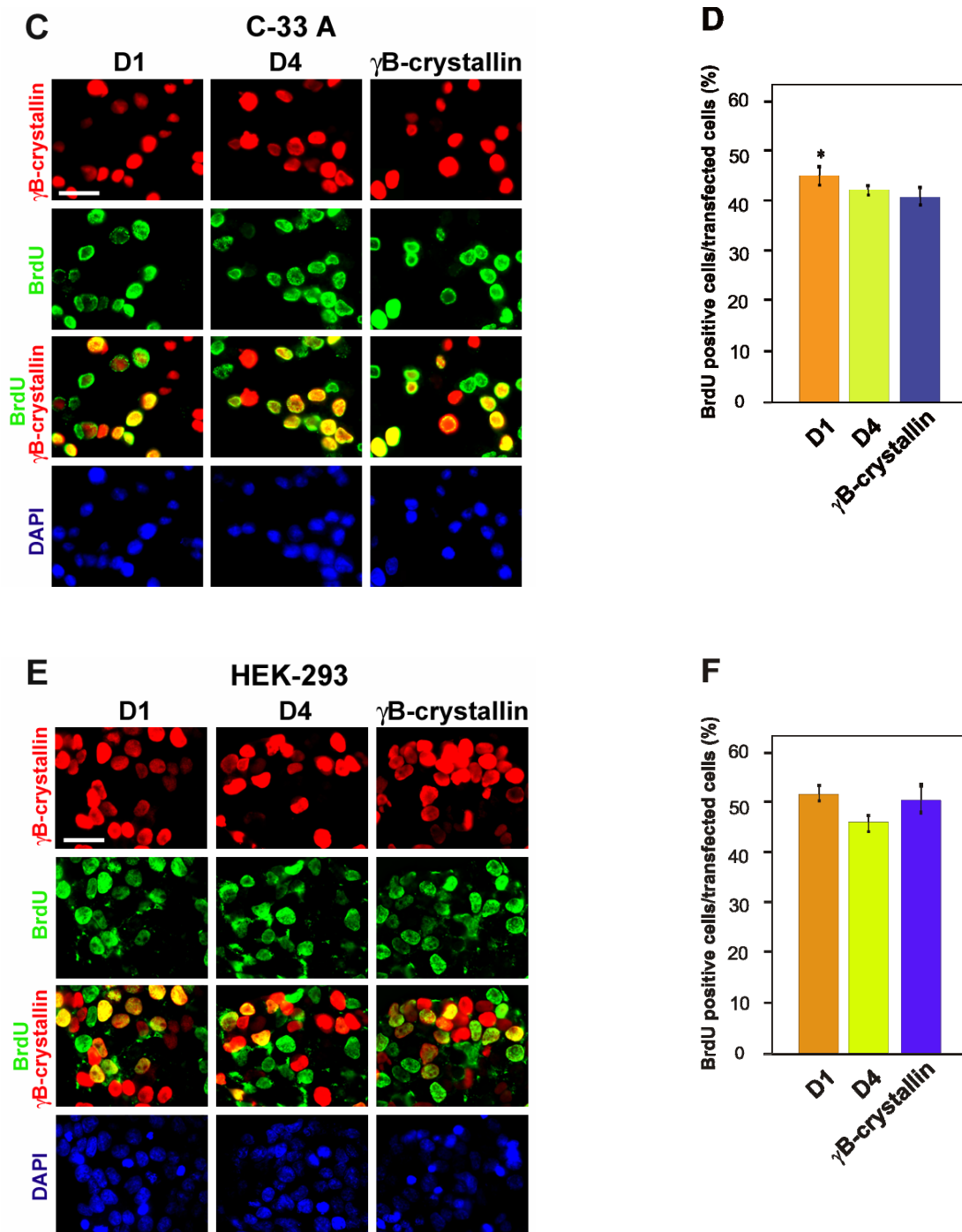


**Figure 35.** Analysis of proliferation of HPV-negative control cell lines, *i.e.* wild-type NIH/3T3 (A, B), C-33 A (C, D) and HEK-293 (E, F) by BrdU incorporation assay. The cells were transiently transfected with vectors for the expression of indicated Affilin molecules or  $\gamma$ B-crystallin. BrdU incorporation was monitored at 48 h post-transfection by staining for BrdU (green). Additionally, the cells were stained for  $\gamma$ B-crystallin (red) and nuclei (DAPI; blue). The percentage of BrdU-positive cells was determined for at least 500 transfected cells counted for each sample (D, E and F). Data were analyzed using the Student's *t*-test where (\*) indicates  $P \leq 0.05$  as compared to values obtained for cells expressing  $\gamma$ B-crystallin. Error bars indicate the standard deviation of the mean calculated from the three independent experiments. The scale bars represent 50  $\mu$ m.

### 3.4.2.2 Influence of the Affilin expression on the apoptosis of E7-positive cells

To further characterize the effect of Affilin expression on the phenotype of E7-positive cells, apoptotic cell death was examined by detection of DNA strand breaks of apoptotic cells *in situ* (2.2.7.6). The principle of this assay is based on the TUNEL (terminal deoxynucleotidyl transferase-mediated dUTP nick end labeling) reaction in which DNA strand breaks are labeled by incorporation of fluorescein-dUTP in an enzymatic reaction catalyzed by terminal deoxynucleotidyl transferase (TdT) (Gavrieli *et al.*, 1992). The fluorescein-dUTP-labeled DNA within apoptotic cells can be visualized directly by fluorescence microscopy.

As shown in Fig. 36, the number of apoptotic cells in the NIH/3T3-E7 cell line expressing D1 and D4 variants was slightly higher as compared to the cells expressing the wild-type  $\gamma$ B-crystallin scaffold. The occurrence of apoptosis in Ca Ski cells following transfection with Affilin D1 and D4 constructs remained unchanged.

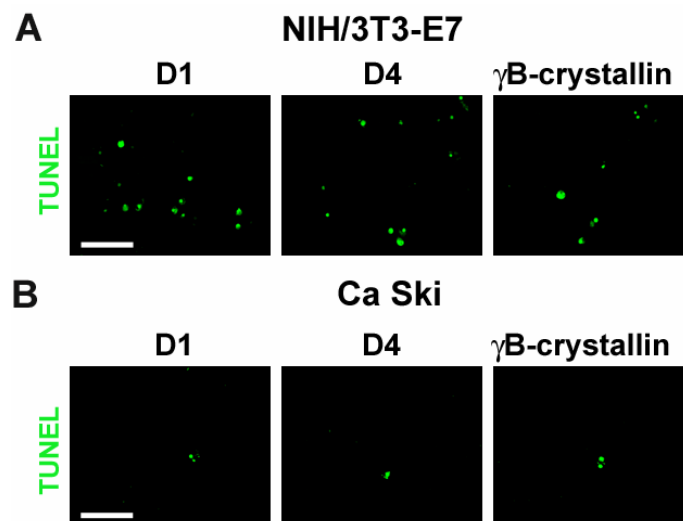


**Figure 36.** Examination of apoptosis in NIH/3T3-E7 (A) and Ca Ski (B) cell lines by detection of fragmented DNA *in situ*. The cells were transiently transfected with vectors for the expression of indicated Affilin molecules or  $\gamma$ B-crystallin. The labeling of DNA strand breaks by fluorescein-dUTP (green) was performed at 72 h after transfection and detected by fluorescence microscopy. The scale bars represent 100  $\mu$ m.

Taken together, these results showed that the transient expression of anti-E7 Affilin molecules D1 and D4 led to the inhibition of cellular proliferation. As shown in Fig. 34, Affilin molecules were detected in the nucleus of target cells, which is where E7 protein is predominantly localized (Greenfield *et al.*, 1991; Guccione *et al.*, 2002). This enables a direct interaction of Affilin molecules with this target protein leading to an impairment of the E7 protein function. The cellular effect was specific as it was found only for E7-positive cells expressing specific anti-E7 Affilin molecules. Thus, this study proves for the first time the effectiveness of Affilin molecules on a cellular level, thereby establishing the potential of these molecules for the generation of novel intracellular binding reagents.

## 4. Discussion

Binding proteins based on non-antibody scaffolds attract growing interest in both academia and industry. The principal applicability of this approach has already been demonstrated in various biotechnological and research areas previously restricted exclusively to antibodies (reviewed in Binz *et al.*, 2005; Hey *et al.*, 2005; Skerra, 2007). With regard to therapeutic applications, the concept of an alternative binding protein has already yielded the first drug candidates currently evaluated in clinical trials with some more undergoing preclinical studies (Gill & Damle, 2006; Skerra, 2007). As numerous alternative binding proteins are based on scaffolds that do not require disulfide bonds for stability, they seem to be optimal for intracellular applications, where single-chain variable antibody fragments show major limitations.

In this work, Affilin molecules based on the  $\gamma$ B-crystallin scaffold were investigated regarding their potential use in intracellular applications. The intrinsic features of the  $\gamma$ B-crystallin scaffold, *i.e.* small size, high thermodynamic stability, lack of disulfide bonds and human origin have been considered advantageous to such type of application.

For evaluation of the intracellular activity of Affilin molecules, the E7 protein encoded by human papillomavirus type 16 has been chosen as a model target.

### 4.1 Recombinant production of the E7 protein

As a prerequisite for the effective phage display selection of anti-E7 Affilin molecules, the HPV-16 E7 protein was produced as a His<sub>6</sub>-tag fusion using recombinant *E. coli* cells. The first attempts to express the E7 protein yielded a very low protein amount despite of optimization of expression parameters and using different *E. coli* strains. Following DNA sequence analysis it was found that the His2 and Gly3 codons form an alternative ATG start codon. It was hypothesized that the presence of an alternative initiation codon may result in translation of the E7 gene from an incorrect reading frame followed by expression of a short peptide and premature termination of translation (see Fig. 11).

To exclude the possibility of alternative translation initiation, a silent mutation into the codon for His2 was introduced. According to the ProteoExpert suggestions (Roche Applied Sciences; [www.proteoexpert.com](http://www.proteoexpert.com)), the codon for Pro6 was also modified. It should be noted that the introduced mutations were not advantageous regarding the codon usage of *E. coli*. However, using the optimized E7 gene it was possible to achieve a high expression yield of the E7 protein accounting for approximately 30% of the total protein.

The recombinant production of the E7 protein has been attempted previously using various expression systems, *e.g.* *E. coli* (Pahel *et al.*, 1993), baculovirus (Park *et al.*, 1993) or yeast (Braspenning *et al.*, 1997). The level of expression of unfused E7 protein in these

cases was low. Considerably higher expression yields were obtained for E7 N-terminally fused to various tags *e.g.*, glutathione S-transferase (Fernando *et al.*, 1999), maltose binding protein (Alonso *et al.*, 2002), ubiquitin (Roth *et al.*, 1992), or chelating peptides (Kasher *et al.*, 1993). It has also been observed that the E7 protein lacking the N-terminal tag showed a greatly reduced level of bacterial expression as compared to the N-terminally tagged variant (Patrick *et al.*, 1992). These data support the hypothesis put forward in this study that the alternative start codon formed by His2 and Gly3 codons is preferentially used by *E. coli* for the initiation of synthesis of the E7 protein.

Following optimization of the E7 gene sequence, the protein was purified from the soluble fraction using standard chromatographic methods. The yield of approximately 30 mg of protein per 1 l of bacterial shake flask culture has been achieved. The E7 protein produced in other *E. coli* expression systems was often insoluble and was purified under denaturing conditions with subsequent refolding (Patrick *et al.*, 1992; Fernando *et al.*, 1999). Thus, the approach presented here has proved to provide a fast and effective method for the production of recombinant E7 protein using soluble expression and purification under native condition.

The purified E7 protein migrated on the reducing SDS-polyacrylamide gel with an apparent molecular weight of ~16 kDa rather than according to its predicted molecular weight of ~12 kDa. The chemically synthesized HPV-16 E7 protein (Rawls *et al.*, 1990) as well as E7 proteins produced in other expression systems have been shown to display an apparent molecular weight of approximately 16 to 20 kDa (Smotkin & Wettstein, 1986; Stacey *et al.*, 1993; Fernando *et al.*, 1999). It has been suggested that the abnormal electrophoretic mobility of E7 on polyacrylamide gels is caused by the high content of acidic residues in this protein. The regions with a high negative charge are thought to interfere with SDS binding and thus to influence the protein migration (Armstrong & Roman, 1993). It has also been proposed that this effect may partially result from the high stability of the E7 structure, which is expected to be resistant to the combined effects of high temperature and SDS (Heck *et al.*, 1992; Alonso *et al.*, 2002).

Following analysis of the elution profile from the preparative size-exclusion chromatography column it was found that the E7 protein existed as an oligomer with a higher apparent molecular weight estimated to be approximately 700 kDa. This is consistent with previous studies in which several degrees of E7 oligomerization have been demonstrated (Chinami *et al.*, 1994; Clemens *et al.*, 1995). The E7 protein has also been reported to self-assemble into defined spherical oligomers with a molecular mass of ~790 kDa (Alonso *et al.*, 2004) which is similar to that observed for E7 oligomers obtained in this study.

The mechanism of E7 oligomerization has not been fully elucidated yet. The two CysXXCys motifs within the C-terminal part of the protein have been proposed to act as a dimerization

domain by way of bound zinc ions (Barbosa *et al.*, 1989; Clemens *et al.*, 1995). However, the formation of E7 oligomers from dimeric protein has been reported to require the zinc removal (Alonso *et al.*, 2004). As a non-specific chelating agent (EDTA) was used in this study, the authors concluded that other metals may play a role in the oligomer assembly (Alonso *et al.*, 2004). Resistance of E7 oligomers to the reducing agent (dithiothreitol) implies that the oligomerization process does not involve intermolecular disulfide bonding (Chinami *et al.*, 1994). Despite of a well-documented property of the E7 protein to form dimers and oligomers *in vitro*, the state of E7 in cervical cancer cells as well as the requirement of dimerization and/or oligomerization for the biological activity of this protein remain to be shown.

E7 is a multifunctional protein known best for its potential to inactivate the tumor suppressor pRb. Here, the biological activity of recombinant E7 protein was demonstrated by its ability to bind to pRb in the ELISA. The calculated apparent dissociation constant of E7-pRb interaction was ~20 nM which is comparable to that of HPV-16 E7 protein previously reported by Dong *et al.*, 2001 ( $K_d$  ~4.5 nM).

In this study, the binding of E7 to pRb was also demonstrated by surface plasmon resonance (see Fig. 17). Due to the complexity of the E7-pRb interaction involving so far undefined molar ratio of the E7 protein as well as the loss of pRb stability during measurements, the evaluation of kinetics and affinity based on the SPR measurements was not possible.

In summary, this study presents a feasible method for the soluble, cytoplasmic expression of the E7 protein using recombinant *E. coli* cells allowing its preparation in a sufficient quantity and quality for the use in phage display selection of Affilin molecules. As E7 proteins from different HPV types show high sequence homology (Munger *et al.*, 1991), the procedure described here may also be applied to the production of other E7 homologs.

## **4.2 Generation of intracellular Affilin molecules**

### **4.2.1 Phage display selection of Affilin molecules from a $\gamma$ B-crystallin library**

Affilin molecules binding E7 were first selected by conventional phage display approach with the E7 protein directly immobilized on a microtiter plate. Following analysis of 20 ELISA-positive clones from the round three of biopanning, two variants named D1 and D4 with E7-binding affinities in the nanomolar range (*i.e.*  $K_d$  ~80 nM and ~260 nM, respectively) were identified. The remaining clones bound the E7 protein with affinities in the micromolar range. Of them, seven clones sharing identical amino acid sequence, which initially suggested an enrichment of the high-affinity binding motif, revealed a relatively low affinity to the E7 protein ( $K_d$  ~5  $\mu$ M). The reason why this sequence dominated the pool of selected

anti-E7 clones is not clear. One possible explanation is that, due to the presence of the amber stop codon, the level of expression of these clones was significantly reduced and bacteria expressing these constructs gained a growth advantage over bacteria producing high amounts of pIII recombinant constructs. Moreover, the lower expression rate of amber containing clones may lead to the efficient transport of these constructs to the periplasm and their beneficial packaging. On the other hand, the enrichment of undesired clones may be associated with the problem of so-called stickiness of the phage particles (Barbass *et al.*, 2001; Paschke & Hohne, 2005). Such phage particles comprise protein sequences which do not fold properly in the periplasm and, as a result of a certain-degree misfolding, attain adhesive properties contributing to the non-stoichiometric and/or non-specific target binding (Paschke & Hohne, 2005). The enrichment of unstructured variants with adhesive properties is caused by limitations of the Sec-dependent translocation pathway utilized in most conventional phage display systems for translocation of pIII-fusion proteins into the bacterial periplasm (Fischer *et al.*, 1994; Rhyner *et al.*, 2002).

The characteristic feature of the Sec-dependent pathway is that it exclusively translocates unfolded polypeptides in a post-translational manner (Driessen *et al.*, 1998). The proteins that fold rapidly in the cytoplasm are therefore refractory to the Sec-mediated transport and are either degraded or, if sufficiently stable, they accumulate in the cytoplasm (Nilsson *et al.*, 1991; Huber *et al.*, 2005). Thus, the post-translational restriction of the Sec system eliminates stable and fast-folding proteins from the pool of phage-displayed library members. In addition, the variants which do not adopt a correctly-folded state in the periplasm, as they may require a cytoplasmic environment for folding, are attached to the phage particles being available for selection (Paschke & Hohne, 2005).

As an alternative to the Sec-dependent system, other *E. coli* translocation pathways can be utilized for the export of pIII-fusion proteins to the periplasm, e.g. the signal recognition particle pathway (SRP), in which the polypeptides are transported cotranslationally (Nagai *et al.*, 2003) or the twin-arginine translocation pathway, in which proteins are transported in a fully folded conformation (Muller, 2005). The phage display systems based on these alternative translocation pathways have already been shown to improve the display levels of pIII-fusion proteins on the filamentous bacteriophage. In these systems, the significant enrichment of functional clones has been achieved (Paschke & Hohne, 2005; Steiner *et al.*, 2008).

An additional problem encountered during the first phage display selection of anti-E7 Affilin molecules was the enrichment of nonfunctional sequences containing insertions or deletions in randomized NNK triplets. Such sequence exchanges resulted in frameshifts followed by one or more non-suppressed stop codons (*i.e.* TGA or TAA). Affilin molecules encoded by these nonfunctional sequences were presumably not functionally displayed on the phage

particles, as they were not in frame with the pIII phage coat protein. These variants, when subcloned into the pET-20b(+) vector and tested for expression in *E. coli*, were apparently not produced as full-length proteins. However, as the truncated peptide sequences contained Cys residues, they could be displayed on the surface of the phage particles by formation of disulfide bonds with the pIII protein (McLafferty *et al.*, 1993; Paschke, 2006).

The phage particles harboring nonfunctional sequences are enriched during selections mainly due to enhanced growth rates of bacteria not expressing the full-length pIII-fusion constructs (Carcamo *et al.*, 1998; Azzazy & Highsmith, 2002). For other randomized protein libraries it has also been observed that nonfunctional clones (which in case of the  $\gamma$ B-crystallin library account for 20% of all library members, Ebersbach *et al.*, 2007) sometimes dominate the selected pool of binders leading to the background binding (Carcamo *et al.*, 1998; Azzazy & Highsmith, 2002).

To improve the selection of high-affinity and functional anti-E7 Affilin molecules, an approach based on proteolytic digestion of phage particles with chymotrypsin was carried out.

In analogy to previous examples in the literature (Pedersen *et al.*, 2002; Bai & Feng, 2004), it was assumed that, when phage particles are treated with proteases, not-correctly folded variants which contribute to the non-specific and/or low-affinity binding should be removed from the library pool as being susceptible to proteolytic digestion. The variants encoded by frameshifted sequences were also expected to be eliminated by protease cleavage.

Following the proteolysis-based phage display selection, the number of nonfunctional clones was significantly reduced (only three frameshifted clones occurred between 22 sequenced clones). Among analyzed clones, one Affilin variant named G6p with nanomolar affinity ( $K_d \sim 520$  nM) and five micromolar affinity clones were identified. In contrast to the previous selection approach, the analyzed clones showed much higher sequence diversity. Furthermore, a common sequence pattern was identified in both selection experiments, which is discussed in more detail in the following section.

#### 4.2.2 Sequence analysis of selected Affilin variants

The sequence analysis of Affilin molecules obtained from both phage display approaches indicated a preference for certain amino acid substitutions (the deduced amino acid sequences of variants exhibiting the highest affinities are shown in Tab. 11). The hydrophobic amino acids, which could mediate the binding to the target protein via hydrophobic interactions, were frequently found within randomized positions. They occurred more frequently at positions 2 and 4. As compared to the theoretical content of Arg and Lys residues in the  $\gamma$ B-crystallin library (*i.e.* one basic residue per eight randomized positions), some variants revealed multiple basic side chain replacements. In case of Affilin D1 and D4

exhibiting the highest affinity to E7 among all identified Affilin clones, three out of eight amino acids were substituted for Lys and Arg residues.

**Table 11.** Deduced amino acid sequence at randomized positions for anti-E7 Affilin variants with the highest affinity arranged according to  $K_d$  values. Yellow boxes highlight hydrophobic amino acid residues (hydropathy index value >0 on the Kyte-Doolittle scale, Kyte & Doolittle, 1982). Basic residues are highlighted in blue and acidic residues in red. The TAG codon was considered as Gln (referred to as Gln\*) due to its suppression in *supE E. coli* strain.

Protein	Randomized position								$K_d$
	2	4	6	15	17	19	36	38	
$\gamma$ B-crystallin	Lys	Thr	Tyr	Ser	Glu	Thr	Arg	Glu	-
D1	Cys	Cys	Gly	Ala	Arg	Arg	Lys	Gly	80 nM
D4	Phe	Met	Thr	Arg	Asp	Gly	Lys	Lys	260 nM
G6p	Leu	Ala	Ser	Phe	Arg	Met	Arg	Ile	520 nM
G5p	Ala	Ala	Cys	Ala	Ala	Gly	Tyr	Cys	1.1 $\mu$ M
D5	Ala	Cys	Ser	Glu	Lys	Leu	Met	Gln*	1.2 $\mu$ M
A1	Ser	Val	Ala	Pro	Thr	Gly	Arg	Tyr	2.1 $\mu$ M
A4p	Cys	Ser	Ser	Thr	Val	Gly	Arg	Asp	2.3 $\mu$ M
H4p	Leu	Phe	Arg	Glu	Ser	Gly	Gln*	Arg	2.6 $\mu$ M
H12	Ala	Val	Gly	Cys	Thr	Ala	Cys	Gln*	3.1 $\mu$ M
A5	Ala	Cys	Ser	Glu	Lys	Leu	Arg	Gln*	5.0 $\mu$ M
E4p	Cys	Ala	Val	Arg	Lys	Arg	Lys	Arg	5.5 $\mu$ M
B12p	Cys	Ala	Val	Pro	Gly	Ser	Val	Lys	6.6 $\mu$ M
C3	Ala	Cys	Ser	Glu	Lys	Leu	Gln	Gly	14 $\mu$ M

The examination of the overall electrostatic potential of Affilin D1 and D4 revealed the presence of basic patches, particularly noticeable on the surface of the D1 variant, as compared to the surface charge distribution of the  $\gamma$ B-crystallin scaffold (Fig. 37).

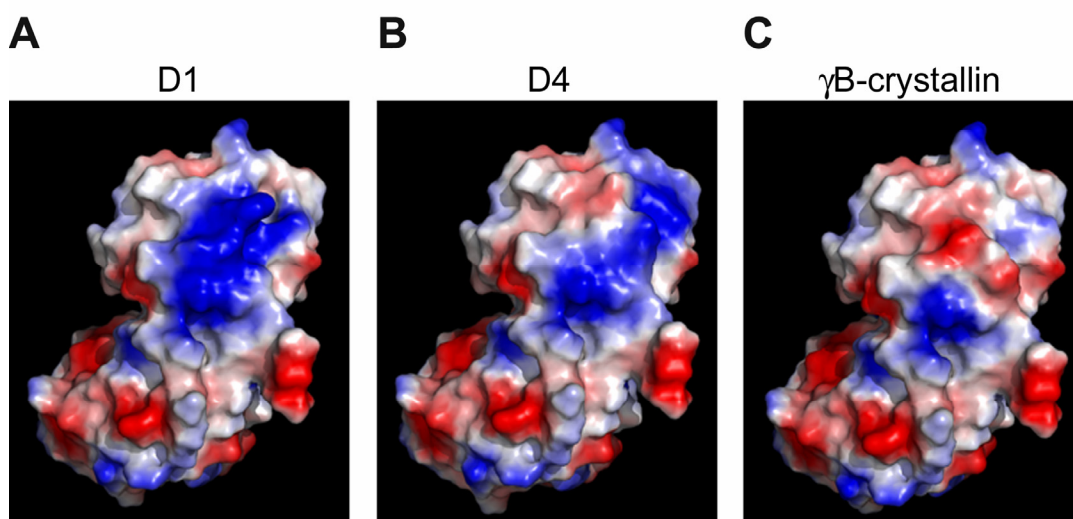


**Figure 37.** Examination of the electrostatic surface potential of Affilin molecules D1 (A), D4 (B) and  $\gamma$ B-crystallin (C). Charged amino acids are indicated in blue (basic: Arg, Lys or His) or red (acidic: Asp or Glu), and other residues are indicated in grey. Models based on coordinates and structure factors of human  $\gamma$ B-crystallin (PDB code 2JDF) were generated using PyMOL (<http://pymol.org>).

Considering the acidic nature of the HPV-16 E7 protein (theoretical pI is ~4.7), this might indicate that electrostatic interactions contributed to the Affilin-E7 binding as well. Similarly, conserved basic residues on the surface of the pRb pocket domain have been reported to make important contacts with acidic residues on E7 (Dick & Dyson, 2002).

As shown in Tab. 11, several Affilin clones revealed the presence of Cys residues within randomized positions in addition to seven free Cys residues present in the wild-type  $\gamma$ B-crystallin scaffold. The Cys residues represent a rather non-favorable amino acid substitution, as they are prone to several modifications such as formation of undesired intramolecular disulfide bonds or covalent dimerization leading to structural changes in protein folds, loss of stability and aggregation. It has been suggested that replacement of free Cys residues can prevent such undesired interactions thereby increasing the stability of the protein (Amaki *et al.*, 1994; Lett *et al.*, 1999; Fremaux *et al.*, 2002). In an attempt to prevent such undesired modification in the D1 variant, two Cys residues at the randomized positions 2 and 4 were exchanged for the structurally similar Ser residues. However, the D1-Ser2,4 mutant revealed a tenfold lower binding affinity as compared to the native D1 variant. As Cys and Ser residues differ in the hydrophobicity of their side chains (Nagano *et al.*, 1999), the Cys removal most probably reduced the binding affinity by the means of decreased hydrophobicity of the binding site.

#### 4.2.3 Comparison of binding affinities of Affilin molecules and other binding proteins

The binding affinities of anti-E7 Affilin molecules calculated here were comparable to those of the first-generation Affilin molecules selected against targets such as human IgG Fc, proNGF or steroid hormones (Ebersbach *et al.*, 2007). These Affilin molecules achieved dissociation constants in the micromolar to nanomolar range with one variant, namely SPC-7-E9 (referred in this study to as E9\*), exhibiting the affinity in the low nanomolar range ( $K_d$  ~6 nM) (Ebersbach *et al.*, 2007).

Considering the relatively small size of the  $\gamma$ B-crystallin library and the fact that Affilin molecules were selected from a primary screening without further maturation, these dissociation constants were quite high. Such affinities are comparable to that of murine monoclonal antibodies generated from a secondary immune response. The dissociation constants of murine monoclonal antibodies usually vary between 10 and 100 nM (Foote & Eisen, 1995). The primary screening of phage-displayed recombinant single-chain antibody fragments typically yields affinities in the micromolar to nanomolar range, which are then improved by several *in vitro* affinity maturation approaches (Rajpal *et al.*, 2005; Wark & Hudson, 2006).

The binding proteins based on alternative scaffolds usually achieve micromolar to nanomolar affinities (Hosse *et al.*, 2006) with some variants reported to show even picomolar binding

(Stoop & Craik, 2003). The alternative binding proteins evaluated in intracellular studies exhibited a broad range of affinities. DARPins derived from designed ankyrin repeat proteins bound their targets with affinities in the micromolar to sub-nanomolar range (Amstutz *et al.*, 2005; Amstutz *et al.*, 2006; Kawe *et al.*, 2006). Other intracellular alternative binding proteins such as monobodies derived from the fibronectin type III scaffold selected against estrogen receptor  $\alpha$ , showed rather low affinities as examined by  $\beta$ -galactosidase assay in the yeast two-hybrid system (Koide *et al.*, 2002).

The affinities of Affilin molecules could be improved by optimization of the selection strategy. Factors that influence the outcome of the phage selection are: concentration of the target molecule, incubation time of the phage library with the target, temperature, pH, ionic strength and stringency of washing conditions as well as the elution strategy and the number of selection cycles (Barbass *et al.*, 2001; Lou *et al.*, 2001). In addition to the selection on immobilized target, as performed in this study, the selection on a biotinylated target in solution may permit a more controlled enrichment of binding molecules with higher affinities (Lou *et al.*, 2001).

It is well recognized that the size of the library determines the affinity of selected binding molecules - the larger the library, the higher the probability of finding high-affinity binders (Ling, 2003; Hoogenboom, 2005). In case of antibody fragments, a library of  $10^7$  -  $10^8$  members typically allows the selection of clones with affinities of up to 10 nM, whereas from libraries with over  $10^9$  members, binders with sub-nanomolar affinities can be selected (Ling, 2003). As the size of the phage display library is limited to  $\sim 10^9$  clones by the efficiency of transfection of DNA into bacteria, fully *in vitro* selection approaches such as ribosome display or mRNA display, which do not require transformation of living cells, allow generation of very large libraries of up to  $10^{14}$  members (Rothe *et al.*, 2006). From such libraries, usually binders with much higher affinities are generated (Lipovsek & Pluckthun, 2004). Thus, the generation of a larger  $\gamma$ B-crystallin library suitable for alternative *in vitro* selection systems would possibly allow selection of binders with higher affinities. Furthermore, to increase the combinatorial complexity of the library, additional amino acid positions could possibly be randomized. However, the diversification of a scaffold is only possible to a limited extent, in that the stability of the scaffold is not altered significantly. Thus, the tolerance of the  $\gamma$ B-crystallin protein architecture for more amino acid exchanges should be tested beforehand.

Finally, several maturation approaches such as error-prone PCR (Thie *et al.*, 2009), hotspot randomization (Yau *et al.*, 2005), site-directed mutagenesis (Furukawa *et al.*, 2007) or mutator strains of *E. coli* (Coia *et al.*, 2001) can be employed for the selection of molecules with higher binding strength.

#### 4.2.4 Specificity of Affilin molecules

The target specificity is an important requirement, which needs to be met when binding reagents are developed for various biotechnological and pharmaceutical applications.

The anti-E7 Affilin molecules generated in this study specifically bound the target and did not cross-react with other proteins tested in the ELISA. The lack of appreciable association with proteins of acidic pI similar to E7 (*i.e.* amyloglucosidase and trypsin inhibitor, pI 3.6 and 4.6, respectively) suggested that electrostatic interactions were specific determinants of the binding of these Affilin molecules to E7.

To provide further evidence of Affilin specificity, the interaction with proteins sharing sequence similarities to E7 target protein would be required. Such specificity testing might include E7 proteins from other HPV types, adenovirus E1A protein or SV40 large tumor antigen. All these proteins share sequence similarities with HPV-16 E7 such as conserved LeuXCysXGlu pRb-binding motif followed by a patch of acidic residues (Dahiya *et al.*, 2000; see Fig. 9). Considering the sequence homology of E7 proteins from different HPV types (Munger *et al.*, 1991), it would be challenging to attempt the selection of Affilin variants recognizing certain conserved E7 epitopes. Such E7 binders could be possibly used for the inhibition of growth of other cells driven by HPV to proliferate.

#### 4.2.5 Recombinant production of Affilin molecules

As a protein scaffold, the  $\gamma$ B-crystallin possesses favorable properties such as high solubility and thermodynamic stability, which is independent from intramolecular disulfide bonds. These intrinsic properties of  $\gamma$ B-crystallin were considered promising for the generation of novel binding molecules in the first place. Such features usually allow the production of functional molecules using expression in bacterial cytoplasm, which is cost-effective and more productive than eukaryotic cell cultures commonly used for antibody production.

The analysis of expression of a number of anti-E7 clones using recombinant *E. coli* cells revealed a high level of expression but was associated with the formation of inclusion bodies. However, in each case the yield of soluble expression was sufficient to purify these protein variants under native conditions. The amount of purified protein obtained from 1 l of shake flask culture under non-optimized conditions varied for individual clones independently of the selection approach, reaching typically 0.4 - 18 mg. For the wild-type  $\gamma$ B-crystallin protein, the amount of purified protein was 65 mg per 1 l of culture. This suggests that amino acid exchanges within the randomized region of Affilin clones influenced the protein folding and solubility. As Affilin variants contained several hydrophobic substitutions, their association during folding in the bacterial cytoplasm could possibly prompt these proteins to form inclusion bodies. Moreover, the oxidative cross-linking of Cys residues might also have induced the aggregation of some clones during purification procedures. However,

as mentioned previously, an approach to exchange undesired Cys residues into Ser was not feasible, as such modification resulted in the reduction of the target-binding affinity (see 3.2.1.5).

Due to demand for increased quantities of Affilin-Tat molecules required for protein delivery experiments, the *E. coli* culture conditions for expression of these variants were optimized. In contrast to generally recommended procedures (Berrow *et al.*, 2006), the induction of expression of D1-Tat at the late mid-log phase of growth of *E. coli* host cells was crucial for improving the level of soluble expression. The D1-Tat protein prepared from such culture was functionally active as it bound E7 with an average dissociation constant of ~80 nM. Other examples in the literature show that in some cases induction of protein expression at the late mid-log phase or even stationary phase of *E. coli* growth may significantly enhance the yield of soluble and functional protein expression (Galloway *et al.*, 2003; Ou *et al.*, 2004). For Affilin variants D1-Tat and D4-Tat, the reduced growth temperature also contributed to higher amounts of soluble protein in *E. coli* cell lysates. Following optimization of expression conditions, the yield of protein preparation from 1 l of shake flask culture increased 13-fold (from 0.6 to 8 mg) and 3-fold (from 5 to 15 mg) for D1-Tat and D4-Tat, respectively.

The protein yields of anti-E7 Affilin clones were similar to that obtained for the first-generation Affilin variants, where the amounts of ~1 to 16 mg of purified protein per 1 l of shake flask culture were obtained (Ebersbach *et al.*, 2007). Similar levels of recombinant protein production have been reported for alternative binding proteins based on other scaffolds. As an example, affibody variants derived from the protein A domain scaffold achieved protein yields of 3 to 10 mg/l of culture (Nord *et al.*, 1997), whereas 2 to 40 mg/l of culture have been obtained for variants based on the tenth human fibronectin type III domain scaffold (Xu *et al.*, 2002; Getmanova *et al.*, 2006). The highest level of soluble expression was achieved by DARPins derived from design ankyrin repeat proteins. It was reported that randomly chosen library members were expressed at the level of 10 - 30% of total *E. coli* protein with up to 200 mg of protein obtained from 1 l of shake flask culture (Kohl *et al.*, 2003). Considerably smaller yields have been reported for anticalins purified from the *E. coli* periplasmic fraction where typically 0.1 to 5 mg of protein was obtained from 1 l of culture (Beste *et al.*, 1999; Mercader & Skerra, 2002).

In conclusion, these results indicate that the  $\gamma$ B-crystallin library allows the selection of Affilin variants that bind the E7 protein with affinity in the nanomolar range. The production of specific anti-E7 clones from soluble fraction of *E. coli* under native condition is feasible. Based on the biophysical analysis, clones D1 and D4 with the highest affinity to E7 were selected for further experiments.

### 4.3 Tat-mediated delivery of Affilin molecules into mammalian cells

The utility of Tat as an intracellular delivery system for varied cargos such as siRNA, DNA, peptides, proteins, phage particles, magnetic nanoparticles and liposomes has been extensively studied during the last two decades (reviewed in Gupta *et al.*, 2005; Wagstaff & Jans, 2006 and Foged & Nielsen, 2008). In addition to the efficient intracellular trafficking, several studies have demonstrated biological activities of Tat-conjugated cargos (Lindsay, 2002; Dietz & Bahr, 2004; Wadia & Dowdy, 2005). In each of these studies, the Tat peptide was chemically linked or genetically fused to the cargo protein and added directly to the cells, where protein internalization was observed.

Here, due to the attributed potential of the Tat peptide as an effective transduction system, an attempt to use it for delivery of Affilin molecules into mammalian cells was undertaken.

To enable a direct visualization of internalized Affilin molecules in living cells, the Affilin variant A1\* fused to the Tat peptide, His<sub>6</sub>-tag and EGFP was evaluated. However, when expressed in *E. coli* cells, the fusion construct was mostly insoluble. Optimization of expression conditions did not improve the amount of protein in soluble form to the level required for protein purification under native conditions. Thus, live cell-imaging studies with Tat-A1\*-EGFP-His<sub>6</sub> fusion protein were not possible.

To monitor the Tat-mediated delivery of Affilin molecules into mammalian cells, Western blot analysis and indirect immunofluorescence microscopy were carried out. The initial data from these experiments suggested an efficient, concentration- and time-dependent uptake. The proteins appeared to localize exclusively to the nucleus. Based on these studies it was concluded that Affilin molecules showed a remarkable intracellular stability as significant levels of Affilin-Tat protein persisted within cells for up to 48 h. However, these results required verification as some reports have implied that the cationic nature of the Tat sequence caused experimental artifacts upon evaluation of Tat uptake using fixed-cell assays (reviewed in Brooks *et al.*, 2005 and Nakase *et al.*, 2008). It has been found that the membrane-bound Tat peptide as well as Tat released from cellular vesicles following fixation redistributed to the cytoplasm and accumulated into the nucleus, probably as a result of electrostatic interaction with cellular DNA. The standard washing techniques, such as incubation of cells in PBS, have been shown to be insufficient to remove peptides associated with cell membranes (Richard *et al.*, 2003; Brooks *et al.*, 2005). Thus, the nonspecific electrostatic interactions and strong membrane association of Affilin-Tat fusion proteins influenced the interpretation of Tat-mediated uptake in this study.

To eliminate externally bound Affilin-Tat molecules, cells were treated with trypsin before final Western blot and immunofluorescence analysis. In contrast to previous experiments, Affilin molecules were not detected within intracellular compartment of analyzed cells. Nevertheless, the possibility that a small fraction of Affilin-Tat protein was internalized could

not be excluded as low amount of protein can escape detection by techniques such as Western blotting or standard imaging studies (Nakase *et al.*, 2008).

Considering endocytosis as a most likely uptake route of Tat conjugates, internalized proteins are expected to be retained in endosomes or to be targeted to lysosomes (Fischer *et al.*, 2004; Richard *et al.*, 2005; Vives *et al.*, 2008). As endosomolysis is a rather infrequent event and proteins within lysosomes are actively degraded, it is at odds with cytoplasmic or nuclear accessibility of Tat-conjugated cargos. The amount of transduced protein released from endosomes can be insufficient to mediate significant biological effects in cells. This has been observed in a study on Tat-mediated uptake of diphtheria toxin A-fragment in which no cytotoxicity of this protein was detected (Falnes *et al.*, 2001). Other studies have also reported ineffective translocation of Tat peptide or Tat conjugated cargos into several cell lines (Koppelhus *et al.*, 2002; Violini *et al.*, 2002; Kramer & Wunderli-Allenspach, 2003). The authors concluded that the very low rate of uptake or rapid degradation of Tat-conjugated proteins in cells might have led to the lack of evidence of Tat-mediated transduction in these experiments.

As mentioned above, even if efficient cellular uptake can be observed, the delivery of intact proteins is often compromised by insufficient endosomal escape and lysosomal degradation of attached proteins (Richard *et al.*, 2005; Vives *et al.*, 2008). Thus, strategies promoting endosomal escape and preventing cleavage of the cargo in the endosomal/lysosomal compartments have to be developed. The treatment of cells with lysosomotropic agents such as chloroquine (Caron *et al.*, 2004) or fusion of Tat to the pH-sensitive fusogenic peptide of the influenza virus hemagglutinin protein (Wadia *et al.*, 2004) have already been shown to induce endosome disruption and improve bioavailability of CPP conjugates to the cytosol and/or nucleus.

Another aspect of the Tat-mediated delivery system that needs to be addressed is a better understanding of the influence of cargo on the relative uptake efficacy and distribution. Several reports have suggested that the molecular size, structure and overall physicochemical properties of molecules attached to the Tat peptide affect the uptake (Yang *et al.*, 2002; Tunnemann *et al.*, 2006), however, a systematic study testing all these parameters has not been conducted yet.

As detection of Tat-mediated internalization has already proved to be problematic, the reliable methods for determination of the uptake, cytoplasmic release and/or nuclear delivery of Tat and Tat-conjugated cargos should be established. As a method which eliminates the requirement of fixation, the microscopic observations of living cells incubated with fluorescently labeled proteins or conjugates with fluorescent proteins such as GFP can be performed. However, microscopic studies are considered to be insufficient for investigation of protein internalization as the amount of cargo released into the cytosol

is often close to background levels (Nakase *et al.*, 2008). A novel approach for real-time analysis of cellular uptake has been proposed by Jones *et al.*, 2006. In this method, photons generated by cytosol-released luciferin were used for quantification of uptake and release in real-time.

Given the difficulties associated with Tat-mediated transduction mentioned above as well as the lack of cellular specificity, several issues have to be addressed in further studies before the potential of Tat peptide as a drug delivery system or as a research tool can be fully realized. These further studies should include a thorough investigation of the transduction process as well as the influence of all involved parameters.

#### **4.4 Intracellular activity of Affilin molecules**

The E6 and E7 proteins are the major transforming factors of human papillomaviruses (zur Hausen, 2000). Both proteins are consistently expressed in HPV-positive malignant tumors and are able to immortalize a wide variety of human cell types (McLaughlin-Drubin & Munger, 2009). These viral genes possess also proliferation-stimulating and transforming activities in a number of cell lines such as rodent NIH/3T3 fibroblasts (Yasumoto *et al.*, 1986; Caldeira *et al.*, 2000).

The transforming activity of E6 and E7 is associated with the inhibition and activation of several cell cycle regulatory proteins (reviewed in Munger *et al.*, 2004). As E7 is a protein distinct from those expressed in the cell, it provided a suitable model for the evaluation of the intracellular activity of Affilin molecules.

Numerous studies have demonstrated that E7 inhibition induces cell growth arrest (Choo *et al.*, 2000; Accardi *et al.*, 2005) or apoptosis (Nauenburg *et al.*, 2001; Jiang & Milner, 2002) in cervical cancer cells. Thus, the intracellular interaction between Affilin molecules and E7 was in this study indirectly examined by analysis of cell proliferation and apoptosis. To enable Affilin-E7 interaction in the cell nucleus, Affilin molecules were transiently expressed from an appropriate vector construct containing the signal sequence for nuclear targeting. In the initial experiments, a model NIH/3T3-E7 mouse cell line, originally established to provide the experimental system for studies on the transforming potential of the E7 protein (Zerfass *et al.*, 1995; Schulze *et al.*, 1998), was used. Following transient expression of Affilin D1 and D4 in NIH/3T3-E7 cells, a significant reduction of the proliferation rate was observed as compared to the cells expressing the wild-type  $\gamma$ B-crystallin scaffold.

To further evaluate the growth-inhibitory effect of Affilin molecules in a cervical cancer cell model, the Ca Ski cell line was employed. The transformed phenotype of Ca Ski cells is associated with the consistent expression of both E6 and E7 proteins from the integrated HPV genome (Yee *et al.*, 1985; Baker *et al.*, 1987). In these cells, the intracellular expression of anti-E7 Affilin molecules led to the growth inhibition as well. The Affilin variant D1 induced

growth suppression in the range of 50% in the population of both NIH/3T3-E7 and Ca Ski cells, whereas Affilin D4 caused less pronounced antiproliferative effect in both investigated cell lines. Although the reason for this difference was not established in this study, it is possible that each Affilin variant recognizes a different binding epitope on the surface of the E7 protein leading to the different degree of target neutralization. The fact that E7 is a multifunctional protein (Munger *et al.*, 2001) supports this hypothesis. To provide knowledge on the intermolecular contacts occurring between these two Affilin molecules and the E7 target protein, further mutational and structural studies would be required. The higher binding affinity of the Affilin D1, although increased only by about fourfold as compared to D4, could also contribute to the more pronounced antiproliferative effect observed for this variant.

To validate the specificity of Affilin-mediated inhibition of the E7 protein in cells, the cell lines negative for HPV, *i.e.* wild-type NIH/3T3, C-33 A and HEK-293 were evaluated under identical experimental conditions. As an additional control, the wild-type  $\gamma$ B-crystallin scaffold protein was expressed in all investigated cell lines. In the control experiments, no significant changes in the proliferation rate were observed. This finding indicated that the antiproliferative effect of Affilin molecules D1 and D4 was specific. The specificity of target inhibition was also supported by the fact that the expression of Affilin clones did not affect the growth of HEK-293 cells. The HEK-293 cell line was originally derived from the human embryonic kidney cells transformed by adenovirus 5 DNA (Graham *et al.*, 1977). The cells stably express E1A protein sharing some sequence similarities with the E7 protein from HPV (see Fig. 9; Chellappan *et al.*, 1992; Dahiya *et al.*, 2000).

To further determine the influence of Affilin expression on the phenotype of E7-positive cells, the apoptotic cell death was examined. Only a slight increase in the number of apoptotic cells was observed for D1 and D4 variants expressed in NIH/3T3-E7 cells, whereas the level of apoptosis in Ca Ski cells remained unchanged. This finding showed that the inhibition of proliferation was a key cellular event induced by expression of anti-E7 Affilin molecules in target cells. As Affilin molecules appeared in the nucleus, which is where E7 protein is predominantly localized (Greenfield *et al.*, 1991; Guccione *et al.*, 2002), it can be concluded that the growth suppression of target cells was a result of Affilin-mediated impairment of the E7 protein function.

The mechanism by which Affilin molecules achieve their antiproliferative effect was not elucidated in this study. The cellular model associated with HPV-induced transformation is characterized by complex cooperative effects caused by expression of both viral proteins, E6 and E7. Thus, identification of a particular cellular event responsible for induction of a growth-suppressive phenotype in Affilin-expressing cells is very challenging. One could speculate that the repression of E7 may restore the growth inhibitory function of the pRb

protein as well as other negative regulators of the cell cycle such as p21 and p27. The re-establishment of their function would down-regulate the genes required for transition from the G<sub>1</sub> to the S phase of the cell cycle as well as for the DNA synthesis. Such hypothesis is supported by the findings of other studies in which the targeting of HPV transcripts by ribozymes, antisense RNA or siRNA resulted in the growth inhibition of HPV-infected cells (Tan & Ting, 1995; Alvarez-Salas *et al.*, 2003; Yamato *et al.*, 2008). Transcriptional suppression of E6/E7 by forced expression of the E2 protein from bovine papillomavirus 1 (BPV-1) has also led to the significant growth inhibition of virus-related cells (Moon *et al.*, 2001). As a result of inhibition of E6/E7 expression, increased levels of cellular proteins such as pRb, p53 and p21 as well as suppression of E2F1 and cyclinE-associated CDK2 activities have been observed (Tan & Ting, 1995; Moon *et al.*, 2001; Yamato *et al.*, 2008). In an attempt to inhibit E7 at the protein level, the anti-E7 scFv antibody fragments selected by phage display have been probed to interfere with the transformed phenotype of cervical cancer cells (Accardi *et al.*, 2005). The selected scFvs exhibited the anti-proliferative effect similar to that observed for Affilin molecules. However, these antibody fragments revealed reduced stability as their expression in bacterial periplasm as well as in the cytoplasm of mammalian cells was impaired (Accardi *et al.*, 2005).

Taken together, these results prove that Affilin molecules can exert their desired effect on a cellular level and stress out their potential for further development of intracellular binding reagents based on the human  $\gamma$ B-crystallin scaffold.

## 5. Conclusions

The data presented in this thesis show that the  $\gamma$ B-crystallin library is applicable for the selection of Affilin variants with high affinity and specificity against a pre-defined target using conventional phage display approach. The recombinant expression of anti-E7 Affilin molecules in *E. coli* was feasible, thereby offering a cost-effective means of production of these proteins.

In the intracellular context, selected Affilin molecules were capable of inducing a specific cellular effect, which can be ascribed to the inhibition of E7 protein function. These findings encourage further development of the Affilin technology for the generation of new intracellular binding reagents. As transfer of genetic material into mammalian cells can be easily achieved in the laboratory via standard transfection methods, such alternative binding molecules can already be used for intracellular target validation as well as for studies on protein function and protein-protein interactions in cells. By targeting cellular protein functions associated with the progression of several human diseases such as cancer or viral infections, the alternative binding proteins could furthermore be developed for therapeutic use. It should be noted, however, that the therapeutic application of intracellular binding reagents requires more efficient, specific and safe methods for their delivery.

## 6. Summary

Engineered binding proteins based on nonimmunoglobulin scaffolds represent a rich source of affinity reagents for potential use as therapeutics, diagnostics and research tools complementing the repertoire of monoclonal antibodies.

Affilin molecules are novel binding reagents that exploit randomized side chains of the rigid  $\beta$ -sheet of the human  $\gamma$ B-crystallin scaffold for molecular recognition. They bind their pre-defined targets with high affinity and specificity preserving the structure and thermodynamic stability of the parental  $\gamma$ B-crystallin scaffold.

In the work underlying this thesis, the  $\gamma$ B-crystallin scaffold was evaluated in terms of its suitability for the generation of intracellular Affilin molecules. As a model target, the human papillomavirus E7 protein implicated in the development of cervical cancer was used.

For the purpose of the phage display selection of anti-E7 Affilin molecules, the E7 target protein was prepared as a His<sub>6</sub>-tag fusion using recombinant *E. coli* cells. Following optimization of the E7 gene sequence as well as expression parameters, the protein was purified under native conditions with a high yield. As determined by analytical size-exclusion chromatography, the protein existed as a soluble higher-order oligomer with a molecular mass of ~700 kDa. The biological activity of the recombinant E7 protein was demonstrated by its ability to bind to the retinoblastoma tumor protein (pRb). The apparent dissociation constant of the E7-pRb interaction was determined by ELISA as ~20 nM.

Using the recombinant E7 protein and a human  $\gamma$ B-crystallin library, anti-E7 Affilin molecules were selected by phage display technique. The first selection approach yielded micromolar to nanomolar anti-E7 binders, however was associated with enrichment of non-functional clones. To reduce the number of irrelevant clones and to isolate variants with higher affinity to E7, an alternative proteolysis-based phage display selection was carried out. Following this selection, the number of background clones was decreased. The isolated Affilin molecules specifically bound the E7 protein with affinities in the micromolar to nanomolar range. Both approaches led to the selection of Affilin variants exhibiting similar sequence pattern, in which the hydrophobic amino acids were frequently found at certain randomized positions in addition to basic amino acid residues enriched in case of some clones. From isolated anti-E7 Affilin variants, two clones named D1 and D4 exhibiting ~80 nM and ~260 nM apparent dissociation constants, respectively, were selected for further evaluation.

To study the internalization of Affilin molecules into mammalian cells, fusion constructs comprising Affilin molecules and the cell-penetrating Tat peptide derived from the HIV-1 Tat protein were generated and characterized. The Affilin-Tat fusion proteins maintained the target-binding affinity and specificity. However, when used in internalization studies using Western blotting and immunofluorescence microscopy, these proteins revealed only enhanced cell surface binding properties but no efficient cellular delivery.

In order to evaluate the intracellular activity of Affilin molecules, the anti-E7 Affilin clones were transiently expressed in E7-positive mammalian cells and the cellular proliferation and apoptosis were examined. The clones D1 and D4 revealed a significant inhibitory effect on the proliferation of target cells. The effect was specific as the growth of E7-negative cells or cells expressing the wild-type  $\gamma$ B-crystallin scaffold remained unaffected. The level of apoptosis in analyzed cells was essentially unchanged implying that the growth suppression was a key cellular event induced upon expression of specific anti-E7 Affilin molecules.

The results presented in this thesis demonstrate for the first time that Affilin molecules are able to fulfill their function in the reducing environment of mammalian cells thereby establishing their potential for the generation of novel intracellular binding reagents. Such intracellular binding molecules can be potentially applied in research for target validation and study of protein function in cells as well as in therapy.

## 7. Zusammenfassung

Die Nutzung stabiler Proteine als Grundgerüst zur Gewinnung künstlicher Bindemoleküle bietet eine ernstzunehmende Alternative für die Erweiterung der bisher allein monoklonalen Antikörpern vorbehaltene Anwendung in Therapie, Diagnostik und Forschung.

Affilin Moleküle sind neuartige künstliche Bindeproteine, die auf Basis des humanen  $\gamma$ B-Kristallins durch zufälligen Aminosäureaustausch an acht Positionen der  $\beta$ -Faltblattstruktur des Proteins entwickelt wurden. Affilin Moleküle binden ihre entsprechenden Zielmoleküle mit hoher Affinität und Spezifität, auch unter Erhalt der Struktur und der thermodynamischen Stabilität des  $\gamma$ B-Kristallin-Wildtyps.

Im Rahmen der vorliegenden Dissertation wurde daher die Eignung der  $\gamma$ B-Kristallin-Struktur für die Entwicklung von Affilin Molekülen mit der Fähigkeit zur Bindung intrazellulärer Zielmoleküle untersucht. Als Modell für ein solches intrazelluläres Zielmolekül wurde das human Papillomavirus E7 Protein, welches bei der Entwicklung von Gebärmutterhalskrebs eine Rolle spielt, ausgewählt.

Für die Selektion mittels Phage Display wurde das E7 Protein zunächst als His<sub>6</sub>-Tag fusioniertes Konstrukt in *E. coli* Zellen hergestellt. Nach Optimierung sowohl der Gensequenz des verwendeten Konstruktes als auch der Expressionsparameter konnte das Protein produziert und unter nativen Bedingungen mit hoher Ausbeute und Reinheit erhalten werden. Die analytische Größenausschluss-Chromatographie zeigte, dass das Protein als ein lösliches Oligomer, höherer Ordnung, mit einer molekularen Masse von ~700 kDa vorlag. Die Funktionalität des rekombinanten Proteins E7 wurde durch Bindung an das Retinoblastom-Protein (pRb) mittels ELISA gezeigt. Die apparente Dissoziationskonstante der E7-pRb Interaktion betrug dabei ~20 nM.

Unter Verwendung des rekombinanten E7 Proteins wurden anschließend entsprechende Affilin Moleküle mittels der Phage-Display-Technik aus der  $\gamma$ B-Kristallin-Bibliothek isoliert. In einem ersten Selektionsprozess konnten erfolgreich Affilin Varianten mit apparenten Dissoziationskonstanten für die Bindung an E7 im nano- bis mikromolaren Bereich isoliert werden. Es zeigte sich jedoch, dass zu einem großen Anteil auch nicht-funktionelle Klone angereichert wurden. Um die Zahl an irrelevanten Klonen zu verringern und Varianten mit höherer Affinität zu E7 zu isolieren, wurde eine alternative Proteolyse-basierte Phage-Display-Selektion durchgeführt. Mit Hilfe dieser Selektion wurde die Zahl von nicht-funktionellen Varianten deutlich verringert. Für die erhaltenen Klone wurde eine spezifische Bindung an das E7 Protein mit Dissoziationskonstanten im mikro- bis nanomolaren Bereich bestimmt. Beide Selektionsexperimente führten zu Isolierung

und Identifizierung von Affilin Varianten, die ähnliche Sequenzen aufwiesen. Dabei traten besonders hydrophobe Aminosäuren häufig an definierten Positionen auf. Zusätzlich wurden im Falle einiger Klone auch basische Aminosäurereste in der Primärsequenz erhaltener Affilin Moleküle angereichert. Von den anti-E7 Affilin Varianten wurden zwei als D1 bzw. D4 bezeichnete Klone mit ~80 nM und ~260 nM Dissoziationskonstanten für die nachfolgenden Studien ausgewählt.

Für die Untersuchung des zielgerichteten intrazellulären Transports in eukaryontischen Zellen wurden aus den Affilin Molekülen sowie dem vom HIV-1 abstammenden zellpenetrierendem Tat-Peptid bestehende Fusionsproteine hergestellt und charakterisiert. Die Herstellung der Fusionsproteine erfolgte dabei unter Erhalt von Affinität und Spezifität für E7. Die Auswertung der Lokalisierungsexperimente mittels Western Blot und Immunfluoreszenzmikroskopie zeigte allerdings, dass für diese Fusionskonstrukte nur eine erhöhte Bindung an die Zelloberfläche, jedoch keine effiziente Internalisierung nachgewiesen werden konnte.

Um die intrazelluläre Funktion der Affilin Moleküle zu analysieren, wurden die E7-spezifischen Affilin Moleküle Klone in eukaryontischen Zellen transient produziert und die zelluläre Proliferation und Apoptose überprüft. Dabei konnte für beide Klone eine signifikante Inhibierung der Proliferation E7-positiver Zellen nachgewiesen werden. Dieser Effekt war spezifisch, da das Wachstum E7-negativer Zellen bzw. von Zellen, die den  $\gamma$ B-Kristallin-Wildtyp produzierten, nicht beeinflusst wurde. Die apoptotische Aktivität in analysierten Zellen war im Wesentlichen unverändert. Dies deutet darauf hin, dass die Erniedrigung der Proliferation nach intrazellulärer Produktion der E7-spezifischen Affilin Moleküle ein zelluläres Schlüsselereignis war.

Die hier präsentierten Ergebnisse belegen damit erstmalig, dass Affilin Moleküle ihre Funktionalität und ihre Bindungseigenschaften auch im reduzierenden Medium des Zellinneren von eukaryontischen Zellen erhalten. Sie sind daher für die Generierung neuartiger intrazellulär funktioneller Bindeproteine grundsätzlich geeignet. Diese intrazellulären Bindemoleküle haben ein großes Potenzial für die Anwendung sowohl bei der Untersuchung von Proteinfunktionen in Zellen, der Validierung von intrazellulären Zielmolekülen als auch bei der Entwicklung neuer Therapieansätze.

## 8. References

- Accardi, L., Dona, M.G., Di Bonito, P. and Giorgi, C.** (2005). Intracellular anti-E7 human antibodies in single-chain format inhibit proliferation of HPV16-positive cervical carcinoma cells. *Int J Cancer* 116(4): 564-70.
- Alonso, L.G., Garcia-Alai, M.M., Nadra, A.D., Lapena, A.N., Almeida, F.L., Gualfetti, P. and Prat-Gay, G.D.** (2002). High-risk (HPV16) human papillomavirus E7 oncoprotein is highly stable and extended, with conformational transitions that could explain its multiple cellular binding partners. *Biochemistry* 41(33): 10510-8.
- Alonso, L.G., Garcia-Alai, M.M., Smal, C., Centeno, J.M., Iacono, R., Castano, E., Gualfetti, P. and de Prat-Gay, G.** (2004). The HPV16 E7 viral oncoprotein self-assembles into defined spherical oligomers. *Biochemistry* 43(12): 3310-7.
- Alvarez-Salas, L.M., Benitez-Hess, M.L. and DiPaolo, J.A.** (2003). Advances in the development of ribozymes and antisense oligodeoxynucleotides as antiviral agents for human papillomaviruses. *Antivir Ther* 8(4): 265-78.
- Amaki, Y., Nakano, H. and Yamane, T.** (1994). Role of cysteine residues in esterase from *Bacillus stearothermophilus* and increasing its thermostability by the replacement of cysteines. *Appl Microbiol Biotechnol* 40(5): 664-8.
- Amstutz, P., Binz, H.K., Parizek, P., Stumpp, M.T., Kohl, A., Grutter, M.G., Forrer, P. and Pluckthun, A.** (2005). Intracellular kinase inhibitors selected from combinatorial libraries of designed ankyrin repeat proteins. *J Biol Chem* 280(26): 24715-22.
- Amstutz, P., Koch, H., Binz, H.K., Deuber, S.A. and Pluckthun, A.** (2006). Rapid selection of specific MAP kinase-binders from designed ankyrin repeat protein libraries. *Protein Eng Des Sel* 19(5): 219-29.
- Antinore, M.J., Birrer, M.J., Patel, D., Nader, L. and McCance, D.J.** (1996). The human papillomavirus type 16 E7 gene product interacts with and trans-activates the AP1 family of transcription factors. *Embo J* 15(8): 1950-60.
- Armstrong, D.J. and Roman, A.** (1993). The anomalous electrophoretic behavior of the human papillomavirus type 16 E7 protein is due to the high content of acidic amino acid residues. *Biochem Biophys Res Commun* 192(3): 1380-7.
- Asada, S., Choi, Y., Yamada, M., Wang, S.C., Hung, M.C., Qin, J. and Uesugi, M.** (2002). External control of Her2 expression and cancer cell growth by targeting a Ras-linked coactivator. *Proc Natl Acad Sci U S A* 99(20): 12747-52.
- Astriab-Fisher, A., Sergueev, D.S., Fisher, M., Shaw, B.R. and Juliano, R.L.** (2000). Antisense inhibition of P-glycoprotein expression using peptide-oligonucleotide conjugates. *Biochem Pharmacol* 60(1): 83-90.
- Attucci, S., Gauthier, A., Korkmaz, B., Delepine, P., Martino, M.F., Saudubray, F., Diot, P. and Gauthier, F.** (2006). EPI-hNE4, a proteolysis-resistant inhibitor of human neutrophil elastase and potential anti-inflammatory drug for treating cystic fibrosis. *J Pharmacol Exp Ther* 318(2): 803-9.
- Atwell, S. and Wells, J.A.** (1999). Selection for improved subtiligases by phage display. *Proc Natl Acad Sci U S A* 96(17): 9497-502.
- Avvakumov, N., Torchia, J. and Mymryk, J.S.** (2003). Interaction of the HPV E7 proteins with the pCAF acetyltransferase. *Oncogene* 22(25): 3833-41.
- Azzazy, H.M. and Highsmith, W.E., Jr.** (2002). Phage display technology: clinical applications and recent innovations. *Clin Biochem* 35(6): 425-45.
- Bai, Y. and Feng, H.** (2004). Selection of stably folded proteins by phage-display with proteolysis. *Eur J Biochem* 271(9): 1609-14.
- Baker, C.C., Phelps, W.C., Lindgren, V., Braun, M.J., Gonda, M.A. and Howley, P.M.** (1987). Structural and transcriptional analysis of human papillomavirus type 16 sequences in cervical carcinoma cell lines. *J Virol* 61(4): 962-71.
- Balsitis, S., Dick, F., Dyson, N. and Lambert, P.F.** (2006). Critical roles for non-pRb targets of human papillomavirus type 16 E7 in cervical carcinogenesis. *Cancer Res* 66(19): 9393-400.

- Baneyx, F. and Mujacic, M.** (2004). Recombinant protein folding and misfolding in *Escherichia coli*. *Nat Biotechnol* 22(11): 1399-408.
- Barbass, C.F., Burton, D.R., Scott, J.K. and Silverman, G.J.** (2001). Phage Display: A Laboratory Manual. New York, Cold Spring Harbor Laboratory Press
- Barbosa, M.S., Lowy, D.R. and Schiller, J.T.** (1989). Papillomavirus polypeptides E6 and E7 are zinc-binding proteins. *J Virol* 63(3): 1404-7.
- Barka, T., Gresik, E.W. and van Der Noen, H.** (2000). Transduction of TAT-HA-beta-galactosidase fusion protein into salivary gland-derived cells and organ cultures of the developing gland, and into rat submandibular gland in vivo. *J Histochem Cytochem* 48(11): 1453-60.
- Barnard, P. and McMillan, N.A.** (1999). The human papillomavirus E7 oncoprotein abrogates signaling mediated by interferon-alpha. *Virology* 259(2): 305-13.
- Berezutskaya, E. and Bagchi, S.** (1997). The human papillomavirus E7 oncoprotein functionally interacts with the S4 subunit of the 26 S proteasome. *J Biol Chem* 272(48): 30135-40.
- Bernard, H.U.** (2004). Established and potential strategies against papillomavirus infections. *J Antimicrob Chemother* 53(2): 137-9.
- Bernat, A., Avvakumov, N., Mymryk, J.S. and Banks, L.** (2003). Interaction between the HPV E7 oncoprotein and the transcriptional coactivator p300. *Oncogene* 22(39): 7871-81.
- Berrow, N.S., Bussow, K., Coutard, B., Diprose, J., Ekberg, M., Folkers, G.E., Levy, N., Lieu, V., Owens, R.J., Peleg, Y., Pinaglia, C., Quevillon-Cheruel, S., Salim, L., Scheich, C., Vincentelli, R. and Busso, D.** (2006). Recombinant protein expression and solubility screening in *Escherichia coli*: a comparative study. *Acta Crystallogr D Biol Crystallogr* 62(Pt 10): 1218-26.
- Beste, G., Schmidt, F.S., Stibora, T. and Skerra, A.** (1999). Small antibody-like proteins with prescribed ligand specificities derived from the lipocalin fold. *Proc Natl Acad Sci U S A* 96(5): 1898-903.
- Binz, H.K., Amstutz, P. and Pluckthun, A.** (2005). Engineering novel binding proteins from nonimmunoglobulin domains. *Nat Biotechnol* 23(10): 1257-68.
- Binz, H.K. and Pluckthun, A.** (2005). Engineered proteins as specific binding reagents. *Curr Opin Biotechnol* 16(4): 459-69.
- Bloemendal, H., de Jong, W., Jaenicke, R., Lubsen, N.H., Slingsby, C. and Tardieu, A.** (2004). Ageing and vision: structure, stability and function of lens crystallins. *Prog Biophys Mol Biol* 86(3): 407-85.
- Borghouts, C., Kunz, C. and Groner, B.** (2005). Peptide aptamers: recent developments for cancer therapy. *Expert Opin Biol Ther* 5(6): 783-97.
- Boyer, S.N., Wazer, D.E. and Band, V.** (1996). E7 protein of human papilloma virus-16 induces degradation of retinoblastoma protein through the ubiquitin-proteasome pathway. *Cancer Res* 56(20): 4620-4.
- Bradford, M.M.** (1976). A rapid and sensitive method for the quantitation of microgram quantities of protein utilizing the principle of protein-dye binding. *Anal Biochem* 72: 248-54.
- Braspenning, J., Manetti, R., Zumbach, K., Meschede, W., Gissmann, L. and Tommasino, M.** (1997). A general purification protocol for E7 proteins from "high- and low-risk" human papillomavirus types expressed in the yeast *Schizosaccharomyces pombe*. *Protein Expr Purif* 10(2): 192-201.
- Brehm, A., Nielsen, S.J., Miska, E.A., McCance, D.J., Reid, J.L., Bannister, A.J. and Kouzarides, T.** (1999). The E7 oncoprotein associates with Mi2 and histone deacetylase activity to promote cell growth. *Embo J* 18(9): 2449-58.
- Brooks, H., Lebleu, B. and Vives, E.** (2005). Tat peptide-mediated cellular delivery: back to basics. *Adv Drug Deliv Rev* 57(4): 559-77.
- Caldeira, S., de Villiers, E.M. and Tommasino, M.** (2000). Human papillomavirus E7 proteins stimulate proliferation independently of their ability to associate with retinoblastoma protein. *Oncogene* 19(6): 821-6.

- Campo-Fernandez, B., Morandell, D., Santer, F.R., Zwerschke, W. and Jansen-Durr, P.** (2007). Identification of the FHL2 transcriptional coactivator as a new functional target of the E7 oncoprotein of human papillomavirus type 16. *J Virol* 81(2): 1027-32.
- Carcamo, J., Ravera, M.W., Brissette, R., Dedova, O., Beasley, J.R., Alam-Moghe, A., Wan, C., Blume, A. and Mandecki, W.** (1998). Unexpected frameshifts from gene to expressed protein in a phage-displayed peptide library. *Proc Natl Acad Sci U S A* 95(19): 11146-51.
- Caron, N.J., Quenneville, S.P. and Tremblay, J.P.** (2004). Endosome disruption enhances the functional nuclear delivery of Tat-fusion proteins. *Biochem Biophys Res Commun* 319(1): 12-20.
- Carter, P.J.** (2006). Potent antibody therapeutics by design. *Nat Rev Immunol* 6(5): 343-57.
- Cattaneo, A. and Biocca, S.** (1999). The selection of intracellular antibodies. *Trends Biotechnol* 17(3): 115-21.
- Chakravarty, S., Mitra, N., Queitsch, I., Surolia, A., Varadarajan, R. and Dubel, S.** (2000). Protein stabilization through phage display. *FEBS Lett* 476(3): 296-300.
- Chellappan, S., Kraus, V.B., Kroger, B., Munger, K., Howley, P.M., Phelps, W.C. and Nevins, J.R.** (1992). Adenovirus E1A, simian virus 40 tumor antigen, and human papillomavirus E7 protein share the capacity to disrupt the interaction between transcription factor E2F and the retinoblastoma gene product. *Proc Natl Acad Sci U S A* 89(10): 4549-53.
- Chen, C.H., Wang, T.L., Hung, C.F., Yang, Y., Young, R.A., Pardoll, D.M. and Wu, T.C.** (2000). Enhancement of DNA vaccine potency by linkage of antigen gene to an HSP70 gene. *Cancer Res* 60(4): 1035-42.
- Cheng, S., Schmidt-Grimminger, D.C., Murrant, T., Broker, T.R. and Chow, L.T.** (1995). Differentiation-dependent up-regulation of the human papillomavirus E7 gene reactivates cellular DNA replication in suprabasal differentiated keratinocytes. *Genes Dev* 9(19): 2335-49.
- Chiang, C.M., Ustav, M., Stenlund, A., Ho, T.F., Broker, T.R. and Chow, L.T.** (1992). Viral E1 and E2 proteins support replication of homologous and heterologous papillomaviral origins. *Proc Natl Acad Sci U S A* 89(13): 5799-803.
- Chinami, M., Sasaki, S., Hachiya, N., Yuge, K., Ohsugi, T., Maeda, H. and Shingu, M.** (1994). Functional oligomerization of purified human papillomavirus types 16 and 6b E7 proteins expressed in *Escherichia coli*. *J Gen Virol* 75 ( Pt 2): 277-81.
- Choo, C.K., Ling, M.T., Suen, C.K., Chan, K.W. and Kwong, Y.L.** (2000). Retrovirus-mediated delivery of HPV16 E7 antisense RNA inhibited tumorigenicity of CaSki cells. *Gynecol Oncol* 78(3 Pt 1): 293-301.
- Clackson, T. and Lowman, H.B.** (2004). *Phage Display: A Practical Approach*. New York, Oxford University Press Inc.
- Clemens, K.E., Brent, R., Gyuris, J. and Munger, K.** (1995). Dimerization of the human papillomavirus E7 oncoprotein in vivo. *Virology* 214(1): 289-93.
- Clements, A., Johnston, K., Mazzarelli, J.M., Ricciardi, R.P. and Marmorstein, R.** (2000). Oligomerization properties of the viral oncoproteins adenovirus E1A and human papillomavirus E7 and their complexes with the retinoblastoma protein. *Biochemistry* 39(51): 16033-45.
- Cobrinik, D.** (2005). Pocket proteins and cell cycle control. *Oncogene* 24(17): 2796-809.
- Cogliano, V., Baan, R., Straif, K., Grosse, Y., Secretan, B. and El Ghissassi, F.** (2005). Carcinogenicity of human papillomaviruses. *Lancet Oncol* 6(4): 204.
- Coia, G., Hudson, P.J. and Irving, R.A.** (2001). Protein affinity maturation in vivo using *E. coli* mutator cells. *J Immunol Methods* 251(1-2): 187-93.
- Collins, A.S., Nakahara, T., Do, A. and Lambert, P.F.** (2005). Interactions with pocket proteins contribute to the role of human papillomavirus type 16 E7 in the papillomavirus life cycle. *J Virol* 79(23): 14769-80.
- Craik, D.J., Daly, N.L. and Waine, C.** (2001). The cystine knot motif in toxins and implications for drug design. *Toxicon* 39(1): 43-60.
- Dahiya, A., Gavin, M.R., Luo, R.X. and Dean, D.C.** (2000). Role of the LXCXE binding site in Rb function. *Mol Cell Biol* 20(18): 6799-805.

- de Villiers, E.M., Fauquet, C., Broker, T.R., Bernard, H.U. and zur Hausen, H. (2004). Classification of papillomaviruses. *Virology* 324(1): 17-27.
- Demarest, S.J. and Glaser, S.M. (2008). Antibody therapeutics, antibody engineering, and the merits of protein stability. *Curr Opin Drug Discov Devel* 11(5): 675-87.
- Demeret, C., Desaintes, C., Yaniv, M. and Thierry, F. (1997). Different mechanisms contribute to the E2-mediated transcriptional repression of human papillomavirus type 18 viral oncogenes. *J Virol* 71(12): 9343-9.
- Derossi, D., Joliot, A.H., Chassaing, G. and Prochiantz, A. (1994). The third helix of the Antennapedia homeodomain translocates through biological membranes. *J Biol Chem* 269(14): 10444-50.
- Dick, F.A. and Dyson, N.J. (2002). Three regions of the pRB pocket domain affect its inactivation by human papillomavirus E7 proteins. *J Virol* 76(12): 6224-34.
- Dietz, G.P. and Bahr, M. (2004). Delivery of bioactive molecules into the cell: the Trojan horse approach. *Mol Cell Neurosci* 27(2): 85-131.
- Dolgilevich, S., Zaidi, N., Song, J., Abe, E., Moonga, B.S. and Sun, L. (2002). Transduction of TAT fusion proteins into osteoclasts and osteoblasts. *Biochem Biophys Res Commun* 299(3): 505-9.
- Dong, W.L., Caldeira, S., Sehr, P., Pawlita, M. and Tommasino, M. (2001). Determination of the binding affinity of different human papillomavirus E7 proteins for the tumour suppressor pRb by a plate-binding assay. *J Virol Methods* 98(1): 91-8.
- Driessen, A.J., Fekkes, P. and van der Wolk, J.P. (1998). The Sec system. *Curr Opin Microbiol* 1(2): 216-22.
- Duchardt, F., Fotin-Mleczek, M., Schwarz, H., Fischer, R. and Brock, R. (2007). A comprehensive model for the cellular uptake of cationic cell-penetrating peptides. *Traffic* 8(7): 848-66.
- Duensing, S., Lee, L.Y., Duensing, A., Basile, J., Piboonniyom, S., Gonzalez, S., Crum, C.P. and Munger, K. (2000). The human papillomavirus type 16 E6 and E7 oncoproteins cooperate to induce mitotic defects and genomic instability by uncoupling centrosome duplication from the cell division cycle. *Proc Natl Acad Sci U S A* 97(18): 10002-7.
- Duensing, S. and Munger, K. (2004). Mechanisms of genomic instability in human cancer: insights from studies with human papillomavirus oncoproteins. *Int J Cancer* 109(2): 157-62.
- Dyson, N., Guida, P., Munger, K. and Harlow, E. (1992). Homologous sequences in adenovirus E1A and human papillomavirus E7 proteins mediate interaction with the same set of cellular proteins. *J Virol* 66(12): 6893-902.
- Dyson, N., Howley, P.M., Munger, K. and Harlow, E. (1989). The human papilloma virus-16 E7 oncoprotein is able to bind to the retinoblastoma gene product. *Science* 243(4893): 934-7.
- Ebersbach, H., Fiedler, E., Scheuermann, T., Fiedler, M., Stubbs, M.T., Reimann, C., Proetzl, G., Rudolph, R. and Fiedler, U. (2007). Affilin-novel binding molecules based on human gamma-B-crystallin, an all beta-sheet protein. *J Mol Biol* 372(1): 172-85.
- Edmonds, C. and Vousden, K.H. (1989). A point mutational analysis of human papillomavirus type 16 E7 protein. *J Virol* 63(6): 2650-6.
- Eksioglu-Demiralp, E., Kitada, S., Carson, D., Garland, J., Andreef, M. and Reed, J.C. (2003). A method for functional evaluation of caspase activation pathways in intact lymphoid cells using electroporation-mediated protein delivery and flow cytometric analysis. *J Immunol Methods* 275(1-2): 41-56.
- el Awady, M.K., Kaplan, J.B., O'Brien, S.J. and Burk, R.D. (1987). Molecular analysis of integrated human papillomavirus 16 sequences in the cervical cancer cell line SiHa. *Virology* 159(2): 389-98.
- Elliott, G. and O'Hare, P. (1997). Intercellular trafficking and protein delivery by a herpesvirus structural protein. *Cell* 88(2): 223-33.

- Epstein, J., Lee, M.M., Kelly, C.E. and Donahoe, P.K.** (1990). Effect of *E. coli* endotoxin on mammalian cell growth and recombinant protein production. *In Vitro Cell Dev Biol* 26(12): 1121-2.
- Ewert, S., Honegger, A. and Pluckthun, A.** (2003). Structure-based improvement of the biophysical properties of immunoglobulin VH domains with a generalizable approach. *Biochemistry* 42(6): 1517-28.
- Falnes, P.O., Wesche, J. and Olsnes, S.** (2001). Ability of the Tat basic domain and VP22 to mediate cell binding, but not membrane translocation of the diphtheria toxin A-fragment. *Biochemistry* 40(14): 4349-58.
- Fehrmann, F., Klumpp, D.J. and Laimins, L.A.** (2003). Human papillomavirus type 31 E5 protein supports cell cycle progression and activates late viral functions upon epithelial differentiation. *J Virol* 77(5): 2819-31.
- Fehrmann, F. and Laimins, L.A.** (2003). Human papillomaviruses: targeting differentiating epithelial cells for malignant transformation. *Oncogene* 22(33): 5201-7.
- Fernando, G.J., Murray, B., Zhou, J. and Frazer, I.H.** (1999). Expression, purification and immunological characterization of the transforming protein E7, from cervical cancer-associated human papillomavirus type 16. *Clin Exp Immunol* 115(3): 397-403.
- Ferrari, A., Pellegrini, V., Arcangeli, C., Fittipaldi, A., Giacca, M. and Beltram, F.** (2003). Caveolae-mediated internalization of extracellular HIV-1 tat fusion proteins visualized in real time. *Mol Ther* 8(2): 284-94.
- Fiedler, E., Fiedler, M., Proetzel, G., Scheuermann, T., Fiedler, U. and Rudolph, R.** (2006). Affilin™ Molecules: Novel Ligands for Bioseparation. *Food and Bioproducts Processing* 84(1): 3-8.
- Fiedler, U. and Rudolph, R.** (2001). Fabrication of beta-pleated sheet proteins with specific binding properties. International Patent Application WO/2001/004144
- Finnen, R.L., Erickson, K.D., Chen, X.S. and Garcea, R.L.** (2003). Interactions between papillomavirus L1 and L2 capsid proteins. *J Virol* 77(8): 4818-26.
- Fischer, P., Leu, S.J., Yang, Y.Y. and Chen, P.P.** (1994). Rapid simultaneous screening for DNA integrity and antigen specificity of clones selected by phage display. *Biotechniques* 16(5): 828-30.
- Fischer, R., Kohler, K., Fotin-Mieczek, M. and Brock, R.** (2004). A stepwise dissection of the intracellular fate of cationic cell-penetrating peptides. *J Biol Chem* 279(13): 12625-35.
- Fittipaldi, A., Ferrari, A., Zoppe, M., Arcangeli, C., Pellegrini, V., Beltram, F. and Giacca, M.** (2003). Cell membrane lipid rafts mediate caveolar endocytosis of HIV-1 Tat fusion proteins. *J Biol Chem* 278(36): 34141-9.
- Foged, C. and Nielsen, H.M.** (2008). Cell-penetrating peptides for drug delivery across membrane barriers. *Expert Opin Drug Deliv* 5(1): 105-17.
- Foote, J. and Eisen, H.N.** (1995). Kinetic and affinity limits on antibodies produced during immune responses. *Proc Natl Acad Sci U S A* 92(5): 1254-6.
- Forrer, P., Jung, S. and Pluckthun, A.** (1999). Beyond binding: using phage display to select for structure, folding and enzymatic activity in proteins. *Curr Opin Struct Biol* 9(4): 514-20.
- Frankel, A.D. and Pabo, C.O.** (1988). Cellular uptake of the tat protein from human immunodeficiency virus. *Cell* 55(6): 1189-93.
- Fremaux, I., Mazeres, S., Brisson-Lougarre, A., Arnaud, M., Ladurantie, C. and Fournier, D.** (2002). Improvement of *Drosophila* acetylcholinesterase stability by elimination of a free cysteine. *BMC Biochem* 3: 21.
- Frolov, M.V. and Dyson, N.J.** (2004). Molecular mechanisms of E2F-dependent activation and pRB-mediated repression. *J Cell Sci* 117(Pt 11): 2173-81.
- Fuchs, E.** (1993). Epidermal differentiation and keratin gene expression. *J Cell Sci Suppl* 17: 197-208.
- Fung, E.T.** (2004). Protein Arrays: Methods and Protocols. Berlin, Springer.
- Furukawa, K., Shimizu, T., Murakami, A., Kono, R., Nakagawa, M., Sagawa, T., Yamato, I. and Azuma, T.** (2007). Strategy for affinity maturation of an antibody with high evolvability to (4-hydroxy-3-nitrophenyl) acetyl hapten. *Mol Immunol* 44(9): 2436-45.

- Futaki, S., Suzuki, T., Ohashi, W., Yagami, T., Tanaka, S., Ueda, K. and Sugiura, Y.** (2001). Arginine-rich peptides. An abundant source of membrane-permeable peptides having potential as carriers for intracellular protein delivery. *J Biol Chem* 276(8): 5836-40.
- Galloway, C.A., Sowden, M.P. and Smith, H.C.** (2003). Increasing the yield of soluble recombinant protein expressed in *E. coli* by induction during late log phase. *Biotechniques* 34(3): 524-6, 528, 530.
- Gavrieli, Y., Sherman, Y. and Ben-Sasson, S.A.** (1992). Identification of programmed cell death in situ via specific labeling of nuclear DNA fragmentation. *J Cell Biol* 119(3): 493-501.
- Gebauer, M. and Skerra, A.** (2009). Engineered protein scaffolds as next-generation antibody therapeutics. *Curr Opin Chem Biol* 13(3): 245-55.
- Getmanova, E.V., Chen, Y., Bloom, L., Gokemeijer, J., Shamah, S., Warikoo, V., Wang, J., Ling, V. and Sun, L.** (2006). Antagonists to human and mouse vascular endothelial growth factor receptor 2 generated by directed protein evolution in vitro. *Chem Biol* 13(5): 549-56.
- Gill, D.S. and Damle, N.K.** (2006). Biopharmaceutical drug discovery using novel protein scaffolds. *Curr Opin Biotechnol* 17(6): 653-8.
- Gillison, M.L. and Shah, K.V.** (2001). Human papillomavirus-associated head and neck squamous cell carcinoma: mounting evidence for an etiologic role for human papillomavirus in a subset of head and neck cancers. *Curr Opin Oncol* 13(3): 183-8.
- Graham, F.L., Smiley, J., Russell, W.C. and Nairn, R.** (1977). Characteristics of a human cell line transformed by DNA from human adenovirus type 5. *J Gen Virol* 36(1): 59-74.
- Graham, F.L. and van der Eb, A.J.** (1973). Transformation of rat cells by DNA of human adenovirus 5. *Virology* 54(2): 536-9.
- Gratzner, H.G.** (1982). Monoclonal antibody to 5-bromo- and 5-iododeoxyuridine: A new reagent for detection of DNA replication. *Science* 218(4571): 474-5.
- Green, I., Christison, R., Voyce, C.J., Bundell, K.R. and Lindsay, M.A.** (2003). Protein transduction domains: are they delivering? *Trends Pharmacol Sci* 24(5): 213-5.
- Green, M. and Loewenstein, P.M.** (1988). Autonomous functional domains of chemically synthesized human immunodeficiency virus tat trans-activator protein. *Cell* 55(6): 1179-88.
- Greenfield, I., Nickerson, J., Penman, S. and Stanley, M.** (1991). Human papillomavirus 16 E7 protein is associated with the nuclear matrix. *Proc Natl Acad Sci U S A* 88(24): 11217-21.
- Guccione, E., Massimi, P., Bernat, A. and Banks, L.** (2002). Comparative analysis of the intracellular location of the high- and low-risk human papillomavirus oncoproteins. *Virology* 293(1): 20-5.
- Gump, J.M. and Dowdy, S.F.** (2007). TAT transduction: the molecular mechanism and therapeutic prospects. *Trends Mol Med* 13(10): 443-8.
- Gupta, B., Levchenko, T.S. and Torchilin, V.P.** (2005). Intracellular delivery of large molecules and small particles by cell-penetrating proteins and peptides. *Adv Drug Deliv Rev* 57(4): 637-51.
- Han, J., Lee, J.D., Bibbs, L. and Ulevitch, R.J.** (1994). A MAP kinase targeted by endotoxin and hyperosmolarity in mammalian cells. *Science* 265(5173): 808-11.
- Harper, D.M., Franco, E.L., Wheeler, C.M., Moscicki, A.B., Romanowski, B., Roteli-Martins, C.M., Jenkins, D., Schuind, A., Costa Clemens, S.A. and Dubin, G.** (2006). Sustained efficacy up to 4.5 years of a bivalent L1 virus-like particle vaccine against human papillomavirus types 16 and 18: follow-up from a randomised control trial. *Lancet* 367(9518): 1247-55.
- He, W., Staples, D., Smith, C. and Fisher, C.** (2003). Direct activation of cyclin-dependent kinase 2 by human papillomavirus E7. *J Virol* 77(19): 10566-74.
- Heck, D.V., Yee, C.L., Howley, P.M. and Munger, K.** (1992). Efficiency of binding the retinoblastoma protein correlates with the transforming capacity of the E7

- oncoproteins of the human papillomaviruses. *Proc Natl Acad Sci U S A* 89(10): 4442-6.
- Heinis, C., Huber, A., Demartis, S., Bertschinger, J., Melkko, S., Lozzi, L., Neri, P. and Neri, D.** (2001). Selection of catalytically active biotin ligase and trypsin mutants by phage display. *Protein Eng* 14(12): 1043-52.
- Helt, A.M., Funk, J.O. and Galloway, D.A.** (2002). Inactivation of both the retinoblastoma tumor suppressor and p21 by the human papillomavirus type 16 E7 oncoprotein is necessary to inhibit cell cycle arrest in human epithelial cells. *J Virol* 76(20): 10559-68.
- Hennessey, P.T., Westra, W.H. and Califano, J.A.** (2009). Human papillomavirus and head and neck squamous cell carcinoma: recent evidence and clinical implications. *J Dent Res* 88(4): 300-6.
- Herce, H.D. and Garcia, A.E.** (2007). Molecular dynamics simulations suggest a mechanism for translocation of the HIV-1 TAT peptide across lipid membranes. *Proc Natl Acad Sci U S A* 104(52): 20805-10.
- Hey, T., Fiedler, E., Rudolph, R. and Fiedler, M.** (2005). Artificial, non-antibody binding proteins for pharmaceutical and industrial applications. *Trends Biotechnol* 23(10): 514-22.
- Holliger, P. and Hudson, P.J.** (2005). Engineered antibody fragments and the rise of single domains. *Nat Biotechnol* 23(9): 1126-36.
- Honegger, A.** (2008). Engineering antibodies for stability and efficient folding. *Handb Exp Pharmacol*(181): 47-68.
- Hoogenboom, H.R.** (2002). Overview of antibody phage-display technology and its applications. *Methods Mol Biol* 178: 1-37.
- Hoogenboom, H.R.** (2005). Selecting and screening recombinant antibody libraries. *Nat Biotechnol* 23(9): 1105-16.
- Hoogenboom, H.R. and Chames, P.** (2000). Natural and designer binding sites made by phage display technology. *Immunol Today* 21(8): 371-8.
- Hoogenboom, H.R., Griffiths, A.D., Johnson, K.S., Chiswell, D.J., Hudson, P. and Winter, G.** (1991). Multi-subunit proteins on the surface of filamentous phage: methodologies for displaying antibody (Fab) heavy and light chains. *Nucleic Acids Res* 19(15): 4133-7.
- Hosse, R.J., Rothe, A. and Power, B.E.** (2006). A new generation of protein display scaffolds for molecular recognition. *Protein Sci* 15(1): 14-27.
- Huber, D., Cha, M.I., Debarbieux, L., Planson, A.G., Cruz, N., Lopez, G., Tasayco, M.L., Chaffotte, A. and Beckwith, J.** (2005). A selection for mutants that interfere with folding of Escherichia coli thioredoxin-1 in vivo. *Proc Natl Acad Sci U S A* 102(52): 18872-7.
- Hufton, S.E., van Neer, N., van den Beuken, T., Desmet, J., Sablon, E. and Hoogenboom, H.R.** (2000). Development and application of cytotoxic T lymphocyte-associated antigen 4 as a protein scaffold for the generation of novel binding ligands. *FEBS Lett* 475(3): 225-31.
- Huh, K., Zhou, X., Hayakawa, H., Cho, J.Y., Libermann, T.A., Jin, J., Harper, J.W. and Munger, K.** (2007). Human papillomavirus type 16 E7 oncoprotein associates with the cullin 2 ubiquitin ligase complex, which contributes to degradation of the retinoblastoma tumor suppressor. *J Virol* 81(18): 9737-47.
- Huh, K.W., DeMasi, J., Ogawa, H., Nakatani, Y., Howley, P.M. and Munger, K.** (2005). Association of the human papillomavirus type 16 E7 oncoprotein with the 600-kDa retinoblastoma protein-associated factor, p600. *Proc Natl Acad Sci U S A* 102(32): 11492-7.
- Ignatovich, I.A., Dizhe, E.B., Pavlotskaya, A.V., Akifiev, B.N., Burov, S.V., Orlov, S.V. and Perevozchikov, A.P.** (2003). Complexes of plasmid DNA with basic domain 47-57 of the HIV-1 Tat protein are transferred to mammalian cells by endocytosis-mediated pathways. *J Biol Chem* 278(43): 42625-36.
- Imoto, T., Yamada, H. and Ueda, T.** (1986). Unfolding rates of globular proteins determined by kinetics of proteolysis. *J Mol Biol* 190(4): 647-9.

- Jaenicke, R.** (1994). Eye-lens proteins: structure, superstructure, stability, genetics. *Naturwissenschaften* 81(10): 423-9.
- Jaenicke, R. and Slingsby, C.** (2001). Lens crystallins and their microbial homologs: structure, stability, and function. *Crit Rev Biochem Mol Biol* 36(5): 435-99.
- Janeway, C.A., Travers, P., Walport, M. and Shlomchik, M.J.** (2001). Immunobiology. New York, Garland Publishing.
- Jason-Moller, L., Murphy, M. and Bruno, J.** (2006). Overview of Biacore systems and their applications. *Curr Protoc Protein Sci* Chapter 19: Unit 19 13.
- Jiang, M. and Milner, J.** (2002). Selective silencing of viral gene expression in HPV-positive human cervical carcinoma cells treated with siRNA, a primer of RNA interference. *Oncogene* 21(39): 6041-8.
- Joliot, A., Pernelle, C., Deagostini-Bazin, H. and Prochiantz, A.** (1991). Antennapedia homeobox peptide regulates neural morphogenesis. *Proc Natl Acad Sci U S A* 88(5): 1864-8.
- Joliot, A. and Prochiantz, A.** (2004). Transduction peptides: from technology to physiology. *Nat Cell Biol* 6(3): 189-96.
- Jones, L.R., Goun, E.A., Shinde, R., Rothbard, J.B., Contag, C.H. and Wender, P.A.** (2006). Releasable luciferin-transporter conjugates: tools for the real-time analysis of cellular uptake and release. *J Am Chem Soc* 128(20): 6526-7.
- Junqueira, D., Cilenti, L., Musumeci, L., Sedivy, J.M. and Zervos, A.S.** (2003). Random mutagenesis of PDZ(Omi) domain and selection of mutants that specifically bind the Myc proto-oncogene and induce apoptosis. *Oncogene* 22(18): 2772-81.
- Kalinin, N.L., Ward, L.D. and Winzor, D.J.** (1995). Effects of solute multivalence on the evaluation of binding constants by biosensor technology: studies with concanavalin A and interleukin-6 as partitioning proteins. *Anal Biochem* 228(2): 238-44.
- Kamio, M., Yoshida, T., Ogata, H., Douchi, T., Nagata, Y., Inoue, M., Hasegawa, M., Yonemitsu, Y. and Yoshimura, A.** (2004). SOCS1 [corrected] inhibits HPV-E7-mediated transformation by inducing degradation of E7 protein. *Oncogene* 23(17): 3107-15.
- Kaplan, I.M., Wadia, J.S. and Dowdy, S.F.** (2005). Cationic TAT peptide transduction domain enters cells by macropinocytosis. *J Control Release* 102(1): 247-53.
- Karlsson, F., Borrebaeck, C.A., Nilsson, N. and Malmberg-Hager, A.C.** (2003). The mechanism of bacterial infection by filamentous phages involves molecular interactions between TolA and phage protein 3 domains. *J Bacteriol* 185(8): 2628-34.
- Kasher, M.S., Wakulchik, M., Cook, J.A. and Smith, M.C.** (1993). One-step purification of recombinant human papillomavirus type 16 E7 oncoprotein and its binding to the retinoblastoma gene product. *Biotechniques* 14(4): 630-41.
- Katterle, Y., Brandt, B.H., Dowdy, S.F., Niggemann, B., Zanker, K.S. and Dittmar, T.** (2004). Antitumour effects of PLC-gamma1-(SH2)2-TAT fusion proteins on EGFR/c-erbB-2-positive breast cancer cells. *Br J Cancer* 90(1): 230-5.
- Kawe, M., Forrer, P., Amstutz, P. and Pluckthun, A.** (2006). Isolation of intracellular proteinase inhibitors derived from designed ankyrin repeat proteins by genetic screening. *J Biol Chem* 281(52): 40252-63.
- Kipriyanov, S.M. and Le Gall, F.** (2004). Generation and production of engineered antibodies. *Mol Biotechnol* 26(1): 39-60.
- Kohl, A., Binz, H.K., Forrer, P., Stumpp, M.T., Pluckthun, A. and Grutter, M.G.** (2003). Designed to be stable: crystal structure of a consensus ankyrin repeat protein. *Proc Natl Acad Sci U S A* 100(4): 1700-5.
- Koide, A., Abbatiello, S., Rothgery, L. and Koide, S.** (2002). Probing protein conformational changes in living cells by using designer binding proteins: application to the estrogen receptor. *Proc Natl Acad Sci U S A* 99(3): 1253-8.
- Koppelhus, U., Awasthi, S.K., Zachar, V., Holst, H.U., Ebbesen, P. and Nielsen, P.E.** (2002). Cell-dependent differential cellular uptake of PNA, peptides, and PNA-peptide conjugates. *Antisense Nucleic Acid Drug Dev* 12(2): 51-63.

- Kramer, S.D. and Wunderli-Allenspach, H.** (2003). No entry for TAT(44-57) into liposomes and intact MDCK cells: novel approach to study membrane permeation of cell-penetrating peptides. *Biochim Biophys Acta* 1609(2): 161-9.
- Krautwald, S., Ziegler, E., Tiede, K., Pust, R. and Kunzendorf, U.** (2004). Transduction of the TAT-FLIP fusion protein results in transient resistance to Fas-induced apoptosis in vivo. *J Biol Chem* 279(42): 44005-11.
- Kyte, J. and Doolittle, R.F.** (1982). A simple method for displaying the hydrophobic character of a protein. *J Mol Biol* 157: 105-132.
- Laemmli, U.K.** (1970). Cleavage of structural proteins during the assembly of the head of bacteriophage T4. *Nature* 227(5259): 680-5.
- Lagrange, M., Boulade-Ladame, C., Maily, L., Weiss, E., Orfanoudakis, G. and Deryckere, F.** (2007). Intracellular scFvs against the viral E6 oncoprotein provoke apoptosis in human papillomavirus-positive cancer cells. *Biochem Biophys Res Commun* 361(2): 487-92.
- Lamla, T. and Erdmann, V.A.** (2003). Searching sequence space for high-affinity binding peptides using ribosome display. *J Mol Biol* 329(2): 381-8.
- Lee, C. and Cho, Y.** (2002). Interactions of SV40 large T antigen and other viral proteins with retinoblastoma tumour suppressor. *Rev Med Virol* 12(2): 81-92.
- Lett, C.M., Rosu-Myles, M.D., Frey, H.E. and Guillemette, J.G.** (1999). Rational design of a more stable yeast iso-1-cytochrome c. *Biochim Biophys Acta* 1432(1): 40-8.
- Lewin, M., Carlesso, N., Tung, C.H., Tang, X.W., Cory, D., Scadden, D.T. and Weissleder, R.** (2000). Tat peptide-derivatized magnetic nanoparticles allow in vivo tracking and recovery of progenitor cells. *Nat Biotechnol* 18(4): 410-4.
- Lewis, H., Webster, K., Sanchez-Perez, A.M. and Gaston, K.** (1999). Cellular transcription factors regulate human papillomavirus type 16 gene expression by binding to a subset of the DNA sequences recognized by the viral E2 protein. *J Gen Virol* 80 ( Pt 8): 2087-96.
- Lindsay, M.A.** (2002). Peptide-mediated cell delivery: application in protein target validation. *Curr Opin Pharmacol* 2(5): 587-94.
- Ling, M.M.** (2003). Large antibody display libraries for isolation of high-affinity antibodies. *Comb Chem High Throughput Screen* 6(5): 421-32.
- Lipovsek, D. and Pluckthun, A.** (2004). In-vitro protein evolution by ribosome display and mRNA display. *J Immunol Methods* 290(1-2): 51-67.
- Liu, X., Clements, A., Zhao, K. and Marmorstein, R.** (2006). Structure of the human Papillomavirus E7 oncoprotein and its mechanism for inactivation of the retinoblastoma tumor suppressor. *J Biol Chem* 281(1): 578-86.
- Lonberg, N.** (2008). Fully human antibodies from transgenic mouse and phage display platforms. *Curr Opin Immunol* 20(4): 450-9.
- Longworth, M.S. and Laimins, L.A.** (2004). Pathogenesis of human papillomaviruses in differentiating epithelia. *Microbiol Mol Biol Rev* 68(2): 362-72.
- Lou, J., Marzari, R., Verzillo, V., Ferrero, F., Pak, D., Sheng, M., Yang, C., Sblattero, D. and Bradbury, A.** (2001). Antibodies in haystacks: how selection strategy influences the outcome of selection from molecular diversity libraries. *J Immunol Methods* 253(1-2): 233-42.
- Lundberg, M., Wikstrom, S. and Johansson, M.** (2003). Cell surface adherence and endocytosis of protein transduction domains. *Mol Ther* 8(1): 143-50.
- Luscher-Firzlaff, J.M., Westendorf, J.M., Zwicker, J., Burkhardt, H., Henriksson, M., Muller, R., Pirollet, F. and Luscher, B.** (1999). Interaction of the fork head domain transcription factor MPP2 with the human papilloma virus 16 E7 protein: enhancement of transformation and transactivation. *Oncogene* 18(41): 5620-30.
- Lutz, S. and Bornscheuer, U.T.** (2009). Protein Engineering Handbook. Weinheim, Germany, Wiley-Vch Verlag.
- Makino, E., Sakaguchi, M., Iwatsuki, K. and Huh, N.H.** (2004). Introduction of an N-terminal peptide of S100C/A11 into human cells induces apoptotic cell death. *J Mol Med* 82(9): 612-20.

- Malumbres, M. and Barbacid, M.** (2001). To cycle or not to cycle: a critical decision in cancer. *Nat Rev Cancer* 1(3): 222-31.
- Mannhardt, B., Weinzimer, S.A., Wagner, M., Fiedler, M., Cohen, P., Jansen-Durr, P. and Zwerschke, W.** (2000). Human papillomavirus type 16 E7 oncoprotein binds and inactivates growth-inhibitory insulin-like growth factor binding protein 3. *Mol Cell Biol* 20(17): 6483-95.
- Mayer, M. and Buchner, J.** (2004). Refolding of inclusion body proteins. *Methods Mol Med* 94: 239-54.
- Mazzarelli, J.M., Atkins, G.B., Geisberg, J.V. and Ricciardi, R.P.** (1995). The viral oncoproteins Ad5 E1A, HPV16 E7 and SV40 TAg bind a common region of the TBP-associated factor-110. *Oncogene* 11(9): 1859-64.
- McBride, A.A., Romanczuk, H. and Howley, P.M.** (1991). The papillomavirus E2 regulatory proteins. *J Biol Chem* 266(28): 18411-4.
- McIntyre, M.C., Frattini, M.G., Grossman, S.R. and Laimins, L.A.** (1993). Human papillomavirus type 18 E7 protein requires intact Cys-X-X-Cys motifs for zinc binding, dimerization, and transformation but not for Rb binding. *J Virol* 67(6): 3142-50.
- McLafferty, M.A., Kent, R.B., Ladner, R.C. and Markland, W.** (1993). M13 bacteriophage displaying disulfide-constrained microproteins. *Gene* 128(1): 29-36.
- McLaughlin-Drubin, M.E., Huh, K.W. and Munger, K.** (2008). Human papillomavirus type 16 E7 oncoprotein associates with E2F6. *J Virol* 82(17): 8695-705.
- McLaughlin-Drubin, M.E. and Munger, K.** (2009). The human papillomavirus E7 oncoprotein. *Virology* 384(2): 335-44.
- Meade, B.R. and Dowdy, S.F.** (2007). Exogenous siRNA delivery using peptide transduction domains/cell penetrating peptides. *Adv Drug Deliv Rev* 59(2-3): 134-40.
- Melikov, K. and Chernomordik, L.V.** (2005). Arginine-rich cell penetrating peptides: from endosomal uptake to nuclear delivery. *Cell Mol Life Sci* 62(23): 2739-49.
- Mercader, J.V. and Skerra, A.** (2002). Generation of anticalins with specificity for a nonsymmetric phthalic acid ester. *Anal Biochem* 308(2): 269-77.
- Milovnik, P., Ferrari, D., Sarkar, C.A. and Pluckthun, A.** (2009). Selection and characterization of DARPins specific for the neurotensin receptor 1. *Protein Eng Des Sel* 22(6): 357-66.
- Modis, Y., Trus, B.L. and Harrison, S.C.** (2002). Atomic model of the papillomavirus capsid. *Embo J* 21(18): 4754-62.
- Moon, M.S., Lee, C.J., Um, S.J., Park, J.S., Yang, J.M. and Hwang, E.S.** (2001). Effect of BPV1 E2-mediated inhibition of E6/E7 expression in HPV16-positive cervical carcinoma cells. *Gynecol Oncol* 80(2): 168-75.
- Moro, A. and Hernandez, P.** (1996). Bacterial expression and immunological detection of human papillomavirus type 16 E7 protein. *Biochem Biophys Res Commun* 226(3): 895-9.
- Muller, M.** (2005). Twin-arginine-specific protein export in Escherichia coli. *Res Microbiol* 156(2): 131-6.
- Munger, K., Baldwin, A., Edwards, K.M., Hayakawa, H., Nguyen, C.L., Owens, M., Grace, M. and Huh, K.** (2004). Mechanisms of human papillomavirus-induced oncogenesis. *J Virol* 78(21): 11451-60.
- Munger, K., Basile, J.R., Duensing, S., Eichten, A., Gonzalez, S.L., Grace, M. and Zacny, V.L.** (2001). Biological activities and molecular targets of the human papillomavirus E7 oncoprotein. *Oncogene* 20(54): 7888-98.
- Munger, K., Phelps, W.C., Bubb, V., Howley, P.M. and Schlegel, R.** (1989). The E6 and E7 genes of the human papillomavirus type 16 together are necessary and sufficient for transformation of primary human keratinocytes. *J Virol* 63(10): 4417-21.
- Munger, K., Werness, B.A., Dyson, N., Phelps, W.C., Harlow, E. and Howley, P.M.** (1989). Complex formation of human papillomavirus E7 proteins with the retinoblastoma tumor suppressor gene product. *Embo J* 8(13): 4099-105.
- Munger, K., Yee, C.L., Phelps, W.C., Pietenpol, J.A., Moses, H.L. and Howley, P.M.** (1991). Biochemical and biological differences between E7 oncoproteins of the high-

- and low-risk human papillomavirus types are determined by amino-terminal sequences. *J Virol* 65(7): 3943-8.
- Nagai, K., Oubridge, C., Kuglstatter, A., Menichelli, E., Isel, C. and Jovine, L.** (2003). Structure, function and evolution of the signal recognition particle. *Embo J* 22(14): 3479-85.
- Nagano, N., Ota, M. and Nishikawa, K.** (1999). Strong hydrophobic nature of cysteine residues in proteins. *FEBS Lett* 458(1): 69-71.
- Nakase, I., Niwa, M., Takeuchi, T., Sonomura, K., Kawabata, N., Koike, Y., Takehashi, M., Tanaka, S., Ueda, K., Simpson, J.C., Jones, A.T., Sugiura, Y. and Futaki, S.** (2004). Cellular uptake of arginine-rich peptides: roles for macropinocytosis and actin rearrangement. *Mol Ther* 10(6): 1011-22.
- Nakase, I., Takeuchi, T., Tanaka, G. and Futaki, S.** (2008). Methodological and cellular aspects that govern the internalization mechanisms of arginine-rich cell-penetrating peptides. *Adv Drug Deliv Rev* 60(4-5): 598-607.
- Nauenburg, S., Zwerschke, W. and Jansen-Durr, P.** (2001). Induction of apoptosis in cervical carcinoma cells by peptide aptamers that bind to the HPV-16 E7 oncoprotein. *Faseb J* 15(3): 592-4.
- Nead, M.A., Baglia, L.A., Antinore, M.J., Ludlow, J.W. and McCance, D.J.** (1998). Rb binds c-Jun and activates transcription. *Embo J* 17(8): 2342-52.
- Nevins, J.R., Leone, G., DeGregori, J. and Jakoi, L.** (1997). Role of the Rb/E2F pathway in cell growth control. *J Cell Physiol* 173(2): 233-6.
- Nguyen, C.L., Eichwald, C., Nibert, M.L. and Munger, K.** (2007). Human papillomavirus type 16 E7 oncoprotein associates with the centrosomal component gamma-tubulin. *J Virol* 81(24): 13533-43.
- Nguyen, C.L. and Munger, K.** (2008). Direct association of the HPV16 E7 oncoprotein with cyclin A/CDK2 and cyclin E/CDK2 complexes. *Virology* 380(1): 21-5.
- Nguyen, C.L. and Munger, K.** (2009). Human papillomavirus E7 protein deregulates mitosis via an association with nuclear mitotic apparatus protein 1. *J Virol* 83(4): 1700-7.
- Nieba, L., Krebber, A. and Pluckthun, A.** (1996). Competition BIAcore for measuring true affinities: large differences from values determined from binding kinetics. *Anal Biochem* 234(2): 155-65.
- Nilsson, B., Berman-Marks, C., Kuntz, I.D. and Anderson, S.** (1991). Secretion incompetence of bovine pancreatic trypsin inhibitor expressed in *Escherichia coli*. *J Biol Chem* 266(5): 2970-7.
- Nolkrantz, K., Farre, C., Hurtig, K.J., Rylander, P. and Orwar, O.** (2002). Functional screening of intracellular proteins in single cells and in patterned cell arrays using electroporation. *Anal Chem* 74(16): 4300-5.
- Nord, K., Gunneriusson, E., Ringdahl, J., Stahl, S., Uhlen, M. and Nygren, P.A.** (1997). Binding proteins selected from combinatorial libraries of an alpha-helical bacterial receptor domain. *Nat Biotechnol* 15(8): 772-7.
- Nord, K., Gunneriusson, E., Uhlen, M. and Nygren, P.A.** (2000). Ligands selected from combinatorial libraries of protein A for use in affinity capture of apolipoprotein A-1M and taq DNA polymerase. *J Biotechnol* 80(1): 45-54.
- Ohlenschlager, O., Seiboth, T., Zengerling, H., Briese, L., Marchanka, A., Ramachandran, R., Baum, M., Korbass, M., Meyer-Klaucke, W., Durst, M. and Goriach, M.** (2006). Solution structure of the partially folded high-risk human papilloma virus 45 oncoprotein E7. *Oncogene* 25(44): 5953-9.
- Orlova, A., Magnusson, M., Eriksson, T.L., Nilsson, M., Larsson, B., Hoiden-Guthenberg, I., Widstrom, C., Carlsson, J., Tolmachev, V., Stahl, S. and Nilsson, F.Y.** (2006). Tumor imaging using a picomolar affinity HER2 binding affibody molecule. *Cancer Res* 66(8): 4339-48.
- Ou, J., Wang, L., Ding, X., Du, J., Zhang, Y., Chen, H. and Xu, A.** (2004). Stationary phase protein overproduction is a fundamental capability of *Escherichia coli*. *Biochem Biophys Res Commun* 314(1): 174-80.
- Pace, C.N., Vajdos, F., Fee, L., Grimsley, G. and Gray, T.** (1995). How to measure and predict the molar absorption coefficient of a protein. *Protein Sci* 4(11): 2411-23.

- Padlan, E.A.** (1994). Anatomy of the antibody molecule. *Mol Immunol* 31(3): 169-217.
- Pahel, G., Aulabaugh, A., Short, S.A., Barnes, J.A., Painter, G.R., Ray, P. and Phelps, W.C.** (1993). Structural and functional characterization of the HPV16 E7 protein expressed in bacteria. *J Biol Chem* 268(34): 26018-25.
- Park, D.S., Selvey, L.A., Kelsall, S.R. and Frazer, I.H.** (1993). Human papillomavirus type 16 E6, E7 and L1 and type 18 E7 proteins produced by recombinant baculoviruses. *J Virol Methods* 45(3): 303-18.
- Park, J., Ryu, J., Kim, K.A., Lee, H.J., Bahn, J.H., Han, K., Choi, E.Y., Lee, K.S., Kwon, H.Y. and Choi, S.Y.** (2002). Mutational analysis of a human immunodeficiency virus type 1 Tat protein transduction domain which is required for delivery of an exogenous protein into mammalian cells. *J Gen Virol* 83(Pt 5): 1173-81.
- Park, J.S., Kim, E.J., Kwon, H.J., Hwang, E.S., Namkoong, S.E. and Um, S.J.** (2000). Inactivation of interferon regulatory factor-1 tumor suppressor protein by HPV E7 oncoprotein. Implication for the E7-mediated immune evasion mechanism in cervical carcinogenesis. *J Biol Chem* 275(10): 6764-9.
- Parkin, D.M., Bray, F., Ferlay, J. and Pisani, P.** (2005). Global cancer statistics, 2002. *CA Cancer J Clin* 55(2): 74-108.
- Paschke, M.** (2006). Phage display systems and their applications. *Appl Microbiol Biotechnol* 70(1): 2-11.
- Paschke, M. and Hohne, W.** (2005). A twin-arginine translocation (Tat)-mediated phage display system. *Gene* 350(1): 79-88.
- Patrick, D.R., Zhang, K., Defeo-Jones, D., Vuocolo, G.R., Maigetter, R.Z., Sardana, M.K., Oliff, A. and Heimbrook, D.C.** (1992). Characterization of functional HPV-16 E7 protein produced in *Escherichia coli*. *J Biol Chem* 267(10): 6910-5.
- Pedersen, J.S., Otzen, D.E. and Kristensen, P.** (2002). Directed evolution of barnase stability using proteolytic selection. *J Mol Biol* 323(1): 115-23.
- Peitz, M., Pfannkuche, K., Rajewsky, K. and Edenhofer, F.** (2002). Ability of the hydrophobic FGF and basic TAT peptides to promote cellular uptake of recombinant Cre recombinase: a tool for efficient genetic engineering of mammalian genomes. *Proc Natl Acad Sci U S A* 99(7): 4489-94.
- Petsch, D. and Anspach, F.B.** (2000). Endotoxin removal from protein solutions. *J Biotechnol* 76(2-3): 97-119.
- Phillips, A.C. and Vousden, K.H.** (1997). Analysis of the interaction between human papillomavirus type 16 E7 and the TATA-binding protein, TBP. *J Gen Virol* 78 ( Pt 4): 905-9.
- Piliarik, M., Vaisocherova, H. and Homola, J.** (2009). Surface plasmon resonance biosensing. *Methods Mol Biol* 503: 65-88.
- Polyakov, V., Sharma, V., Dahlheimer, J.L., Pica, C.M., Luker, G.D. and Piwnica-Worms, D.** (2000). Novel Tat-peptide chelates for direct transduction of technetium-99m and rhenium into human cells for imaging and radiotherapy. *Bioconjug Chem* 11(6): 762-71.
- Prathapam, T., Kuhne, C. and Banks, L.** (2001). The HPV-16 E7 oncoprotein binds Skip and suppresses its transcriptional activity. *Oncogene* 20(52): 7677-85.
- Presta, L.G.** (2006). Engineering of therapeutic antibodies to minimize immunogenicity and optimize function. *Adv Drug Deliv Rev* 58(5-6): 640-56.
- Raghava, G.P. and Agrewala, J.N.** (1994). Method for determining the affinity of monoclonal antibody using non-competitive ELISA: a computer program. *J Immunoassay* 15(2): 115-28.
- Rajpal, A., Beyaz, N., Haber, L., Cappuccilli, G., Yee, H., Bhatt, R.R., Takeuchi, T., Lerner, R.A. and Crea, R.** (2005). A general method for greatly improving the affinity of antibodies by using combinatorial libraries. *Proc Natl Acad Sci U S A* 102(24): 8466-71.
- Rawls, J.A., Pusztai, R. and Green, M.** (1990). Chemical synthesis of human papillomavirus type 16 E7 oncoprotein: autonomous protein domains for induction of cellular DNA synthesis and for trans activation. *J Virol* 64(12): 6121-9.

- Reichert, J.M.** (2008). Monoclonal antibodies as innovative therapeutics. *Curr Pharm Biotechnol* 9(6): 423-30.
- Reina, J., Lacroix, E., Hobson, S.D., Fernandez-Ballester, G., Rybin, V., Schwab, M.S., Serrano, L. and Gonzalez, C.** (2002). Computer-aided design of a PDZ domain to recognize new target sequences. *Nat Struct Biol* 9(8): 621-7.
- Renberg, B., Shiroyama, I., Engfeldt, T., Nygren, P.K. and Karlstrom, A.E.** (2005). Affibody protein capture microarrays: synthesis and evaluation of random and directed immobilization of affibody molecules. *Anal Biochem* 341(2): 334-43.
- Rey, O., Lee, S., Baluda, M.A., Swee, J., Ackerson, B., Chiu, R. and Park, N.H.** (2000). The E7 oncoprotein of human papillomavirus type 16 interacts with F-actin in vitro and in vivo. *Virology* 268(2): 372-81.
- Rhyner, C., Kodzius, R. and Cramer, R.** (2002). Direct selection of cDNAs from filamentous phage surface display libraries: potential and limitations. *Curr Pharm Biotechnol* 3(1): 13-21.
- Richard, J.P., Melikov, K., Brooks, H., Prevot, P., Lebleu, B. and Chernomordik, L.V.** (2005). Cellular uptake of unconjugated TAT peptide involves clathrin-dependent endocytosis and heparan sulfate receptors. *J Biol Chem* 280(15): 15300-6.
- Richard, J.P., Melikov, K., Vives, E., Ramos, C., Verbeure, B., Gait, M.J., Chernomordik, L.V. and Lebleu, B.** (2003). Cell-penetrating peptides. A reevaluation of the mechanism of cellular uptake. *J Biol Chem* 278(1): 585-90.
- Roberts, S., Ashmole, I., Gibson, L.J., Rookes, S.M., Barton, G.J. and Gallimore, P.H.** (1994). Mutational analysis of human papillomavirus E4 proteins: identification of structural features important in the formation of cytoplasmic E4/cytokeratin networks in epithelial cells. *J Virol* 68(10): 6432-45.
- Roggenbuck, B., Larsen, P.M., Fey, S.J., Bartsch, D., Gissmann, L. and Schwarz, E.** (1991). Human papillomavirus type 18 E6\*, E6, and E7 protein synthesis in cell-free translation systems and comparison of E6 and E7 in vitro translation products to proteins immunoprecipitated from human epithelial cells. *J Virol* 65(9): 5068-72.
- Romanczuk, H. and Howley, P.M.** (1992). Disruption of either the E1 or the E2 regulatory gene of human papillomavirus type 16 increases viral immortalization capacity. *Proc Natl Acad Sci U S A* 89(7): 3159-63.
- Roth, E.J., Kurz, B., Liang, L., Hansen, C.L., Dameron, C.T., Winge, D.R. and Smotkin, D.** (1992). Metal thiolate coordination in the E7 proteins of human papilloma virus 16 and cottontail rabbit papilloma virus as expressed in *Escherichia coli*. *J Biol Chem* 267(23): 16390-5.
- Rothe, A., Hosse, R.J. and Power, B.E.** (2006). In vitro display technologies reveal novel biopharmaceuticals. *Faseb J* 20(10): 1599-610.
- Ruben, S., Perkins, A., Purcell, R., Joung, K., Sia, R., Burghoff, R., Haseltine, W.A. and Rosen, C.A.** (1989). Structural and functional characterization of human immunodeficiency virus tat protein. *J Virol* 63(1): 1-8.
- Rudolph, C., Plank, C., Lausier, J., Schillinger, U., Muller, R.H. and Rosenecker, J.** (2003). Oligomers of the arginine-rich motif of the HIV-1 TAT protein are capable of transferring plasmid DNA into cells. *J Biol Chem* 278(13): 11411-8.
- Rudolph, R., Siebendritt, R., Nesslauer, G., Sharma, A.K. and Jaenicke, R.** (1990). Folding of an all-beta protein: independent domain folding in gamma II-crystallin from calf eye lens. *Proc Natl Acad Sci U S A* 87(12): 4625-9.
- Rui, M., Chen, Y., Zhang, Y. and Ma, D.** (2002). Transfer of anti-TFAR19 monoclonal antibody into HeLa cells by in situ electroporation can inhibit the apoptosis. *Life Sci* 71(15): 1771-8.
- Russel, M.** (1991). Filamentous phage assembly. *Mol Microbiol* 5(7): 1607-13.
- Sambrook, J. and Russell, D.W.** (2001). *Molecular Cloning: A Laboratory Manual*. New York, Cold Spring Harbor Laboratory Press.
- Sanger, F., Nicklen, S. and Coulson, A.R.** (1977). DNA sequencing with chain-terminating inhibitors. *Proc Natl Acad Sci U S A* 74(12): 5463-7.

- Sato, H., Watanabe, S., Furuno, A. and Yoshiike, K.** (1989). Human papillomavirus type 16 E7 protein expressed in *Escherichia coli* and monkey COS-1 cells: immunofluorescence detection of the nuclear E7 protein. *Virology* 170(1): 311-5.
- Schein, C.H.** (1991). Optimizing protein folding to the native state in bacteria. *Curr Opin Biotechnol* 2(5): 746-50.
- Schilling, B., De-Medina, T., Syken, J., Vidal, M. and Munger, K.** (1998). A novel human DnaJ protein, hTid-1, a homolog of the *Drosophila* tumor suppressor protein Tid56, can interact with the human papillomavirus type 16 E7 oncoprotein. *Virology* 247(1): 74-85.
- Schlehuber, S. and Skerra, A.** (2005). Lipocalins in drug discovery: from natural ligand-binding proteins to "anticalins". *Drug Discov Today* 10(1): 23-33.
- Schulze, A., Mannhardt, B., Zerfass-Thome, K., Zwerschke, W. and Jansen-Durr, P.** (1998). Anchorage-independent transcription of the cyclin A gene induced by the E7 oncoprotein of human papillomavirus type 16. *J Virol* 72(3): 2323-34.
- Schwarze, S.R., Ho, A., Vocero-Akbani, A. and Dowdy, S.F.** (1999). In vivo protein transduction: delivery of a biologically active protein into the mouse. *Science* 285(5433): 1569-72.
- Schwarze, S.R., Hruska, K.A. and Dowdy, S.F.** (2000). Protein transduction: unrestricted delivery into all cells? *Trends Cell Biol* 10(7): 290-5.
- Sedman, S.A., Barbosa, M.S., Vass, W.C., Hubbert, N.L., Haas, J.A., Lowy, D.R. and Schiller, J.T.** (1991). The full-length E6 protein of human papillomavirus type 16 has transforming and trans-activating activities and cooperates with E7 to immortalize keratinocytes in culture. *J Virol* 65(9): 4860-6.
- Siddiqui, M.A. and Perry, C.M.** (2006). Human papillomavirus quadrivalent (types 6, 11, 16, 18) recombinant vaccine (Gardasil). *Drugs* 66(9): 1263-71; discussion 1272-3.
- Sieber, V., Pluckthun, A. and Schmid, F.X.** (1998). Selecting proteins with improved stability by a phage-based method. *Nat Biotechnol* 16(10): 955-60.
- Silverman, J., Liu, Q., Bakker, A., To, W., Duguay, A., Alba, B.M., Smith, R., Rivas, A., Li, P., Le, H., Whitehorn, E., Moore, K.W., Swimmer, C., Perlroth, V., Vogt, M., Kolkman, J. and Stemmer, W.P.** (2005). Multivalent avimer proteins evolved by exon shuffling of a family of human receptor domains. *Nat Biotechnol* 23(12): 1556-61.
- Skerra, A.** (2000). Engineered protein scaffolds for molecular recognition. *J Mol Recognit* 13(4): 167-87.
- Skerra, A.** (2000). Lipocalins as a scaffold. *Biochim Biophys Acta* 1482(1-2): 337-50.
- Skerra, A.** (2007). Alternative non-antibody scaffolds for molecular recognition. *Curr Opin Biotechnol* 18(4): 295-304.
- Smotkin, D. and Wettstein, F.O.** (1986). Transcription of human papillomavirus type 16 early genes in a cervical cancer and a cancer-derived cell line and identification of the E7 protein. *Proc Natl Acad Sci U S A* 83(13): 4680-4.
- Sorensen, H.P. and Mortensen, K.K.** (2005). Soluble expression of recombinant proteins in the cytoplasm of *Escherichia coli*. *Microb Cell Fact* 4(1): 1.
- Speck, L.M. and Tyring, S.K.** (2006). Vaccines for the prevention of human papillomavirus infections. *Skin Therapy Lett* 11(6): 1-3.
- Spitkovsky, D., Aengeneyndt, F., Braspenning, J. and von Knebel Doeberitz, M.** (1996). p53-independent growth regulation of cervical cancer cells by the papillomavirus E6 oncogene. *Oncogene* 13(5): 1027-35.
- Stacey, S.N., Ghosh, A., Bartholomew, J.S., Tindle, R.W., Stern, P.L., Mackett, M. and Arrand, J.R.** (1993). Expression of human papillomavirus type 16 E7 protein by recombinant baculovirus and use for the detection of E7 antibodies in sera from cervical carcinoma patients. *J Med Virol* 40(1): 14-21.
- Steiner, D., Forrer, P. and Pluckthun, A.** (2008). Efficient selection of DARPins with sub-nanomolar affinities using SRP phage display. *J Mol Biol* 382(5): 1211-27.
- Stoop, A.A. and Craik, C.S.** (2003). Engineering of a macromolecular scaffold to develop specific protease inhibitors. *Nat Biotechnol* 21(9): 1063-8.

- Stubenrauch, F. and Laimins, L.A.** (1999). Human papillomavirus life cycle: active and latent phases. *Semin Cancer Biol* 9(6): 379-86.
- Stumpp, M.T. and Amstutz, P.** (2007). DARPinS: a true alternative to antibodies. *Curr Opin Drug Discov Devel* 10(2): 153-9.
- Stumpp, M.T., Binz, H.K. and Amstutz, P.** (2008). DARPinS: a new generation of protein therapeutics. *Drug Discov Today* 13(15-16): 695-701.
- Tan, T.M. and Ting, R.C.** (1995). In vitro and in vivo inhibition of human papillomavirus type 16 E6 and E7 genes. *Cancer Res* 55(20): 4599-605.
- Theiss, C. and Meller, K.** (2002). Microinjected anti-actin antibodies decrease gap junctional intercellular communication in cultured astrocytes. *Exp Cell Res* 281(2): 197-204.
- Thie, H., Voedisch, B., Dubel, S., Hust, M. and Schirrmann, T.** (2009). Affinity maturation by phage display. *Methods Mol Biol* 525: 1-14.
- Thomas, J.T., Hubert, W.G., Ruesch, M.N. and Laimins, L.A.** (1999). Human papillomavirus type 31 oncoproteins E6 and E7 are required for the maintenance of episomes during the viral life cycle in normal human keratinocytes. *Proc Natl Acad Sci U S A* 96(15): 8449-54.
- Thurber, G.M., Schmidt, M.M. and Wittrup, K.D.** (2008). Antibody tumor penetration: transport opposed by systemic and antigen-mediated clearance. *Adv Drug Deliv Rev* 60(12): 1421-34.
- Tommasino, M., Contorni, M., Scarlato, V., Bugnoli, M., Maundrell, K. and Cavalieri, F.** (1990). Synthesis, phosphorylation, and nuclear localization of human papillomavirus E7 protein in *Schizosaccharomyces pombe*. *Gene* 93(2): 265-70.
- Torchilin, V.P., Levchenko, T.S., Rammohan, R., Volodina, N., Papahadjopoulos-Sternberg, B. and D'Souza, G.G.** (2003). Cell transfection in vitro and in vivo with nontoxic TAT peptide-liposome-DNA complexes. *Proc Natl Acad Sci U S A* 100(4): 1972-7.
- Torchilin, V.P., Rammohan, R., Weissig, V. and Levchenko, T.S.** (2001). TAT peptide on the surface of liposomes affords their efficient intracellular delivery even at low temperature and in the presence of metabolic inhibitors. *Proc Natl Acad Sci U S A* 98(15): 8786-91.
- Tunnemann, G., Martin, R.M., Haupt, S., Patsch, C., Edenhofer, F. and Cardoso, M.C.** (2006). Cargo-dependent mode of uptake and bioavailability of TAT-containing proteins and peptides in living cells. *Faseb J* 20(11): 1775-84.
- van der Gun, B.T., Monami, A., Laarmann, S., Rasko, T., Slaska-Kiss, K., Weinhold, E., Wasserkort, R., de Leij, L.F., Ruiters, M.H., Kiss, A. and McLaughlin, P.M.** (2007). Serum insensitive, intranuclear protein delivery by the multipurpose cationic lipid SAINT-2. *J Control Release* 123(3): 228-38.
- Vendeville, A., Rayne, F., Bonhoure, A., Bettache, N., Montcourrier, P. and Beaumelle, B.** (2004). HIV-1 Tat enters T cells using coated pits before translocating from acidified endosomes and eliciting biological responses. *Mol Biol Cell* 15(5): 2347-60.
- Vieira, J. and Messing, J.** (1987). Production of single-stranded plasmid DNA. *Methods Enzymol* 153: 3-11.
- Violini, S., Sharma, V., Prior, J.L., Dyszlewski, M. and Piwnicka-Worms, D.** (2002). Evidence for a plasma membrane-mediated permeability barrier to Tat basic domain in well-differentiated epithelial cells: lack of correlation with heparan sulfate. *Biochemistry* 41(42): 12652-61.
- Viti, F., Nilsson, F., Demartis, S., Huber, A. and Neri, D.** (2000). Design and use of phage display libraries for the selection of antibodies and enzymes. *Methods Enzymol* 326: 480-505.
- Vives, E., Brodin, P. and Lebleu, B.** (1997). A truncated HIV-1 Tat protein basic domain rapidly translocates through the plasma membrane and accumulates in the cell nucleus. *J Biol Chem* 272(25): 16010-7.
- Vives, E., Schmidt, J. and Pelegrin, A.** (2008). Cell-penetrating and cell-targeting peptides in drug delivery. *Biochim Biophys Acta*.

- Vocero-Akbani, A.M., Heyden, N.V., Lissy, N.A., Ratner, L. and Dowdy, S.F.** (1999). Killing HIV-infected cells by transduction with an HIV protease-activated caspase-3 protein. *Nat Med* 5(1): 29-33.
- von Knebel Doeberitz, M., Rittmuller, C., Aengeneyndt, F., Jansen-Durr, P. and Spitkovsky, D.** (1994). Reversible repression of papillomavirus oncogene expression in cervical carcinoma cells: consequences for the phenotype and E6-p53 and E7-pRB interactions. *J Virol* 68(5): 2811-21.
- von Knebel Doeberitz, M., Rittmuller, C., zur Hausen, H. and Durst, M.** (1992). Inhibition of tumorigenicity of cervical cancer cells in nude mice by HPV E6-E7 anti-sense RNA. *Int J Cancer* 51(5): 831-4.
- Voss, S. and Skerra, A.** (1997). Mutagenesis of a flexible loop in streptavidin leads to higher affinity for the Strep-tag II peptide and improved performance in recombinant protein purification. *Protein Eng* 10(8): 975-82.
- Vousden, K.H. and Jat, P.S.** (1989). Functional similarity between HPV16E7, SV40 large T and adenovirus E1a proteins. *Oncogene* 4(2): 153-8.
- Wadia, J.S. and Dowdy, S.F.** (2005). Transmembrane delivery of protein and peptide drugs by TAT-mediated transduction in the treatment of cancer. *Adv Drug Deliv Rev* 57(4): 579-96.
- Wadia, J.S., Stan, R.V. and Dowdy, S.F.** (2004). Transducible TAT-HA fusogenic peptide enhances escape of TAT-fusion proteins after lipid raft macropinocytosis. *Nat Med* 10(3): 310-5.
- Wagstaff, K.M. and Jans, D.A.** (2006). Protein transduction: cell penetrating peptides and their therapeutic applications. *Curr Med Chem* 13(12): 1371-87.
- Wark, K.L. and Hudson, P.J.** (2006). Latest technologies for the enhancement of antibody affinity. *Adv Drug Deliv Rev* 58(5-6): 657-70.
- Wigler, M., Silverstein, S., Lee, L.S., Pellicer, A., Cheng, Y. and Axel, R.** (1977). Transfer of purified herpes virus thymidine kinase gene to cultured mouse cells. *Cell* 11(1): 223-32.
- Wikman, M., Steffen, A.C., Gunneriusson, E., Tolmachev, V., Adams, G.P., Carlsson, J. and Stahl, S.** (2004). Selection and characterization of HER2/neu-binding affibody ligands. *Protein Eng Des Sel* 17(5): 455-62.
- Wille, J.J., Park, J. and Elgavish, A.** (1992). Effects of growth factors, hormones, bacterial lipopolysaccharides, and lipotechoic acids on the clonal growth of normal ureteral epithelial cells in serum-free culture. *J Cell Physiol* 150(1): 52-8.
- Williams, A. and Baird, L.G.** (2003). DX-88 and HAE: a developmental perspective. *Transfus Apher Sci* 29(3): 255-8.
- Wistow, G.J. and Piatigorsky, J.** (1988). Lens crystallins: the evolution and expression of proteins for a highly specialized tissue. *Annu Rev Biochem* 57: 479-504.
- Wittrup, K.D.** (2001). Protein engineering by cell-surface display. *Curr Opin Biotechnol* 12(4): 395-9.
- Worn, A., Auf der Maur, A., Escher, D., Honegger, A., Barberis, A. and Pluckthun, A.** (2000). Correlation between in vitro stability and in vivo performance of anti-GCN4 intrabodies as cytoplasmic inhibitors. *J Biol Chem* 275(4): 2795-803.
- Worn, A. and Pluckthun, A.** (2001). Stability engineering of antibody single-chain Fv fragments. *J Mol Biol* 305(5): 989-1010.
- Wu, S., Meng, L., Wang, S., Wang, W., Xi, L., Tian, X., Chen, G., Wu, Y., Zhou, J., Xu, G., Lu, Y. and Ma, D.** (2006). Reversal of the malignant phenotype of cervical cancer CaSki cells through adeno-associated virus-mediated delivery of HPV16 E7 antisense RNA. *Clin Cancer Res* 12(7 Pt 1): 2032-7.
- Xu, L., Aha, P., Gu, K., Kuimelis, R.G., Kurz, M., Lam, T., Lim, A.C., Liu, H., Lohse, P.A., Sun, L., Weng, S., Wagner, R.W. and Lipovsek, D.** (2002). Directed evolution of high-affinity antibody mimics using mRNA display. *Chem Biol* 9(8): 933-42.
- Yamato, K., Yamada, T., Kizaki, M., Ui-Tei, K., Natori, Y., Fujino, M., Nishihara, T., Ikeda, Y., Nasu, Y., Saigo, K. and Yoshinouchi, M.** (2008). New highly potent and specific E6 and E7 siRNAs for treatment of HPV16 positive cervical cancer. *Cancer Gene Ther* 15(3): 140-53.

- Yang, T.T., Cheng, L. and Kain, S.R.** (1996). Optimized codon usage and chromophore mutations provide enhanced sensitivity with the green fluorescent protein. *Nucleic Acids Res* 24(22): 4592-3.
- Yang, Y., Ma, J., Song, Z. and Wu, M.** (2002). HIV-1 TAT-mediated protein transduction and subcellular localization using novel expression vectors. *FEBS Lett* 532(1-2): 36-44.
- Yasumoto, S., Burkhardt, A.L., Doniger, J. and DiPaolo, J.A.** (1986). Human papillomavirus type 16 DNA-induced malignant transformation of NIH 3T3 cells. *J Virol* 57(2): 572-7.
- Yau, K.Y., Dubuc, G., Li, S., Hirama, T., Mackenzie, C.R., Jermutus, L., Hall, J.C. and Tanha, J.** (2005). Affinity maturation of a V(H)H by mutational hotspot randomization. *J Immunol Methods* 297(1-2): 213-24.
- Yee, C., Krishnan-Hewlett, I., Baker, C.C., Schlegel, R. and Howley, P.M.** (1985). Presence and expression of human papillomavirus sequences in human cervical carcinoma cell lines. *Am J Pathol* 119(3): 361-6.
- Yuste, R.** (2005). Fluorescence microscopy today. *Nat Methods* 2(12): 902-4.
- Zelphati, O., Wang, Y., Kitada, S., Reed, J.C., Felgner, P.L. and Corbeil, J.** (2001). Intracellular delivery of proteins with a new lipid-mediated delivery system. *J Biol Chem* 276(37): 35103-10.
- Zerfass-Thome, K., Zwerschke, W., Mannhardt, B., Tindle, R., Botz, J.W. and Jansen-Durr, P.** (1996). Inactivation of the cdk inhibitor p27KIP1 by the human papillomavirus type 16 E7 oncoprotein. *Oncogene* 13(11): 2323-30.
- Zerfass, K., Schulze, A., Spitkovsky, D., Friedman, V., Henglein, B. and Jansen-Durr, P.** (1995). Sequential activation of cyclin E and cyclin A gene expression by human papillomavirus type 16 E7 through sequences necessary for transformation. *J Virol* 69(10): 6389-99.
- Zheng, Z.M. and Baker, C.C.** (2006). Papillomavirus genome structure, expression, and post-transcriptional regulation. *Front Biosci* 11: 2286-302.
- zur Hausen, H.** (2000). Papillomaviruses causing cancer: evasion from host-cell control in early events in carcinogenesis. *J Natl Cancer Inst* 92(9): 690-8.
- zur Hausen, H.** (2002). Papillomaviruses and cancer: from basic studies to clinical application. *Nat Rev Cancer* 2(5): 342-50.
- Zwerschke, W., Mannhardt, B., Massimi, P., Nauenburg, S., Pim, D., Nickel, W., Banks, L., Reuser, A.J. and Jansen-Durr, P.** (2000). Allosteric activation of acid alpha-glucosidase by the human papillomavirus E7 protein. *J Biol Chem* 275(13): 9534-41.
- Zwerschke, W., Mazurek, S., Massimi, P., Banks, L., Eigenbrodt, E. and Jansen-Durr, P.** (1999). Modulation of type M2 pyruvate kinase activity by the human papillomavirus type 16 E7 oncoprotein. *Proc Natl Acad Sci U S A* 96(4): 1291-6.

## 9. Publications

Parts of this thesis have been published in the following journals:

**Mirecka, E. A.**, Rudolph, R. & Hey, T. (2006). Expression and purification of His-tagged HPV16 E7 protein active in pRb binding. *Protein Expr Purif* 48, 281-91.

**Mirecka, E. A.**, Hey, T., Fiedler, U., Rudolph, R. & Hatzfeld, M. (2009). Affilin molecules selected against the human papillomavirus E7 protein inhibit the proliferation of target cells. *J Mol Biol* 390, 710-21.

## 10. Abbreviations

<b>A, C, G, T</b>	Adenine, Cytosine, Guanine, Thymine
<b>2x YT</b>	Two times yeast tryptone
<b>A<sub>x</sub></b>	Absorption at x nm
<b>bp</b>	base pair
<b>BrdU</b>	Bromodeoxyuridine
<b>BSA</b>	Bovine serum albumin
<b>DMEM</b>	Dulbecco/Vogt modified Eagle's minimal essential medium
<b>DMSO</b>	Dimethylsulfoxide
<b>DNA</b>	Deoxyribonucleic acid
<b>dNTP</b>	Deoxynucleotide triphosphate
<b><i>E. coli</i></b>	<i>Escherichia coli</i>
<b><i>e.g.</i></b>	<i>exempli gratia</i> (for example)
<b>EDTA</b>	Ethylene diamine tetraacetic acid
<b>ELISA</b>	Enzyme-linked immunosorbent assay
<b><i>et al.</i></b>	<i>et alii</i> (and others)
<b>FBS</b>	Fetal bovine serum
<b>h</b>	hour
<b>HBS</b>	HEPES-buffered saline
<b>HEPES</b>	2-[(4-(hydroxyethyl)-1-piperazin)ethanesulfonic acid
<b>HIV</b>	Human immunodeficiency virus
<b>HPV</b>	Human papillomavirus
<b><i>i.e.</i></b>	<i>id est</i> (that is)
<b>IgG</b>	Immunoglobulin G
<b>IMAC</b>	Immobilized metal-ion affinity chromatography
<b>IPTG</b>	Isopropyl β-D-1-thiogalactopyranoside
<b>kDa</b>	kilodalton
<b>K<sub>d</sub></b>	Dissociation constant
<b>LB</b>	Luria-Bertani
<b>MES</b>	2-( <i>N</i> -morpholino)ethanesulfonic acid
<b>min</b>	minute
<b>MWCO</b>	molecular weight cut off
<b>NLS</b>	Nuclear localization signal
<b>No.</b>	Number
<b>OD<sub>600</sub></b>	Optical density at 600 nm
<b>PBS</b>	Phosphate buffered saline
<b>PCR</b>	Polymerase chain reaction
<b>PDB</b>	Protein Data Bank
<b>PMSF</b>	Phenylmethanesulfonylfluorid
<b>pRb</b>	Retinoblastoma tumor suppressor protein
<b>RPMI</b>	Roswell Park Memorial Institute medium
<b>RT</b>	Room temperature
<b>RU</b>	Resonance unit
<b>scFv</b>	single chain variable antibody fragment
<b>SDS</b>	Sodium dodecyl sulfate
<b>SDS-PAGE</b>	SDS-polyacrylamide gel electrophoresis
<b>sec</b>	second
<b>siRNA</b>	Small interfering ribonucleic acid
<b>SPR</b>	Surface plasmon resonance
<b>SV40</b>	Simian virus 40
<b>TMB</b>	3,3',5,5'-tetramethylbenzidine
<b>Tris</b>	N-[tris-(hydroxymethyl-)]aminomethane
<b>v/v</b>	volume per volume
<b>w/v</b>	weight per volume

## **Erklärung**

Hiermit erkläre ich an Eides statt, dass ich mich bisher mit dieser Arbeit weder an der Martin-Luther-Universität Halle-Wittenberg, noch an einer anderen Einrichtung um die Erlangung eines akademischen Grades beworben habe. Ich versichere weiterhin, dass die vorliegende Arbeit selbstständig und nur unter Benutzung der angegeben Quellen und Hilfsmittel erstellt wurde. Den benutzten Werken wörtlich oder inhaltlich entnommene Stellen sind als solche gekennzeichnet.

Halle (Saale), 19.11.2009

Ewa Mirecka